Universidade de Aveiro Departamento de Química
2012

Helena Isabel Sousa Passos

Extração de biocompostos com soluções aquosas de líquidos iónicos

Extraction of bioactive compounds with ionic liquid aqueous solutions

Universidade de Aveiro Departamento de Química
2012

Helena Isabel Sousa Passos

Extração de biocompostos com soluções aquosas de líquidos iónicos

Extraction of bioactive compounds with ionic liquid aqueous solutions

Dissertação apresentada à Universidade de Aveiro para cumprimento dos requisitos necessários à obtenção do grau de Mestre em Engenharia Química, realizada sob a orientação científica do Professor Dr. João Manuel da Costa Araújo Pereira Coutinho, Professor Associado com agregação do Departamento de Química da Universidade de Aveiro e co-orientação da Dr^{a}. Mara Guadalupe Freire Martins, Estagiária de Pós-Doutoramento do Instituto de Tecnologia Química e Biológica, ITQB 2, da Universidade Nova de Lisboa.

Aos meus pais, porque sem eles nada seria possível…

o júri

presidente

Prof[a]. Dr[a]. Maria Inês Purcell de Portugal Branco
professora auxiliar do Departamento de Química da Universidade de Aveiro

Prof. Dr. João Manuel da Costa Araújo Pereira Coutinho
professor associado com agregação do Departamento de Química da Universidade de Aveiro

Dr[a]. Ana Belén Pereiro Estévez
investigadora Marie Curie do Instituto de Tecnologia Química e Biológica, ITQB 2 da Universidade Nova de Lisboa

Dr[a]. Mara Guadalupe Freire Martins
estagiária de Pós-Doutoramento do Instituto de Tecnologia Química e Biológica, ITQB 2 da Universidade Nova de Lisboa

Dr[a]. Ana Catarina Almeida Sousa
estagiária de Pós-Doutoramento do Centro de Investigação em Ciências da Saúde, CICS-UBI, da Universidade da Beira Interior

agradecimentos

Gostaria de começar por agradecer ao meu orientador, o Prof. João Coutinho, não só pelo excelente acompanhamento ao longo deste trabalho mas também, por me ter dado a possibilidade de crescer a nível profissional e, principalmente, a nível pessoal. Um especial obrigado à minha co-orientadora, a Mara, porque todas as manhãs traz um grande sorriso para partilhar, está sempre bem-disposta e cheia de energia positiva. Obrigada, por estares sempre presente, por me teres dado força quando os dias eram menos bons, por teres acreditado sempre em mim e, claro, por toda a paciência que gastaste comigo. Ao Path e ao mini-Path, muito obrigada a todos por me terem acolhido tão bem e por me deixarem sentir que fiz parte desse grupo. Em especial, deixo um obrigado à Ana Filipa porque foi ela que me abriu a porta e que me mostrou a casa que partilhei com todos vocês.

Joana devo-te muito do que aprendi e do que fiz ao longo destes anos e, por isso, também este trabalho é fruto da tua presença e apoio. Obrigada, minha compincha… Obrigada ainda a todos os amigos, que fizeram parte desta caminhada, que partilharam os bons e os maus momentos e que me fizeram sempre sorrir. Um especial obrigado à Ana Maria e à Cláudia, por serem as amigas que são, por estarem sempre por perto e por acreditarem em mim.

E como há coisas que nunca mudam, Inês, mais uma vez te agradeço por confiares tanto em mim, por aturares as minhas breves loucuras, os meus medos e angústias, por me fazeres sempre acreditar que sou capaz de mais e ainda de mais um pouco… Tu foste peça indispensável neste trabalho.

Pai e Mãe, sem vocês, sem o vosso apoio, nada disto seria possível. Muito obrigada por estarem sempre presentes, por me ouvirem, por me aconselharem e por estarem sempre dispostos a ajudar em tudo o que preciso. Madrinha, Padrinho e avó Rosa, obrigada também a vocês por acreditarem tanto em mim. Obrigada a toda a minha família e a todos os amigos que sempre tiveram uma palavra de apoio para dar.

Bruno, não sei se sem ti teria conseguido chegar onde cheguei mas, mesmo que conseguisse, certamente não seria quem sou hoje. Obrigada por teres percorrido esta estrada comigo…

palavras-chave

Extração líquido-líquido, sistemas aquosos bifásicos, líquidos iónicos, coeficientes de partição, compostos bioativos, bisfenol A, alcaloides.

resumo

O principal objetivo do presente trabalho é estudar a aplicação dos líquidos iónicos (LIs) na formação de sistemas aquosos bifásicos (SAB) e avaliar a sua capacidade para extrair compostos bioativos. Deste modo, este estudo foca essencialmente a procura de sistemas mais benignos, através da aplicação de sais orgânicos, e uma melhor compreensão dos mecanismos que regem a partição de biomoléculas entre as duas fases destes sistemas.

Os SAB constituídos por LIs apresentam uma grande aplicabilidade na extração e purificação de uma vasta gama de compostos, sendo capazes de preservar as suas características. Assim, com o intuito de fomentar os estudos efetuados nesta área, e de melhorar a *performance* destes sistemas, iniciou-se o presente trabalho com a caracterização de SAB compostos por vários LIs e o sal orgânico citrato de potássio. O conjunto de LIs selecionados permitiu estudar o efeito da natureza do anião e do catião central sobre a capacidade de formação destes sistemas. Adicionalmente analisou-se o efeito do tamanho da cadeia alquílica do catião imidazólio e o efeito do pH.

A extração de um conjunto de alcaloides foi efetuada, não apenas para verificar a aplicabilidade dos SAB compostos por LIs e um sal orgânico, mas também para estudar o efeito da agregação dos LIs, e o seu consequente impacto na partição de diferentes biomoléculas. Os resultados obtidos mostraram que a agregação dos LIs tem um efeito significativo e permite uma manipulação das extrações.

Por fim, investigou-se a aplicabilidade dos SAB compostos por LIs na extração e concentração de compostos que apresentam riscos para a saúde humana. Normalmente, a baixa concentração do bisfenol A (um disruptor endócrino) nos fluídos humanos dificulta a sua deteção através de técnicas analíticas convencionais. Estudou-se o efeito do catião central e otimizaram-se as condições de extração. Os resultados obtidos demonstraram uma elevada capacidade de extração por parte dos SAB selecionados e a possibilidade de concentrar até 100 vezes o bisfenol A presente nos fluidos biológicos.

keywords

Liquid-liquid extraction, aqueous two-phase systems, ionic liquids, partition coefficients, bioactive compounds, bisphenol A, alkaloids.

abstract

The main objective of the present work is to study the application of ionic liquids (ILs) in the formation of aqueous two-phase systems (ATPS) and to evaluate their capability in the extraction of bioactive compounds. This study is essentially focused on the finding of more benign systems, making use of organic salts, and in the gathering of a deeper understanding on the mechanisms which rule the partitioning of biomolecules between the coexisting phases of ATPS.

IL-based ATPS display a widespread applicability in the extraction and purification of a large range of compounds, while preserving their characteristics. Thus, with the purpose of fostering the studies conducted in this area and to improve the performance of these systems, this work starts with the characterization of ATPS composed of several ILs and the organic salt potassium citrate. The selected ILs allowed the study of the effect of the anion nature and cation core towards the phase diagrams behavior. Additionally, it was analyzed the influence of the imidazolium cation alkyl side chain length, as well as the pH, in the formation of these systems.

The extraction of a series of alkaloids was carried out not only to verify the applicability of ATPS formed by imidazolium-based ILs and an organic salt, but also to study the effect of the ILs self-aggregation and subsequent impact on the partitioning pathway of different biomolecules. The obtained results show that the self-aggregation of ILs has a significant effect and allows tailored extractions.

Finally, the actual applicability of IL-based ATPS in the extraction and concentration of compounds of human concern from biological fluids was investigated. Usually, the low concentrations of bisphenol A, an endocrine disruptor, in human fluids make it difficult to detect *via* conventional techniques. The effect of the IL cation core was investigated and the extraction conditions were optimized. The results showed a high extraction efficiency and concentration up to 100-fold of bisphenol A from biological fluids.

Contents

List of tables

List of figures

List of symbols

wt % – weight percentage (%);

λ – wavelength (nm);

σ – standard deviation;

Abs – absorbance (dimensionless);

Mw – molecular weight ($g \cdot mol^{-1}$);

K_a – acid dissociation constant ($mol \cdot L^{-1}$);

K_{OW} – octanol-water partition coefficient (dimensionless);

R^2 – correlation coefficient (dimensionless);

α – ratio between the top weight and the total weight of the mixture (dimensionless);

$[IL]$ – concentration of ionic liquid (wt % or $mol \cdot kg^{-1}$);

$[IL]_{\mathrm{IL}}$ – concentration of ionic liquid in ionic liquid-rich phase (wt %);

$[IL]_{\mathrm{Salt}}$ – concentration of ionic liquid in salt-rich phase (wt %);

$[IL]_{\mathrm{M}}$ – concentration of ionic liquid in mixture point (wt %);

$[Salt]$ – concentration of salt (wt % or $mol \cdot kg^{-1}$);

$[Salt]_{\mathrm{IL}}$ – concentration of salt in ionic liquid-rich phase (wt %);

$[Salt]_{\mathrm{Salt}}$ – concentration of salt in salt-rich phase (wt %);

$[Salt]_{\mathrm{M}}$ – concentration of salt in mixture point (wt %);

$[Alk]_{\mathrm{IL}}$ – concentration of an alkaloid in ionic liquid-rich phase (wt %);

$[Alk]_{\mathrm{Salt}}$ – concentration of an alkaloid in salt-rich phase (wt %);

$[X]$ – concentration of compound X (wt %, $g \cdot dm^{-3}$ or $mol \cdot kg^{-1}$);

[BPA] – concentration of bisphenol A ($g \cdot dm^{-3}$);

[Nicotine] – concentration of nicotine ($g \cdot dm^{-3}$);

[Caffeine] – concentration of caffeine ($g \cdot dm^{-3}$);

[Theophylline] – concentration of theophylline ($g \cdot dm^{-3}$);

[Theobromine] – concentration of theobromine ($g \cdot dm^{-3}$);

[K_3PO_4] – concentration of K_3PO_4 (wt %);

[$C_6H_5K_3O_7$] – concentration of $C_6H_5K_3O_7$ (wt % or $mol \cdot kg^{-1}$);

[$C_6H_5K_3O_7/C_6H_8O_7$] – concentration of the buffer $C_6H_5K_3O_7/C_6H_8O_7$ (wt % or $mol \cdot kg^{-1}$);

m_{BPA}^{IL} – amount of bisphenol A in the ionic-liquid-rich phase (g);

m_{BPA}^{Salt} – amount of bisphenol A in the salt-rich phase (g);

$EE_{\mathrm{BPA}}\%$ – percentage extraction efficiencies of bisphenol A (%);

K_{Alk} – partition coefficient of an alkaloid (dimensionless);

K_{Nic} – partition coefficient of nicotine (dimensionless);

K_{Caf} – partition coefficient of caffeine (dimensionless);

K_{Tph} – partition coefficient of theophylline (dimensionless);

K_{Tbr} – partition coefficient of theobromine (dimensionless).

List of abbreviations

ATPS – aqueous two-phase system;

BPA – bisphenol A;

CMC – critical micelle concentration;

DMSO – dimethyl sulfoxide;

ED – electrochemical detector;

ESI – electrospray ionization;

HPLC – high-performance liquid chromatography;

IL – ionic liquid;

MS – mass spectrometry;

MTBE – methyl *t*-butyl ether;

NMR – nuclear magnetic resonance;

SPE – solid-phase extraction;

TL – tie-line;

TLL – tie-line length;

TDI – tolerable daily intake;

TEM – transmission electron microscopy;

UV – ultraviolet;

US – United States;

VOC – volatile organic compound;

$[C_n mim]^+$ – 1-alkyl-3-methylimidazolium cation;

$[C_n mim]Cl$ – 1-alkyl-3-methylimidazolium chloride;

[amim]Cl – 1-allyl-3-methylimidazolium chloride;

$[C_2 mim]Cl$ – 1-ethyl-3-methylimidazolium chloride;

$[OHC_2 mim]Cl$ – 1-hydroxyethyl-3-methylimidazolium chloride;

$[C_4 mpyr]Cl$ – 1-butyl-1-methylpyrrolidinium chloride;

$[C_4 mpip]Cl$ – 1-butyl-1-methylpiperidinium chloride;

$[C_4 mim]Br$ – 1-butyl-3-methylimidazolium bromide;

$[C_4 mim]Cl$ – 1-butyl-3-methylimidazolium chloride;

$[C_4 mim][CH_3CO_2]$ – 1-butyl-3-methylimidazolium acetate;

$[C_4 mim][N(CN)_2]$ – 1-butyl-3-methylimidazolium dicyanamide;

$[C_4 mim][PO_4(CH_3)_2]$ – 1-butyl-3-methylimidazolium dimethylphosphate;

$[C_4 mim][CH_3SO_3]$ – 1-butyl-3-methylimidazolium methanesulfonate;

$[C_4mim][SCN]$ – 1-butyl-3-methylimidazolium thiocyanate;

$[C_4mim][CF_3CO_2]$ – 1-butyl-3-methylimidazolium trifluoroacetate;

$[C_4mim][CF_3SO_3]$ – 1-butyl-3-methylimidazolium trifluoromethanesulfonate;

$[C_4mpy]Cl$ – 1-butyl-3-methylpyridinium chloride;

$[C_6mim]Cl$ – 1-hexyl-3-methylimidazolium chloride;

$[C_7mim]Cl$ – 1 -heptyl-3-methylimidazolium chloride;

$[C_8mim]Cl$ – 1-octyl-3-methylimidazolium chloride;

$[C_{10}mim]Cl$ – 1-decyl-3-methylimidazolium chloride;

$[N_{1112OH}]Cl$ – choline chloride;

$[N_{4444}]Cl$ – tetrabutylammonium chloride;

$[P_{4444}]Cl$ – tetrabutylphosphonium chloride;

$[BF_4]^-$ – tetrafluoroborate anion.

1. General introduction

1.1. Ionic liquids (ILs)

In 1914, when Paul Walden was testing new explosives for the substitution of nitroglycerin, it was synthesized the first ionic liquid (IL), the ethylammonium nitrate ($[CH_3CH_2NH_3][NO_3]$) with a melting point of 12 °C[1]. However, only in 1934, the first patent regarding an industrial application of ILs was filled in the preparation of cellulose solutions, by Charles Graenacher[2]. During the 2nd World War, new patents involving the use of ILs in mixtures of aluminium chloride (III) and 1-ethylpyridinium bromide for the electrodeposition of aluminium were filled[3, 4]. Nevertheless, only in the past few years, with the appearance of air and water stable ILs, the research and development of novel ILs and their possible applications increased significantly. The number of articles concerning ILs, and published between 1990 and 2011, are depicted in Figure 1.

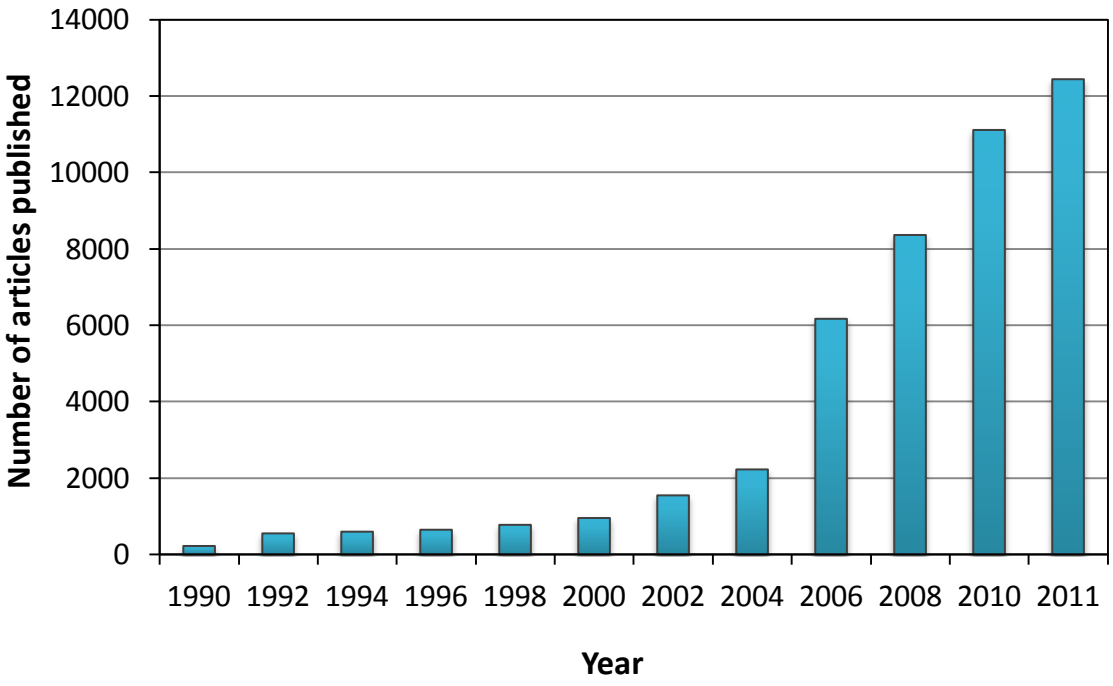

Figure 1. Number of papers published *per* year involving ILs. Values taken from ISI Web of Knowledge in July 04th, 2012.

ILs are salts, liquid at or near room temperature – a resulting characteristic of their low symmetry[5, 6], low intermolecular interactions[7, 8] and ions with a high distribution of charge[9]. ILs are thus only constituted by ionic species, usually a large organic cation and an organic or inorganic anion[10]. The most commonly studied ILs are nitrogen-based and their general cation structures are presented in Figure 2.

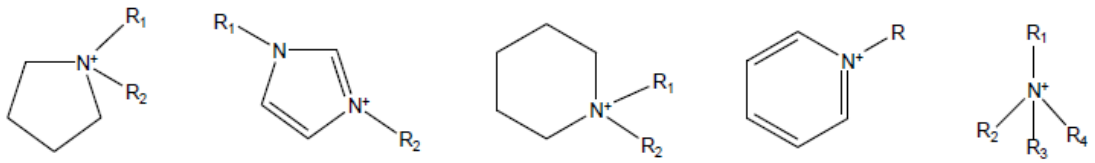

Figure 2. Cation structures of nitrogen-based ILs.

Due to their ionic character, ILs exhibit unique properties, namely negligible vapor pressure, low flammability, high thermal and chemical stabilities, broad liquid temperature range, high ionic conductivity, high solvation ability for organic, inorganic and organometallic compounds, improved selectivity and an easy recycling[11-13]. All these properties made of them improved alternatives to volatile organic compounds (VOCs) in the most diverse applications, such as in biphasic catalysis, in organic synthesis[14], in polymerization[15], in separation and extraction processes[16] and in the dissolution of biomaterials[17]. In fact, nowadays, ILs are used in a wide range of applications, namely in organic chemistry (homogeneous catalysis[18], Heck reaction[19, 20] or Suzuki reaction[21]), as well as in new materials chemistry (electrolytes for the electrochemical industry[22, 23] and liquid crystals[24, 25], for instance). ILs are also a good alternative to the common volatile solvents employed in biocatalysis, since they can provide a non-denaturing environment for biomolecules, maintaining protein structure and enzymatic activity[26, 27].

ILs are commonly described as “designer solvents”, because of the possibility of tuning their properties (such as hydrophobicity and solution behavior, thermophysical properties and variable biodegradation ability or toxicological features) through the manipulation of the type and structure of the ions that compose them aiming at fulfilling a specific application[28-31].

ILs are also described as “green solvents” due to the several physical and chemical advantages that they present over the conventional molecular organic solvents. However, the fact of showing negligible vapor pressure, and consequently reduce the air pollution risks, is not enough to assure that these compounds are in fact “green”. For example, ILs have non-negligible miscibility with water, which can results in contamination of aqueous streams. Thus, in recent years, several studies[32-38] have been focused in the toxicity and biodegradability of ILs. In general, the toxicity of ILs is primordially determined by the cation nature and increases with the increase of the length of the alkyl side chain (increase in hydrophobicity). Nonetheless, it should be stressed that the solubility of ILs in water decreases with their hydrophobicity, what means that

the more toxic ILs present lower water solubilities and the environmental impact of ILs in aquatic streams is thus minimized[34].

1.2. Extraction of biomolecules using aqueous two-phase systems (ATPS)

Separation and purification stages in biotechnological processes usually require numerous steps with high energy and chemical consumption, representing about 60-90 % of the cost of the final product[39, 40]. There have been considerable efforts addressing the development of fast, efficient and cost-effective separation techniques. Liquid–liquid extractions offer advantages, such as high yields, improved purification, better selectivity and a good combination between the recovery and purification steps, while keeping the technological simplicity and a lower associated cost[39, 41]. However, the liquid-liquid extraction of biomolecules is typically carried out making use of VOCs because of their immiscibility with the aqueous media where the biomolecules tend to be produced[42]. Although, these organic compounds present a high volatility and toxicity, as well as the possibility of denaturing enzymes and proteins to be recovered[39].

In 1958, P. A. Albertson introduced aqueous two-phases systems (ATPS) for the separation of biomolecules by their partitioning between two liquid aqueous phases[43]. These systems consist in two aqueous-rich phases and are classified in three main types: polymer/polymer, polymer/salt and salt/salt. In the last few years, liquid-liquid extraction by ATPS has been intensively explored and used to separate and purify several biological products[44-46] and also to recover metal ions, radiochemicals, drugs molecules, dyes, small organic species and inorganic particles from complex mixtures[47, 48].

Recently, a new type of ATPS consisting of hydrophilic ILs and inorganic salts was reported by Gutowski et al.[49]. These systems form above given concentrations of both the IL and inorganic salt in aqueous solutions, and where the spontaneous phase separation occurs. Usually an upper IL-rich phase and a lower salt-rich phase are formed[49]. These new ATPS present additional advantages over typical polymer-based systems, such as low viscosity, quick phase separation, and high and tailored extraction efficiency.

Nowadays it is possible to find a large number of studies regarding the phase behavior of ternary systems composed of ILs + water + inorganic salts[50-56]. The influence of the inorganic ion in the liquid-liquid demixing seems to be well described by the Hofmeister series (ions classification based on their salting-out/-in ability)[57]. It was previously shown that IL-based ATPS are potential extractive systems for distinct compounds, namely testosterone and

epitestosterone[53], alkaloids[54, 58-61] , antibiotics[55, 56], amino acids[51, 52], proteins[62], short chain alcohols[63], aromatic and phenolic compounds[60, 61, 64-66] and metals[67, 68].

In summary, IL-based ATPS are a promising alternative for the extraction of a large variety of biomolecules with an outstanding tailored ability on the extraction efficiencies (that can be achieved by a proper combination of the IL and salt that compose a given system and their concentrations).

1.3. Scope and objectives

Pioneering studies have already demonstrated the potential of IL-based ATPS for the extraction of some added-value compounds[69]. In this context, the main objective of this work is to study the application of novel IL-based systems in the extraction of compounds of human concern, to find more benign systems by substitution of the high charge density salts usually employed, as well as to gather a deeper understanding on the mechanisms which rule the partitioning of biomolecules among the coexisting phases.

The most common IL-based ATPS are formed by ILs, water and inorganic salts. However, there are environmental concerns associated with the use of inorganic salts which tend to be toxic and non-biodegradable. Thus, it is important to find more benign alternatives to IL-based ATPS, such as by substituting the high charge density inorganic salts by biodegradable organic ones. Therefore, a biodegradable and non-toxic organic salt, potassium citrate ($C_6H_5K_3O_7$), was studied here as a main constituent of IL-based ATPS. A large array of novel systems was investigated and proposed by the combination of potassium citrate with 15 ILs. Besides the proposal of novel ternary phase diagrams (and respective tie-lines (TLs) and tie-line lengths (TLLs)), and since ILs with long alkyl side chains were also investigated, the effect of micelles formation and of the pH of the medium towards their extraction ability were also evaluated making use of a series of model alkaloids. All of these tests allowed a deeper analysis, at the molecular level, of the mechanisms which rule the partitioning of charged or non-charged molecules in IL-based ATPS.

The last step of this work addresses the real and prospective application of IL-based ATPS for the extraction of bioactive compounds - substances that have biological activity*, i.e.*, with adverse or beneficial effects on living organisms. Among this class of compounds, bisphenol A (BPA) was selected as a main example due to its serious effects on human health and because it has been identified in several human fluids. Albeit BPA is a ubiquitous compound in the atmosphere, its normally low levels in biological fluids make it difficult to detect *via* conventional techniques. In

this context, several ternary systems composed of ILs, water and K_3PO_4 were evaluated with the goal of finding an improved system capable of completely extracting and concentrating BPA from biological fluids for clinical analysis. The influence of the IL cation core and its alkyl side chain length were investigated. Moreover, aiming at reducing overall costs associated with the consumption of ILs, the influence of the system composition was also investigated. Besides the evaluation of the extraction in model systems, urine-type samples were also studied.

2. IL + H_2O + $C_6H_5K_3O_7$ ternary systems

2.1. Organic salts

IL-based ATPS have great applicability in the design of new "green" and efficient separation technologies for the development of clean manufacturing processes. The most common kosmotropic salts used on the formulation of these systems[49, 50, 53, 54, 70-72] consist of selected cations (ammonium, sodium or potassium) and anions (phosphate, hydroxide, sulfate or carbonate). The high concentration of inorganic salts necessary to induce IL-based ATPS is the cause of some environmental concerns. Nonetheless, in the last years, some authors have been studying the replacement of inorganic salts by biodegradable solutes, such as amino acids[58, 73] and carbohydrates[74-76]. However, these compounds do not have the ability to form ATPS with the most common hydrophilic ILs (such as [C_4mim]Cl[73-76] and [C_4mim]Br[74-76]).

Recent works have introduced biodegradable and non-toxic organic salts, such as the citrate-, tartrate- or acetate-based[77-84] in the formulation of IL-based ATPS. The works dealing with organic salts[77-87] addressed ILs based essentially on the imidazolium cation with the bromide, chloride, and tetrafluoroborate counterions. Besides the water-stable chloride and bromide-based ILs, [BF_4]-based fluids tend to be the most largely explored[77-87] , and it should be remarked that [BF_4]-based ILs are not water stable and form hydrofluoridric acid in aqueous media[88].

Since citrate-based salts are biodegradable and non-toxic, it was studied here a large array of IL-based ATPS, making use of potassium citrate, as "greener" alternatives to the previously studied systems[49, 51, 52, 58, 60, 89-91]. In this work it was evaluated the individual IL cation and anion influences in promoting IL-based ATPS and the impact of the pH towards their phase behavior.

2.2. Experimental section

2.2.1. Chemicals

The ATPS studied in this work were established by using an aqueous solution of potassium citrate tribasic monohydrate, $C_6H_5K_3O_7{\cdot}H_2O$ (≥ 99 wt % pure from Sigma-Aldrich) and different aqueous solutions of hydrophilic ILs. Citric acid monohydrate ($C_6H_8O_7{\cdot}H_2O$), 100 wt % pure from Fisher Scientific, was used for prepare the aqueous solution of the potassium citrate buffer (aqueous mixture of potassium citrate tribasic (94 mol %) and citric acid (6 mol %))[83]. The ILs studied were: 1-butyl-3-methylimidazolium chloride, [C_4mim]Cl (99 wt %); 1-hexyl-3-methylimidazolium chloride, [C_6mim]Cl (> 98 wt %); 1-heptyl-3-methylimidazolium chloride, [C_7mim]Cl (> 98 wt %); 1-octyl-3-methylimidazolium chloride, [C_8mim]Cl (> 98 wt %); 1-decyl-3-methylimidazolium chloride, [C_{10}mim]Cl (> 98 wt %); 1-butyl-3-methylpyridinium

chloride, [C_4mpy]Cl (> 98 wt %); 1-butyl-1-methylpiperidinium chloride, [C_4mpip]Cl (99 wt %); 1-butyl-1-methylpyrrolidinium chloride, [C_4mpyr]Cl (99 wt %); tetrabutylammonium chloride, [N_{4444}]Cl (≥ 97 wt %); tetrabutylphosphonium chloride, [P_{4444}]Cl (98 wt %); 1-butyl-3-methylimidazolium bromide, [C_4mim]Br (99 wt %); 1-butyl-3-methylimidazolium acetate, [C_4mim][CH_3CO_2] (> 98 wt %); 1-butyl-3-methylimidazolium methanesulfonate, [C_4mim][CH_3SO_3] (99 wt %); 1-butyl-3-methylimidazolium trifluoroacetate, [C_4mim][CF_3CO_2] (> 97 wt %); 1-butyl-3-methylimidazolium trifluoromethanesulfonate, [C_4mim][CF_3SO_3] (99 wt %); 1-butyl-3-methylimidazolium dicyanamide, [C_4mim][$N(CN)_2$] (> 98 wt %); 1-butyl-3-methylimidazolium thiocyanate, [C_4mim][SCN] (> 98 wt %); and 1-butyl-3-methylimidazolium dimethylphosphate, [C_4mim][$PO_4(CH_3)_2$] (> 98 wt %). The ILs chemical structures are shown in Figure 3. All imidazolium-, pyridinium- and pyrrolidinium-based ILs were purchased from Iolitec. The [P_{4444}]Cl was kindly supplied by Cytec Industries Inc. and the [N_{4444}]Cl was from Aldrich. To reduce the water and volatile compounds content to negligible values, ILs individual samples were dried under constant stirring at vacuum and moderate temperature (≈ 353 K) for a minimum of 24 h. After this step, the purity of each IL was checked by ^{1}H and ^{13}C NMR spectra and found to be in accordance with the purity given by the suppliers. The water used was ultra-pure water, double distilled, passed by a reverse osmosis system and further treated with a Milli-Q plus 185 water purification apparatus.

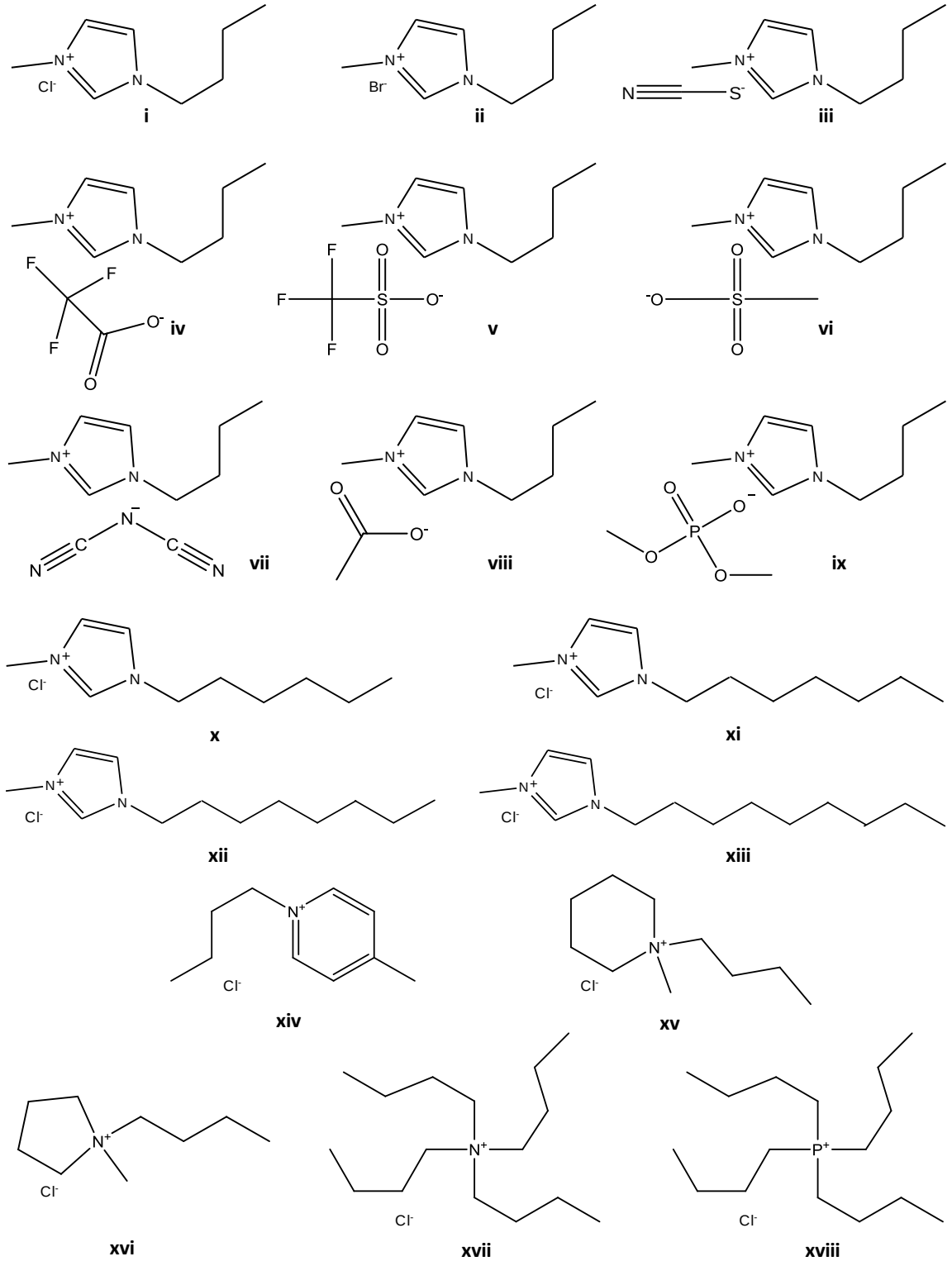

Figure 3. Chemical structures of the ILs studied: (i) $[C_4mim]Cl$; (ii) $[C_4mim]Br$; (iii) $[C_4mim][SCN]$; (iv) $[C_4mim][CF_3CO_2]$; (v) $[C_4mim][CF_3SO_3]$; (vi) $[C_4mim][CH_3SO_3]$; (vii) $[C_4mim][N(CN)_2]$; (viii) $[C_4mim][CH_3CO_2]$; (ix) $[C_4mim][PO_4(CH_3)_2]$; (x) $[C_6mim]Cl$; (xi) $[C_7mim]Cl$; (xii) $[C_8mim]Cl$; (xiii) $[C_{10}mim]Cl$; (xiv) $[C_4mpy]Cl$; (xv) $[C_4mpip]Cl$; (xvi) $[C_4mpyr]Cl$; (xvii) $[N_{4444}]Cl$; (xviii) $[P_{4444}]Cl$.

2.2.2. Experimental procedure

2.2.2.1. Phase diagrams

The binodal curves of the phase diagrams were determined through the cloud point titration method[60] at 298 K (± 1 K) and atmospheric pressure. This procedure was initially validated with the phase diagrams obtained for [C_4mim]Cl + $C_6H_5K_3O_7$ + water, [C_4mim]Br + $C_6H_5K_3O_7$ + water and [C_4mim]Br + $C_6H_5K_3O_7$/$C_6H_8O_7$ + water ternary systems against literature data[79, 82, 83] (*cf.* Appendix A - Figure A 1 and Figure A 2). Aqueous solutions of $C_6H_5K_3O_7$ and of the buffer $C_6H_5K_3O_7$/$C_6H_8O_7$ at 50 wt %, and aqueous solutions of the different hydrophilic ILs at variable concentrations, were prepared gravimetrically and used for the determination of the binodal curves. Repetitive drop-wise addition of the aqueous organic salt solution to each IL aqueous solution was carried out until the detection of a cloudy solution (biphasic region), followed by the drop-wise addition of ultra-pure water until the detection of a clear and limpid solution (monophasic region) (Figure 4). Drop-wise additions were carried out under constant stirring. The ternary system compositions were determined by the weight quantification of all components added within an uncertainty of ± 10^{-4} g.

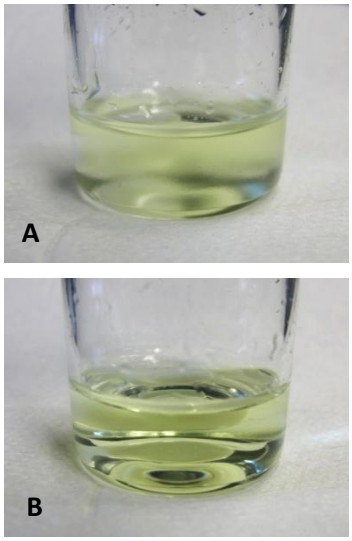

Figure 4. Experimental determination of the binodal curves for IL + $C_6H_5K_3O_7$ ATPS. A) Cloudy solution – biphasic region; B) Limpid and clear solution – monophasic region.

For systems composed of [C_{10}mim]Cl + organic salt + water it was used the turbidometric method[46]. Various and different mixtures of these systems at the biphasic region were initially prepared. Then, under constant stirring, ultra-pure water was added until the detection of a clear and limpid solution (monophasic region). Each mixture corresponds to one point of the binodal curve of the system. The mixture compositions were gravimetrically determined within ± 10^{-4} g.

2.2.2.2. Determination of tie-lines (TLs)

The tie-lines (TLs) were determined by a gravimetric method originally described by Merchuck et al.[92]. A mixture at the biphasic region was gravimetrically prepared with IL + salt + water, vigorously stirred, and allowed to reach the equilibrium by the separation of both phases for at least 12 h at (298 ± 1) K. After the separation step, both top and bottom phases were weighed. Finally, each individual TL was determined by application of the lever-arm rule to the

relationship between the top phase weight and the overall system composition. Experimental binodal curves were fitted using Equation 1[92],

$$[IL] = Aexp[(B[Salt]^{0.5}) - (C[Salt]^3)] \quad (1)$$

where $[IL]$ and $[Salt]$ are, respectively, the IL and salt weight percentages and A, B and C are constants obtained by the regression.

For the determination of TLs it was solved the following system of four equations (Equations 2 to 5) and four unknown values ($[IL]_{\mathrm{IL}}$, $[IL]_{\mathrm{Salt}}$, $[Salt]_{\mathrm{IL}}$ and $[Salt]_{\mathrm{Salt}}$):

$$[IL]_{\mathrm{IL}} = Aexp\left[\left(B[Salt]_{\mathrm{IL}}^{0.5}\right) - \left(C[Salt]_{\mathrm{IL}}^{3}\right)\right] \quad (2)$$

$$[IL]_{\mathrm{Salt}} = Aexp\left[\left(B[Salt]_{\mathrm{Salt}}^{0.5}\right) - \left(C[Salt]_{\mathrm{Salt}}^{3}\right)\right] \quad (3)$$

$$[IL]_{\mathrm{IL}} = \frac{[IL]_{\mathrm{M}}}{\alpha} - \left(\frac{1-\alpha}{\alpha}\right)[IL]_{\mathrm{Salt}} \quad (4)$$

$$[Salt]_{\mathrm{IL}} = \frac{[Salt]_{\mathrm{M}}}{\alpha} - \left(\frac{1-\alpha}{\alpha}\right)[Salt]_{\mathrm{Salt}} \quad (5)$$

The subscripts IL, $Salt$ and M represent the top, bottom and the mixture phases, respectively. The parameter α is the ratio between the top weight and the total weight of the mixture. The solution of the referred system gives the concentration of the IL and salt in the top and bottom phases. For the calculation of the tie-line lengths (TLLs) it was applied Equation 6.

$$TLL = \sqrt{([Salt]_{\mathrm{IL}} - [Salt]_{\mathrm{Salt}})^2 - ([IL]_{\mathrm{IL}} - [IL]_{\mathrm{Salt}})^2} \quad (6)$$

2.2.2.3. pH measurement

The pH values of both the IL-rich and organic-salt-rich aqueous phases were measured at (298 ± 1) K using a METTLER TOLEDO SevenMulti pH meter within an uncertainty of ± 0.02.

2.3. Results and discussion

Novel ternary phase diagrams were determined for several ILs + water + potassium citrate, at 298 K and at atmospheric pressure. The respective ternary phase diagrams are illustrated in

Figure 5 to Figure 9. The experimental weight fraction data of each phase diagram are given at Appendix A (Table A 1 to Table A 14).

The systems composed of potassium citrate, water and [C_4mim]Br or [C_4mim]Cl have already been reported by Zafarani-Moattar and Hamzehzadeh[79, 82, 83]. It should be remarked that a good agreement was observed between literature data and the results obtained in this work[79, 82, 83] (*cf.* Appendix A - Figure A 1 and Figure A 2).

In the studied ATPS, the top phase corresponds to the IL-rich aqueous phase, while the bottom phase is mainly composed of the citrate-based salt. The only exception was observed with the [C_4mim][CF_3SO_3]-based system. This feature was observed before with other salts[51, 52, 91] and is a consequence of the high density of the fluorinated IL.

In Figure 5 to Figure 9, the solubility curves are presented in molality units for a better understanding of the impact of the ILs structure on the phase diagrams behavior, avoiding differences that could result from different molecular weights. In all phase diagrams the biphasic region is localized above the solubility curve. The larger this region, the higher the ability of the IL to undergo liquid-liquid demixing, *i.e.*, the easier the IL is salted-out by the citrate-based salt. The experimental phase diagrams are divided in different figures to allow the individual evaluation of the influence of the cation alkyl side chain length, the cation core, and the anion nature of the diverse ILs through the formation of ATPS.

Figure 5 and Figure 6 depict the effect of the imidazolium alkyl side chain length in the formation of ATPS, at pH 9 and 7, respectively. Aqueous solutions of $C_6H_5K_3O_7$ confer a pH *circa* to 9 to all the systems, whereas an aqueous solution of citrate buffer ($C_6H_5K_3O_7$/$C_6H_8O_7$) confers a pH around 7.

In general, an increase in length of the aliphatic chain of the imidazolium cation facilitates the creation of ATPS. Longer aliphatic chains at the cation contribute to an enhanced hydrophobicity displayed by the IL. Indeed, as the IL becomes more hydrophobic there is a reduction on the water-IL affinity and, therefore, an improved phase separation occurs. Binary liquid-liquid equilibrium data further supports this idea: an increase in the cation side alkyl chain length decreases the solubility of the IL in water[34]. Moreover, this pattern is in close agreement with previous results on IL-based ATPS composed of distinct salts, such as Na_2SO_4 and K_3PO_4[52, 91]. However, the increase of the alkyl side chain length also promotes the IL self-aggregation and supports the superposition of the binodal curves of the systems composed of [C_6mim]Cl, [C_7mim]Cl, [C_8mim]Cl and [C_{10}mim]Cl. This trend is already well documented in literature for ATPS composed of [$C_n$mim]Cl + K_3PO_4[70]. The authors quantitatively[70] evaluated the effect of the alkyl

side chain length of the imidazolium cation making use of salting-out coefficients derived from a Setschenow-type behavior. In general, for the [$C_n$mim]Cl series, the authors[70] concluded that a multifaceted ratio between entropic contributions and the ability of each IL to self-aggregate in aqueous media control the phase behavior of ATPS.

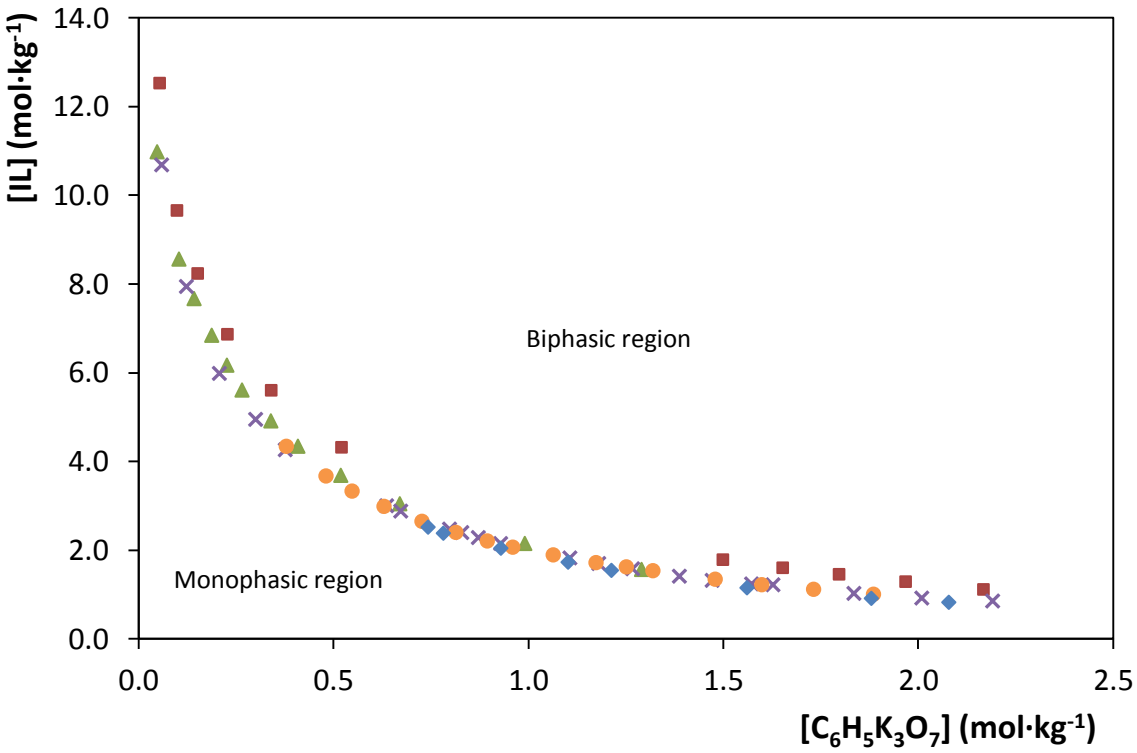

Figure 5. Evaluation of the cation alkyl side chain length in the ternary phase diagrams composed of IL + H_2O + $C_6H_5K_3O_7$ (pH ≈ 9): [C_4mim]Cl (■); [C_6mim]Cl (▲); [C_7mim]Cl (×); [C_8mim]Cl (●); [C_{10}mim]Cl (◆).

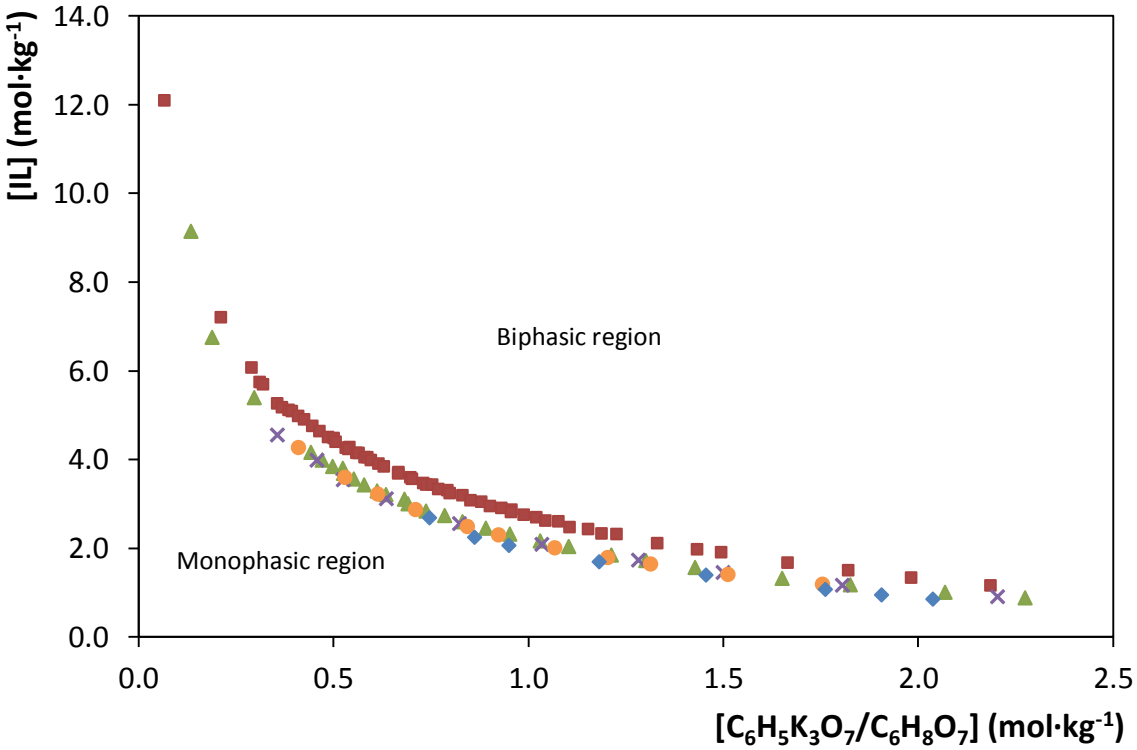

Figure 6. Evaluation of the cation alkyl side chain length in the ternary phase diagrams composed of IL + H_2O + $C_6H_5K_3O_7/C_6H_8O_7$ (pH ≈ 7): [C_4mim]Cl (■); [C_6mim]Cl (▲); [C_7mim]Cl (×); [C_8mim]Cl (●); [C_{10}mim]Cl (◆).

Figure 7 depicts the phase diagrams of a common IL at the two pH values. The phase diagrams of [C_4mim]Cl and [C_{10}mim]Cl at pH 7 and 9 indicate that the pH influence is more relevant in ILs with longer alkyl side chains. However, even for [C_{10}mim]Cl it is almost marginal. The comparison of the systems composed of [C_6mim]Cl, [C_7mim]Cl and [C_8mim]Cl are given in Appendix A (Figure A 3).

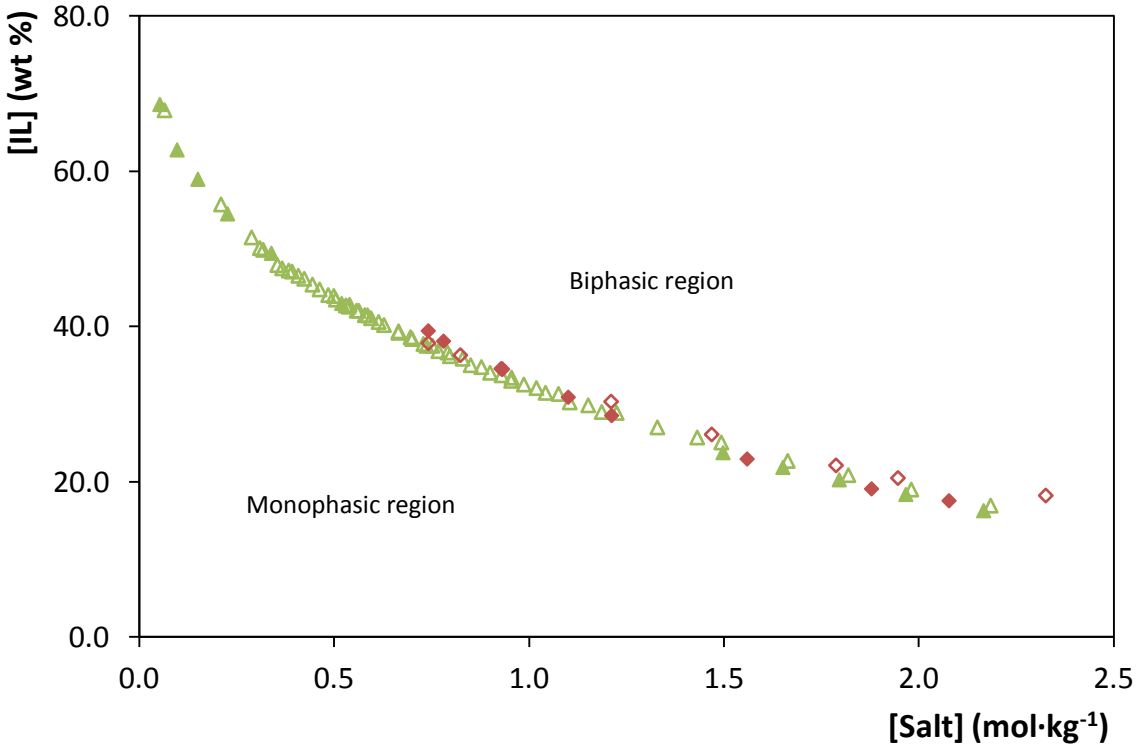

Figure 7. Evaluation of the pH effect in the ternary phase diagrams composed of [C_4mim]Cl + H_2O + $C_6H_5K_3O_7$ (▲); [C_4mim]Cl + H_2O + $C_6H_5K_3O_7$/$C_6H_8O_7$ (△); [C_{10}mim]Cl + H_2O + $C_6H_5K_3O_7$ (◆); [C_{10}mim]Cl + H_2O + $C_6H_5K_3O_7$/$C_6H_8O_7$ (◇). Full symbols correspond to systems with a pH *circa* to 9 while the empty symbols represent the phase diagrams at pH ≈ 7.

It should be stressed that 3 additional ILs were tested according to their ability to form liquid-liquid aqueous phases, namely 1-ethyl-3-methylimidazolium chloride ([C_2mim]Cl), 1-allyl-3-methylimidazolium chloride ([amim]Cl), and 1-hydroxyethyl-3-methylimidazolium chloride ([OHC_2mim]Cl). However, it was not possible to detect the coexisting liquid aqueous phases with these ILs. Only solid-liquid equilibrium was observed. The solid phases were further identified by ^{1}H and ^{13}C NMR spectra and correspond merely to the IL (*cf.* Appendix B). Therefore, it is safe to admit that there is no ion exchange among the studied ILs and the citrate-based salt (at least not above the detection limit of the equipment). Since the potassium citrate has a higher affinity for water, compared to the ILs, there is the preferential exclusion of the IL from the aqueous solution. The reason behind the formation of solid-liquid equilibrium instead of liquid-liquid equilibrium with these ILs is a consequence of their higher melting temperature (85 °C for [C_2mim]Cl[93], 52 °C for [amim]Cl[94], and 86 °C for [OHC_2mim]Cl[95]) compared with the remaining ILs. Indeed, these ILs are more structurally similar to conventional salts and thus present higher melting temperatures.

Despite the immense versatility inherent to the cation-anion permutations in ILs, all authors who explored the use of organic salts in the creation of IL-based ATPS used imidazolium-based compounds[77-87]. The first investigation on the effect of the cation core regarding the formation of ATPS was conducted by Bridges et al.[89] with imidazolium-, pyridinium-, ammonium-, and phosphonium-based cations combined with chloride; yet, salted-out by the salts K_3PO_4, K_2HPO_4, K_2CO_3, KOH and $(NH_4)_2SO_4$. Later on, Ventura et al.[96] compared the influence of imidazolium-, pyridinium-, pyrrolidinium- and piperidinium-based fluids in the formation of ATPS with a phosphate buffer aqueous solution. Therefore, this study constitutes the most complete evaluation of the IL cation effect on ATPS formation for a common organic salt.

The effect of the cation core is displayed in Figure 8. The IL cation ability to form ATPS, for instance at 0.5 mol·kg^{-1} of potassium citrate, follows the order: $[P_{4444}]^+ > [N_{4444}]^+ >> [C_4mpy]^+ \approx [C_4mpip]^+ > [C_4mpyr]^+ > [C_4mim]^+$. This trend reflects the aptitude of the IL cation to be solvated by water (since the chloride anion is the counterion common to all ILs), and which is regulated by steric and entropic contributions[34, 96]. This trend follows the hydrophobic sequence of the IL cations. Quaternary phosphonium- and ammonium-based cations are those that present the higher ability to form ATPS since they present four butyl chains which are responsible for their higher hydrophobicity. Their water miscibility essentially results from the strong solvation of the chloride anion. From the comparison among the cyclic nitrogen-based ILs, it is clear that the 6-sided ring cations, such as pyridinium and piperidinium, are more able to induce ATPS when compared with the smaller 5-sided rings of imidazolium and pyrrolidinium. Hence, the inherent hydrophobicity of the cation, which is also ruled by their carbon number, is the main factor behind the ability of these compounds to form ATPS. The trends obtained here are in agreement with the results previously reported for additional IL-based ATPS composed of different salts[96] and also correlate with the solubility of these ILs in water[97]. From the results obtained it is evident that a large number of combinations of IL cations can be employed in the formation of IL-based ATPS, and that these systems allow the tailoring of the phases' polarities aiming at performing specific extractions.

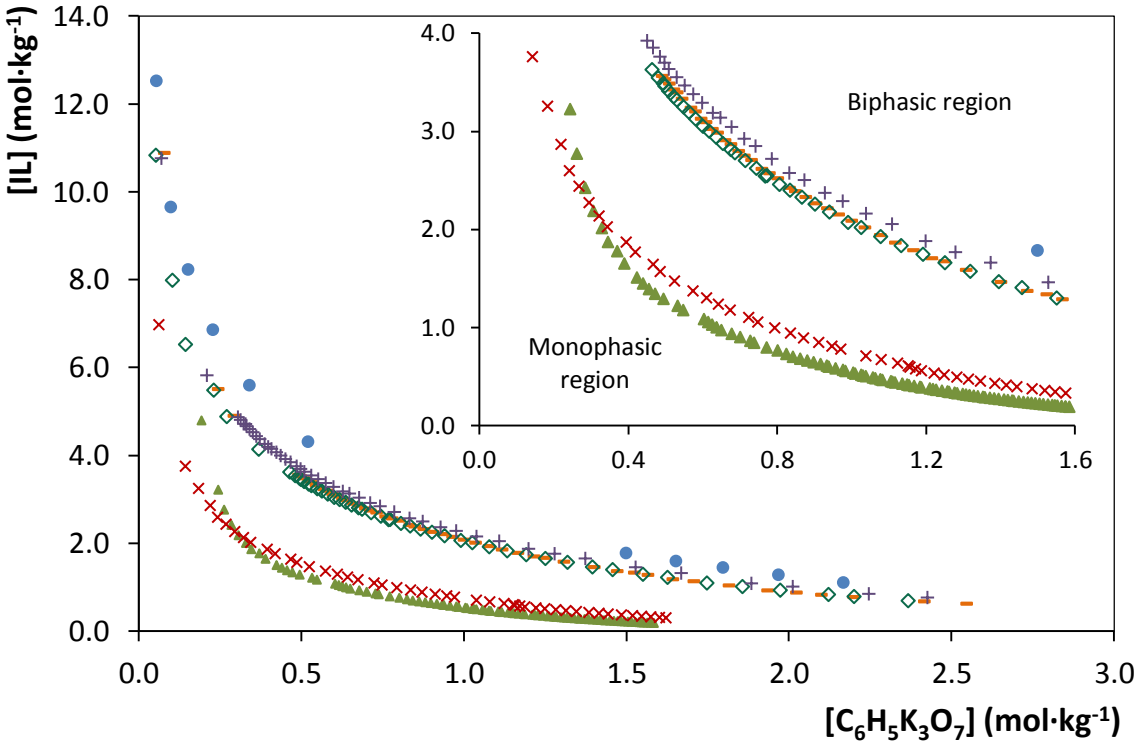

Figure 8. Evaluation of the cation core in the ternary phase diagrams composed of IL + H_2O + $C_6H_5K_3O_7$: $[C_4mim]Cl$ (●), $[C_4mpip]Cl$ (◇), $[C_4mpyr]Cl$ (+), $[C_4mpy]Cl$ (-), $[P_{4444}]Cl$ (▲), $[N_{4444}]Cl$ (×).

The effect of the anion nature on the ATPS phase behavior was studied with several ILs containing the common $[C_4mim]^+$ cation, while combined with the following anions: Cl^-, Br^-, $[CH_3SO_3]^-$, $[CH_3CO_2]^-$, $[CF_3SO_3]^-$, $[CF_3CO_2]^-$, $[SCN]^-$, $[N(CN)_2]^-$, and $[PO_4(CH_3)_2]^-$. The corresponding ternary phase diagrams are depicted in Figure 9 which reveals that a large number of ILs constituted by different anions can be combined with organic salts besides the chloride-, bromide-, and tetrafluoroborate-based fluids commonly investigated[77-87]. At 0.5 mol·kg^{-1} of potassium citrate, the IL anion ability to form ATPS is as follows: $[CH_3CO_2]^-$ < $[PO_4(CH_3)_2]^-$ < $[CH_3SO_3]^-$ < Cl^- << Br^- < $[CF_3CO_2]^-$ << $[N(CN)_2]^-$ < $[SCN]^-$ < $[CF_3SO_3]^-$. This rank is in close agreement with previous works using inorganic salts such as K_3PO_3[51] and Na_2SO_4[91]. The good agreement on the anion trend observed among systems constituted by different salts suggests that the IL ability for creating ATPS is not affected by the salt nature or the pH of the aqueous salt solution employed.

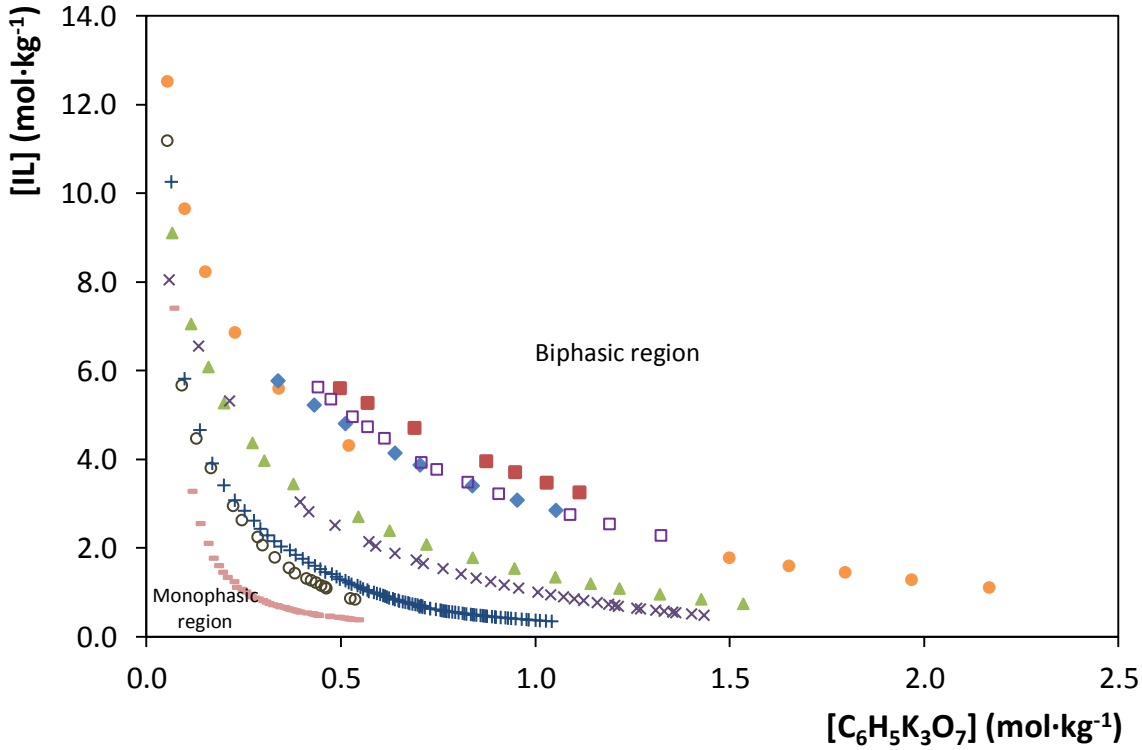

Figure 9. Evaluation of the anion nature in the ternary phase diagrams composed of IL + H_2O + $C_6H_5K_3O_7$: [C_4mim][CF_3SO_3] (–); [C_4mim][SCN] (○); [C_4mim][$N(CN)_2$] (+); [C_4mim][CF_3CO_2] (×); [C_4mim]Br (▲); [C_4mim]Cl (●); [C_4mim][CH_3SO_4] (◆); [C_4mim][$PO_4(CH_3)_2$] (□); [C_4mim][CH_3CO_2] (■).

The anions of ILs compete with the salt ions for the formation of hydration complexes. Usually this competition is won by the ions with a higher charge density, *i.e.*, ions that are capable of stronger interactions with water. For a common cation, ILs composed of anions with lower hydrogen bond basicity are more able to form ATPS. In this context, a close agreement was identified between the ILs ability to form ATPS and their hydrogen bond basicity values determined by solvatochromic probes[98], and as previously identified by Coutinho and co-workers[51, 91]. Moreover, the fluorination of the anions, which further implies a lower ability of the anion for hydrogen-bonding, leads to an enhanced capability of the IL to undergo liquid-liquid demixing. For instance, [C_4mim][CF_3CO_2] and [C_4mim][CF_3SO_3] are more easily salted-out than [C_4mim][CH_3CO_2] and [C_4mim][CH_3SO_3], respectively. Therefore, fluorinated ILs require a less amount of salt to form two aqueous liquid phases.

For the studied systems, the experimental binodal data were further fitted by the empirical relationship described by Equation 1. The regression parameters were estimated by the least-squares regression method, and their values and corresponding standard deviations (σ) are

provided in Table 1. In general, good correlation coefficients were obtained for all systems, indicating that these fittings can be used to predict data in a given region of the phase diagram where no experimental results are available.

The experimental TLs, along with their respective length (TLL), are reported in Table 2 and Table 3. An example of the TLs obtained is depicted in Figure 10. In general, the TLs are closely parallel to each other.

Table 1. Correlation parameters used to describe the experimental binodals data by Equation 1.

IL	$A \pm \sigma$	$B \pm \sigma$	$10^5(C \pm \sigma)$	R^2
IL + $C_6H_5K_3O_7$ ATPS				
[C_4mim]Cl	86.0 ± 0.5	-0.180 ± 0.003	0.84 ± 0.03	0.9998
[C_4mim]Br	92.4 ± 0.6	-0.228 ± 0.003	1.87 ± 0.06	0.9997
[C_4mim][CF_3SO_3]	208.8 ± 5.0	-0.829 ± 0.012	1.00 ± 1.44	0.9968
[C_4mim][CF_3CO_2]	93.7 ± 1.9	-0.222 ± 0.008	3.40 ± 0.15	0.9958
[C_4mim][SCN]	120.9 ± 4.3	-0.470 ± 0.019	13.34 ± 2.37	0.9951
[C_4mim][$N(CN)_2$]	121.8 ± 1.8	-0.444 ± 0.006	6.56 ± 0.24	0.9968
[C_4mim][CH_3SO_3]	85.0 ± 2.8	-0.123 ± 0.010	1.02 ± 0.15	0.9987
[C_4mim][CH_3CO_2]	82.6 ± 3.7	-0.117 ± 0.013	0.95 ± 0.13	0.9994
[C_4mim][$PO_4(CH_3)_2$]	112.2 ± 2.2	-0.179 ± 0.006	0.54 ± 0.05	0.9996
[C_6mim]Cl	85.9 ± 1.0	-0.173 ± 0.005	1.61 ± 0.14	0.9983
[C_7mim]Cl	93.0 ± 0.9	-0.206 ± 0.004	0.82 ± 0.04	0.9994
[C_8mim]Cl	108.8 ± 1.0	-0.238 ± 0.003	0.64 ± 0.02	0.9999
[C_{10}mim]Cl	131.9 ± 9.7	-0.272 ± 0.018	0.57 ± 0.07	0.9997
[C_4mpip]Cl	87.1 ± 0.3	-0.210 ± 0.001	0.85 ± 0.01	0.9997
[C_4mpyr]Cl	87.8 ± 0.5	-0.214 ± 0.002	0.74 ± 0.02	0.9993
[C_4mpy]Cl	94.3 ± 0.4	-0.232 ± 0.001	0.80 ± 0.01	0.9996
[P_{4444}]Cl	170.0 ± 5.7	-0.484 ± 0.011	1.64 ± 0.14	0.9944
[N_{4444}]Cl	99.3 ± 0.9	-0.318 ± 0.003	1.79 ± 0.06	0.9990
IL + $C_6H_5K_3O_7$/$C_6H_8O_7$ ATPS				
[C_4mim]Cl	88.1 ± 0.3	-0.190 ± 0.001	0.71 ± 0.01	0.9995
[C_6mim]Cl	99.5 ± 1.0	-0.224 ± 0.003	0.69 ± 0.03	0.9990
[C_7mim]Cl	98.2 ± 2.0	-0.216 ± 0.006	0.68 ± 0.04	0.9996
[C_8mim]Cl	104.7 ± 1.3	-0.222 ± 0.003	0.68 ± 0.02	0.9999
[C_{10}mim]Cl	115.7 ± 23.0	-0.236 ± 0.047	0.70 ± 0.20	0.9958

Table 2. Experimental data for TLs and TLLs of IL + $C_6H_5K_3O_7$ ATPS.

IL	Weight fraction composition (wt %)								TLL
	$[IL]_{IL}$	$[Salt]_{IL}$	pH_{IL}	$[IL]_{M}$	$[Salt]_{M}$	$[IL]_{Salt}$	$[Salt]_{Salt}$	pH_{Salt}	
[C_4mim]Cl	41.26	15.32	9.18	26.68	29.92	13.04	43.59	9.06	39.94
	52.68	7.33	9.00	39.74	20.35	5.83	54.47	8.98	66.46
	56.57	5.39	8.99	42.82	19.08	4.57	57.16	9.07	73.37
[C_4mim]Br	60.81	3.36	9.19	29.92	24.91	5.14	42.20	9.23	67.87
	73.40	1.02	9.52	40.01	25.03	1.07	53.04	9.04	89.08
[C_4mim][CF_3SO_3]	98.08	0.83	8.60	15.04	14.99	7.00	16.36	8.68	92.39
	73.16	1.60	8.95	24.93	10.18	10.64	12.72	8.60	63.50
[C_4mim][SCN]	56.77	2.57	7.79	14.93	15.05	9.61	16.64	7.84	49.21
	75.97	0.98	7.71	14.93	20.03	1.85	24.71	7.95	77.65
[C_4mim][$N(CN)_2$]	47.57	4.43	8.76	21.82	15.14	9.67	20.19	8.83	41.05
	52.21	3.62	8.80	24.70	15.13	6.98	22.55	8.68	49.03
	58.81	2.68	8.87	29.95	14.97	3.98	26.04	8.66	59.60
[C_4mim][CH_3SO_3]	61.89	6.49	9.36	36.88	29.91	2.95	61.68	8.93	80.74
[C_6mim]Cl	46.52	11.53	8.48	23.46	29.90	8.89	41.53	8.48	48.1
	48.55	10.20	8.28	36.92	20.01	4.93	47.00	8.24	57.07
	54.20	6.90	8.39	44.89	15.02	2.62	51.86	8.88	68.43
[C_7mim]Cl	51.43	8.15	7.43	34.97	24.00	7.62	50.33	7.64	60.82
	56.66	5.75	7.77	34.96	25.98	6.33	52.68	7.79	68.82
[C_8mim]Cl	39.49	17.02	9.15	27.03	29.87	11.97	45.40	9.20	39.53
	47.50	11.82	8.34	33.12	25.84	10.00	48.40	8.33	52.38
	58.37	6.80	8.44	36.91	25.91	8.16	51.51	8.50	67.22
[C_{10}mim]Cl	38.70	19.03	8.28	27.75	29.89	13.09	44.42	8.39	36.06
[C_4mpip]Cl	49.13	7.38	9.41	32.05	24.96	5.83	51.94	9.29	62.13
	59.43	3.32	9.61	43.00	19.96	2.44	61.04	9.49	81.11
[C_4mpyr]Cl	54.34	4.99	9.41	39.93	19.92	4.54	56.62	10.09	71.73
	55.52	4.56	9.31	41.98	18.59	4.07	57.86	11.04	74.08
[C_4mpy]Cl	45.12	9.90	8.31	30.03	25.05	8.70	46.47	8.23	51.61
	55.51	5.20	8.18	34.76	25.10	5.04	53.61	8.18	69.94
[P_{4444}]Cl	39.56	8.94	7.99	30.06	14.96	8.93	28.33	7.86	36.25
	50.66	6.23	8.32	34.80	15.21	7.14	30.88	8.22	50.01
[N_{4444}]Cl	42.92	6.86	8.81	26.97	20.05	5.19	38.07	8.95	48.96
	52.43	4.02	9.12	31.81	20.18	3.08	42.70	9.03	62.70

Table 3. Experimental data for TLs and TLLs of IL + $C_6H_5K_3O_7$/$C_6H_8O_7$ ATPS.

IL	Weight fraction composition (wt %)								TLL
	$[IL]_{IL}$	$[Salt]_{IL}$	pH_{IL}	$[IL]_{M}$	$[Salt]_{M}$	$[IL]_{Salt}$	$[Salt]_{Salt}$	pH_{Salt}	
	41.44	14.80	7.13	27.04	29.97	13.11	44.65	7.11	41.16
$[C_4mim]Cl$	48.17	9.86	7.19	28.99	30.01	8.47	51.56	7.09	57.58
	54.85	6.17	7.34	40.67	20.87	5.39	57.45	7.41	71.25
	37.80	17.27	7.01	25.89	29.99	11.65	45.19	7.06	38.25
$[C_6mim]Cl$	45.15	12.03	7.06	31.71	25.78	9.52	48.46	7.08	50.96
	54.19	7.28	7.13	35.13	25.92	6.48	53.94	7.33	66.74
	42.99	14.00	6.85	27.03	29.97	13.43	43.57	6.93	41.81
$[C_7mim]Cl$	48.24	10.61	6.85	34.89	23.92	9.63	49.12	6.86	54.54
	55.24	7.05	7.05	35.31	26.24	7.24	53.26	7.11	66.63
	43.75	14.69	6.94	27.58	29.96	15.37	41.48	6.89	39.03
$[C_8mim]Cl$	52.11	9.70	7.00	34.99	26.01	8.49	51.26	7.06	60.24
	63.92	4.92	7.15	40.08	26.01	5.81	56.32	7.37	77.57
	42.56	16.79	6.84	33.49	24.96	15.99	40.71	6.72	35.75
$[C_{10}mim]Cl$	43.47	16.18	7.16	28.19	29.99	14.89	42.03	7.17	38.53
	43.73	16.01	6.84	33.30	25.44	14.74	42.21	6.73	39.08

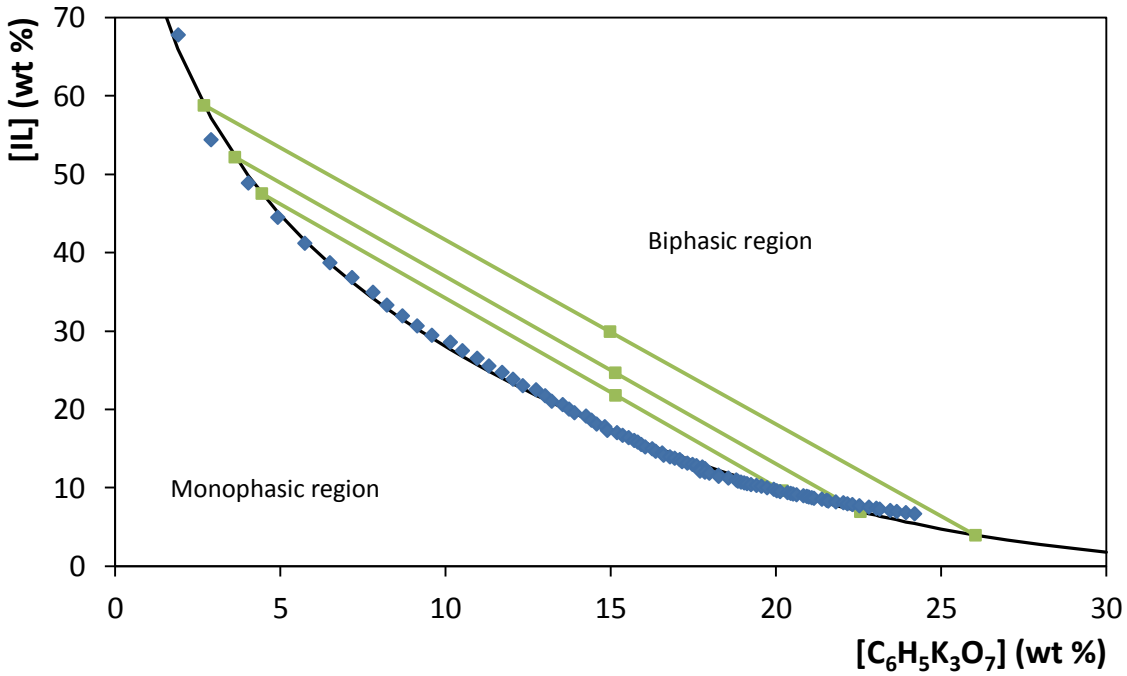

Figure 10. Phase diagram for the ternary system composed of $[C_4mim][N(CN)_2]$ + $C_6H_5K_3O_7$ + H_2O: binodal curve data (◆); TL data (■); adjusted binodal data through Equation 1 (—).

The pH values of both phases in each ATPS, and for the compositions for which the TLs were determined, are given in Table 2 and Table 3. The pH values of the systems composed of IL + $C_6H_5K_3O_7$ + H_2O are in the alkaline region (pH = 8 - 10) and indicate their possible applicability for the extraction of a given (bio)molecule. Since an aqueous solution at 50 wt % of potassium citrate presents a pH value of *circa* 9.2, the differences observed in the pH values are due to the presence of the ILs in the aqueous media. The pH values of the systems composed of IL + $C_6H_5K_3O_7$/$C_6H_8O_7$ + H_2O are neutral (pH ≈ 7) and differences promoted by ILs are not observed in the buffered systems.

2.4. Conclusions

In this section novel phase diagrams for ATPS, TLs and TLLs were determined, making use of a large range of ILs, a biodegradable organic salt and water. The large array of ILs investigated and the distinct phase behaviors observed indicate that the tailoring of the phases' polarities can be properly achieved. In general, an increase in the IL hydrophobicity facilitates the formation of ATPS. The pH effect was evaluated in parallel with the effect of the cation alkyl side chain length and it was found to be negligible.

3. Extraction of alkaloids: self-aggregation in IL-based ATPS

3.1. Self-aggregation in IL-based ATPS

ILs based on 1-alkyl-3-methylimidazolium cation ($[C_n mim]^+$) are structurally similar to ionic surfactants (Figure 11). Due to their amphiphilic nature, related to their molecular structure which consists of a charged hydrophilic head group (imidazolium cation) and one hydrophobic tail (alkyl side chain), they present surface activity in solution and undergo micelle formation. In fact, several authors have already shown the ILs micelle formation in aqueous solutions[99-106].

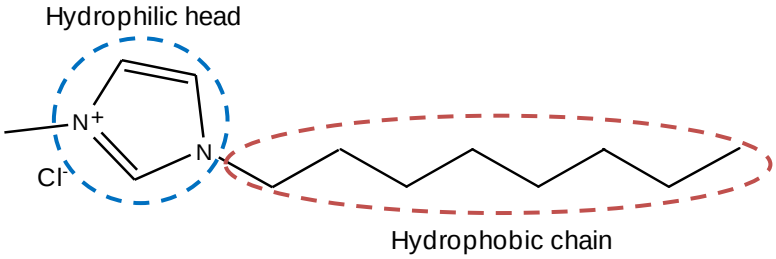

Figure 11. Chemical structure of 1-decyl-3-methylimidazolium chloride ($[C_{10}mim]Cl$).

The possibility of tuning and changing the physical properties of ILs, such as their hydrophobicity, make of these compounds a new class of surfactants with unique abilities. For example, the critical micelle concentration (CMC), *i.e.*, the concentration of IL for which the micelle formation occurs, strongly depends on the IL hydrophobicity, which can be controlled by the alkyl side chain length[10]. It has been reported that in the case of 1-alkyl-3-methylimidazolium chloride ($[C_n mim]Cl$) ILs the micelle formation takes place in solutions containing the ILs with longer alkyl chains (larger than hexyl)[10]. However, to the best of our knowledge, the formation of micelles in 1-heptyl-3-methylimidazolium ($[C_7 mim]Cl$) has not been studied yet, and was only reported for systems composed of $[C_8 mim]Cl$[10]. Besides the common micelles formation, the formation of reverse micelles in an IL continuous phase, using common surfactants, has also been reported[107, 108]. Reverse micelles are water droplets stabilized in non-polar solvents by a layer of surfactant molecules. This type of micelles have a large range of applications, such as media for biocatalysis [109], drugs delivery[110], protein refolding[111], nanomaterial synthesis[112], etc.

Micelle-mediated extraction can be used to increase or decrease the extraction efficiencies of a given molecule[113, 114]. Indeed, Cláudio et al.[64, 65] and Freire et al.[59] have already reported different patterns in the extraction of several (bio)molecules, making use of IL-based ATPS, with an increase in the cation alkyl side chain length of the IL. Albeit the turnover on the trends was attributed to micelle formation, no major conclusions were provided and a molecular based

scenario of the phenomenon ruling the micelle-mediated extractions was far from being achieved[59, 64, 65].

The main aim of the present section is to investigate the partitioning of a series of model alkaloids and in which extent the micelles formation in IL-based ATPS can affect their partitioning. Thus, the extraction of four alkaloids (nicotine, caffeine, theophylline and theobromine) was carried out in ATPS composed of [$C_n$mim]Cl (*n* = 4, 6, 7, 8 and 10), potassium citrate or potassium citrate – citric acid buffer (to confer different pH values in the medium) and water. The molecular structures of the studied alkaloids are presented in Figure 12 and their main physicochemical properties in Table 4.

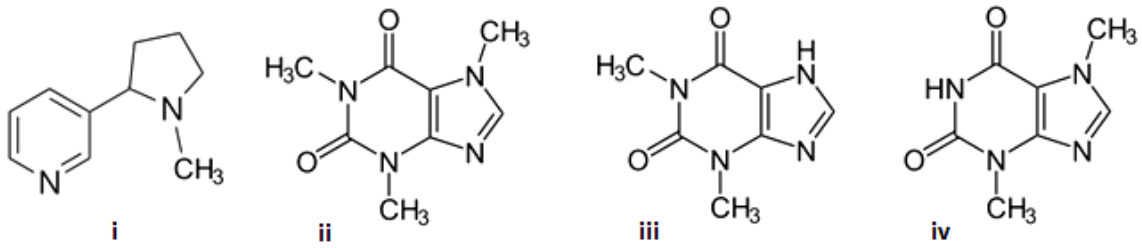

Figure 12. Molecular structures of (i) nicotine, (ii) caffeine, (iii) theophylline and (iv) theobromine.

Table 4. Thermophysical properties of the studied alkaloids[115-118].

	Nicotine	Caffeine	Theophylline	Theobromine
Molecular Weight ($g \cdot mol^{-1}$)	162.23	194.19	180.16	180.16
Melting Temperature (K)	194	511	546	630
Boiling Temperature (K)	520	----	----	----
Solubility in Water at 298 K ($g \cdot dm^{-3}$)	Completely miscible	21.60	7.36	0.33
logK_{OW}	1.17	-0.07	-0.02	-0.81
pK_a at 298 K	3.12 – 8.02	0.6 - 14	3.5 – 8.6	0.12 – 10.5

This group of four alkaloids was selected because they allow the study of a large range of hydrophobicities as well as the manipulation of their charged or non-charged forms at different pH values.

3.2. Experimental section

3.2.1. Chemicals

The ATPS studied in this work were established by using the organic salt potassium citrate tribasic monohydrate ($C_6H_5K_3O_7 \cdot H_2O$), ≥ 99 wt % pure from Sigma-Aldrich, the potassium citrate buffer (an aqueous mixture of tri-potassium citrate monohydrate and citric acid monohydrate ($C_6H_8O_7 \cdot H_2O$), 100 wt % pure, from Fisher Scientific) and different aqueous solutions of hydrophilic ILs. The ILs studied were: 1-butyl-3-methylimidazolium chloride, [C_4mim]Cl (99 wt %), 1-hexyl-3-methylimidazolium chloride, [C_6mim]Cl (> 98 wt %), 1-heptyl-3-methylimidazolium chloride, [C_7mim]Cl (> 98 wt %), 1-octyl-3-methylimidazolium chloride, [C_8mim]Cl (> 98 wt %) and 1-decyl-3-methylimidazolium chloride, [C_{10}mim]Cl (> 98 wt %). The ILs molecular structures are shown in Figure 13. All ILs used in this work were supplied by Iolitec. To reduce the impurities content to negligible values, ILs individual samples were dried under constant stirring at vacuum and moderate temperature (≈ 353 K) for a minimum of 24 h. After this procedure, the purity of each IL was checked by ^{1}H and ^{13}C NMR spectra. The nicotine, ≥ 99.0 wt % pure, was supplied from Fluka, caffeine, > 98.5 wt % pure, was acquired at Marsing & Co. Ltd. A/S. and theophylline (≥ 99 wt %) and theobromine (≥ 99.0 wt %) were from Sigma. The water used was ultra-pure water, double distilled, passed by a reverse osmosis system and further treated with a Milli-Q plus 185 water purification apparatus.

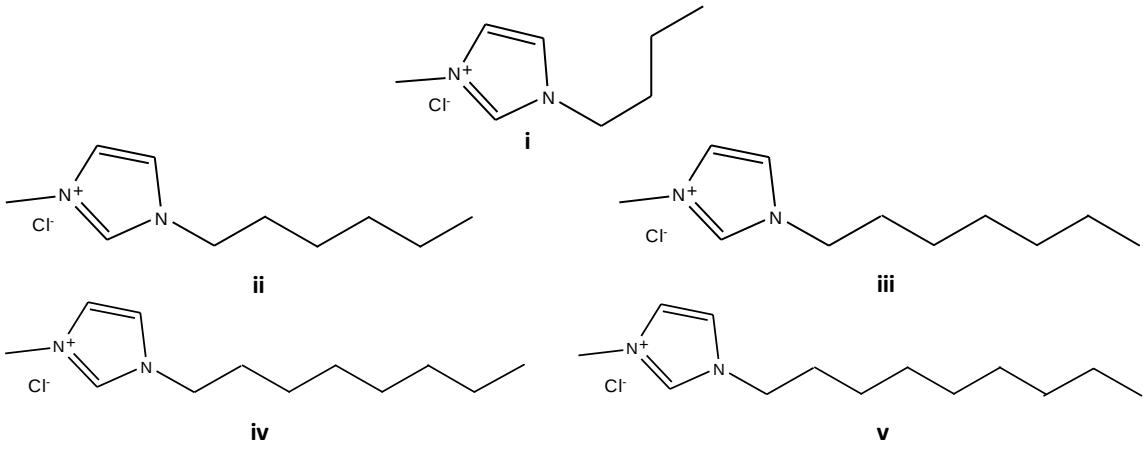

Figure 13. Chemical structures of the ILs studied: (i) [C_4mim]Cl; (ii) [C_6mim]Cl; (iii) [C_7mim]Cl; (iv) [C_8mim]Cl; (v) [C_{10}mim]Cl.

3.2.2. Experimental procedures

3.2.2.1. Partitioning of alkaloids

Aqueous solutions of each alkaloid were prepared with the following concentrations: 0.76 g·dm^{-3} (4.7 × 10^{-3} mol·dm^{-3}) for nicotine, 0.91 g·dm^{-3} (4.7 × 10^{-3} mol·dm^{-3}) for caffeine, 0.85 g·dm^{-3} (4.7 × 10^{-3} mol·dm^{-3}) for theophylline, 0.20 g·dm^{-3} (1.1 × 10^{-3} mol·dm^{-3}) for theobromine. At these concentrations, all alkaloids can be considered at infinite dilution and completely solvated in aqueous media, avoiding thus specific interactions between biomolecules.

Figure 14. ATPS formed by IL + $C_6H_5K_3O_7$/$C_6H_8O_7$ + H_2O.

The ternary mixtures compositions were chosen based on the phase diagrams determined before for each IL-$C_6H_5K_3O_7$/$C_6H_8O_7$ and IL-$C_6H_5K_3O_7$ systems. Moreover, to avoid discrepancies in the results which could arise from the different compositions of the phases, all the partitioning studies were performed at a constant TLL. The mixture compositions which correspond to a TLL of 40 are as follows: 27 wt % of [C_4mim]Cl + 30 wt % of $C_6H_5K_3O_7$/$C_6H_8O_7$, 26 wt % of [C_6mim]Cl + 30 wt % of $C_6H_5K_3O_7$/$C_6H_8O_7$, 27 wt % of [C_7mim]Cl + 30 wt % of $C_6H_5K_3O_7$/$C_6H_8O_7$, 27.5 wt % of [C_8mim]Cl + 30 wt % of $C_6H_5K_3O_7$/$C_6H_8O_7$, 28.2 wt % of [C_{10}mim]Cl + 30 wt % of $C_6H_5K_3O_7$/$C_6H_8O_7$, 26.8 wt % of [C_4mim]Cl + 30 wt % of $C_6H_5K_3O_7$, 23.5 wt % of [C_6mim]Cl + 30 wt % of $C_6H_5K_3O_7$, 27 wt % of [C_8mim]Cl + 30 wt % of $C_6H_5K_3O_7$, and 27.8 wt % of [C_{10}mim]Cl + 30 wt % of $C_6H_5K_3O_7$.

For each system the composition of the coexisting aqueous phases and respective pH values are presented in Table 2 and Table 3 of Section 2.

Each mixture was vigorously stirred and left to equilibrate for at least 12 h (a time period established in previous optimizing experiments), to achieve the complete partitioning of each alkaloid between the two phases. For all the ternary mixtures evaluated, and at the compositions used, the IL-rich aqueous phase is the top layer while the salt-rich aqueous phase corresponds to the bottom layer, as shown in Figure 14. After a careful separation of both phases, the alkaloids quantification in each phase was carried by UV-spectroscopy, using a SHIMADZU UV-1700, Pharma-Spec Spectrometer, at a wavelength of 260 nm for nicotine, 272 nm for theophylline and 273 nm for caffeine and theobromine using calibration curves previously established (*cf.* Appendix C - Figure C 1 to Figure C 4). At least three individual samples of each phase were quantified in order to determine the average in the alkaloids partition coefficients and the respective standard

deviations. Possible interferences of the organic salt and ILs with the analytical method were investigated. Blank control samples were always used. The stability of the alkaloids in the coexisting phases of all systems was also confirmed and it is safe to admit that all the biomolecules are stable up to at least 72 h.

The partition coefficients of studied biomolecules, K_{Nic} for nicotine, K_{Caf} for caffeine, K_{Tph} for theophylline and K_{Tbr} for theobromine are defined as the ratio of the concentration of the each biomolecule in the IL to that in the salt aqueous-rich phases according to Equation 7,

$$K_{\mathrm{Alk}} = \frac{[Alk]_{\mathrm{IL}}}{[Alk]_{\mathrm{Salt}}} \tag{7}$$

where $[Alk]_{\mathrm{IL}}$ and $[Alk]_{\mathrm{Salt}}$ are the concentration of each alkaloid in the IL- and in the salt-rich aqueous phases, respectively.

3.2.2.2. Characterization of micelles

The formation of micelles in the studied IL-based ATPS was qualitatively evaluated by microscopy using a microscope OLYMPUS BX51. Both aqueous phases of each system, with the same composition of mixtures used for the extraction, were analyzed.

3.3. Results and discussion

In Figure 15 and Figure 16 are depicted the results obtained for the partition coefficients of alkaloids in the several IL-based ATPS, at a common TTL ≈ 40, and at different pH values in the aqueous media.

The partition coefficients of caffeine, theophylline and theobromine are presented in Figure 15. The application of citrate buffer ($C_6H_5K_3O_7/C_6H_8O_7$) confers to the ATPS a pH equal to 7. At this pH value the alkaloids listed are predominantly in a non-charged form as can be seen in the dissociation curves shown in Appendix D (Figure D 1 to Figure D 4).

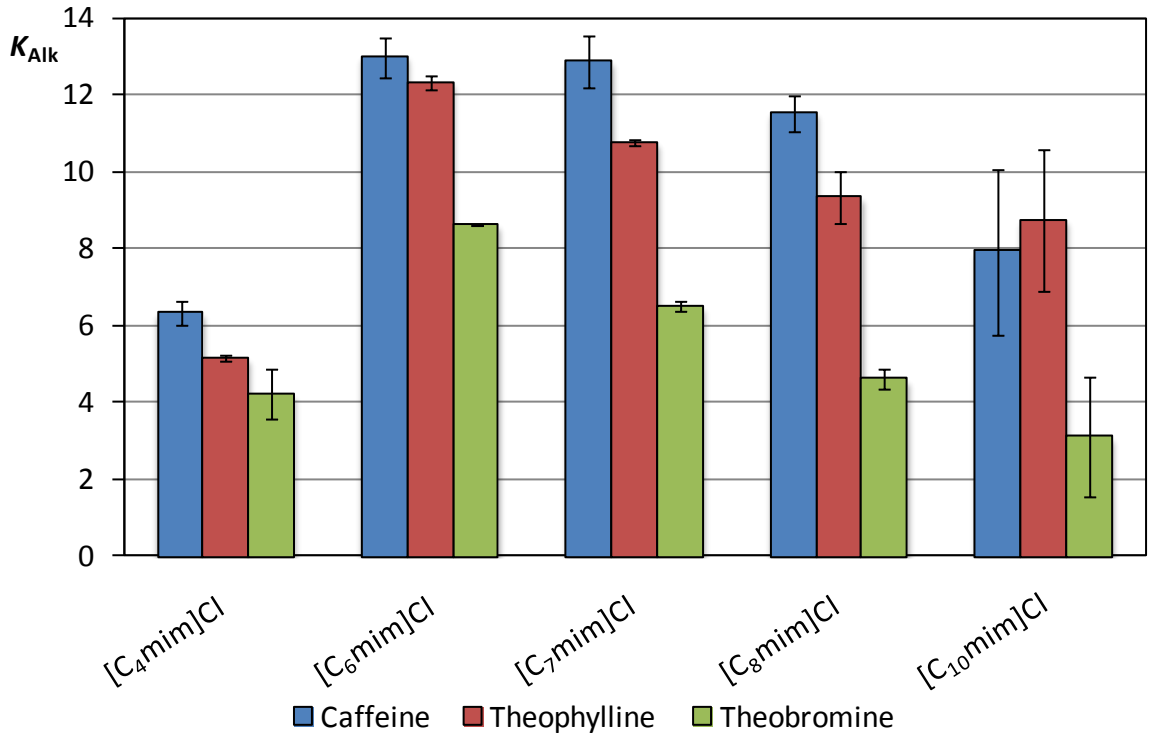

Figure 15. Partition coefficients of caffeine, theophylline and theobromine neutral molecules in imidazolium-based ILs + $C_6H_5K_3O_7$/$C_6H_8O_7$ + H_2O at 298 K and pH 7.

The partition coefficients of caffeine, theophylline and theobromine range between 6.42 and 13.00, 5.16 and 12.53, and 4.22 and 8.62, respectively. In all systems it is verified a preferential partitioning of the alkaloids for the IL-rich aqueous phase.

Through the analysis of the results it is possible to distinguish a well-defined trend in the partition coefficients of the three alkaloids: between [C_4mim]Cl and [C_6mim]Cl there is a substantial increase, with a maximum in [C_6mim]Cl, and after which there is a progressive reduction in the partition coefficients with the alkyl side chain increase. For systems composed of ILs with longer alkyl chains than [C_6mim]Cl it seems that the micelle formation is not favorable for the extraction of the non-charged alkaloids.

Figure 16 depicts the partition coefficients for theophylline at pH 9 (induced by the utilization of the $C_6H_5K_3O_7$ salt) against the partition coefficients obtained at pH 7.

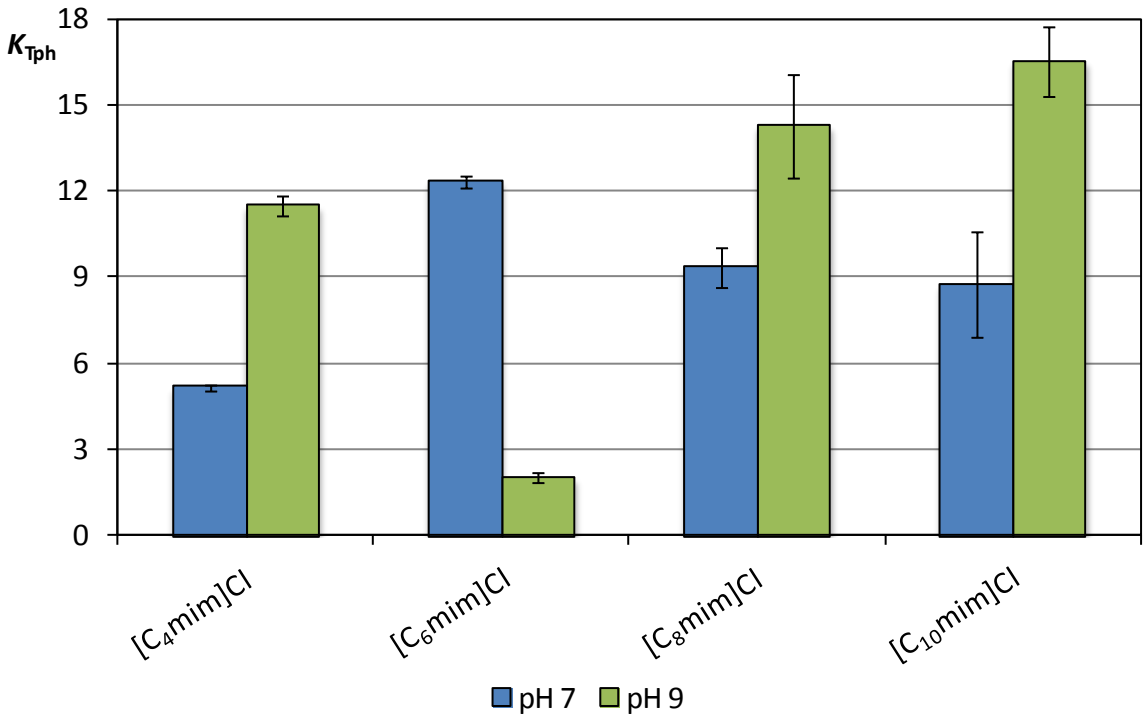

Figure 16. Partition coefficients of theophylline in imidazolium-based ILs + $C_6H_5K_3O_7/C_6H_8O_7$ + H_2O (pH ≈ 7) and ILs + $C_6H_5K_3O_7$ + H_2O (pH ≈ 9) at 298 K.

At pH 9 theophylline is mainly negative charged and the partition coefficients behavior along the series of ILs is completely inverse to that observed at pH 7. Instead of a maximum in [C_6mim]Cl there is a minimum. The highest partition coefficient was indeed observed with [C_{10}mim]Cl with a value of 16.52. This behavior can be explained by the main charge of the alkaloid present at this pH – *cf.* dissociation curves in Appendix D (Figure D 1 to Figure D 4). The negatively charged theophylline has a higher affinity to the positively charged "heads" of the imidazolium cations. Therefore, contrarily to that observed at a neutral pH where the micelles do not favor the partitioning of theophylline, in this example, there is an increase in the partition coefficients by systems which self-aggregate in aqueous media. In summary, it seems that the theophylline anions act as counterions and stabilize the micelles. This phenomenon is well known in literature and seems to be applied also to ILs[119, 120]. A schematic view of the probable mechanism of interactions is presented in Figure 17.

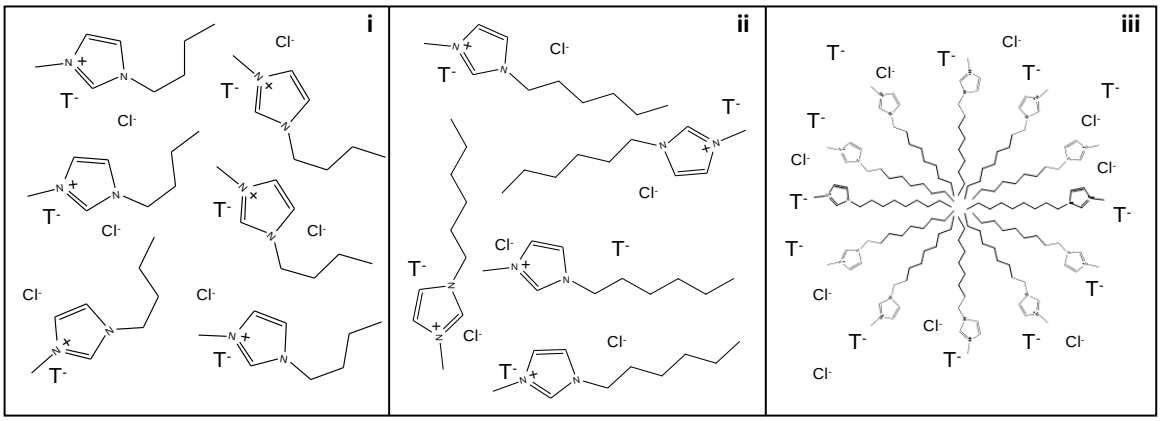

Figure 17. Schematic representation of the theophylline anions their interactions with (i) [C_4mim]Cl, (ii) [C_6mim]Cl and (iii) [C_{10}mim]Cl.

Figure 18 depicts the partition coefficients for nicotine at pH 9 against the partition coefficients obtained at pH 7.

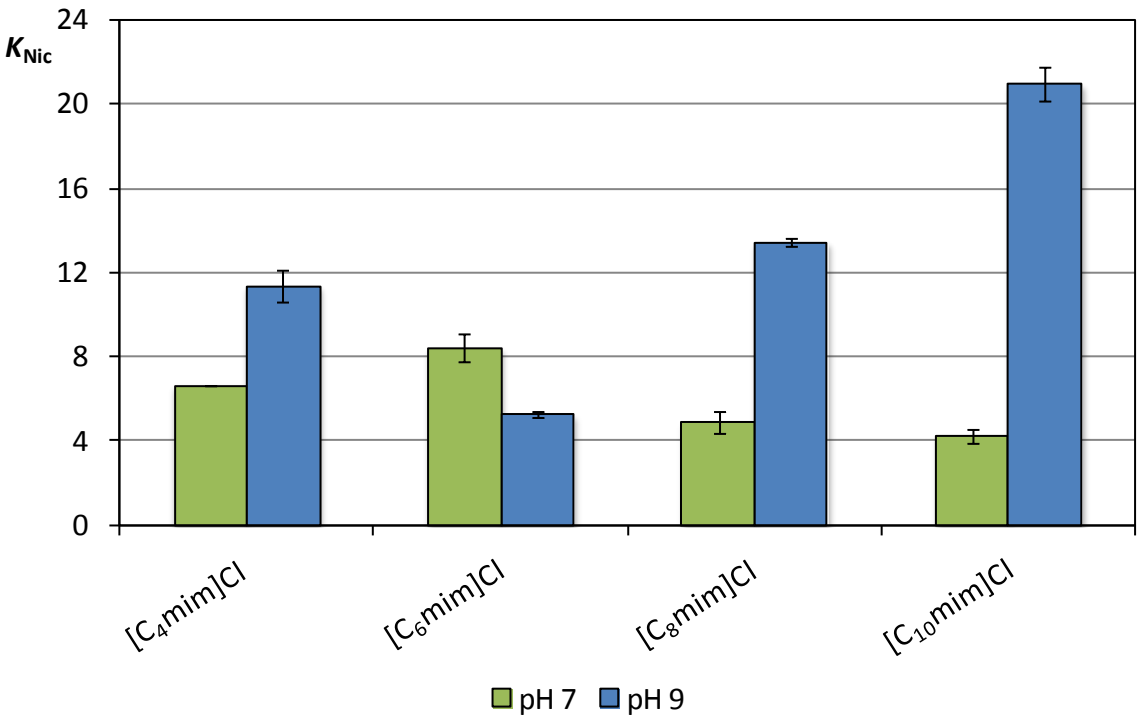

Figure 18. Partition coefficients of nicotine in imidazolium-based ILs + $C_6H_5K_3O_7$ + H_2O (pH ≈ 9) and ILs + $C_6H_5K_3O_7$/$C_6H_8O_7$ + H_2O (pH ≈ 7) at 298 K.

At pH 7, nicotine is predominantly present as a positively charged species as can be gauged in the dissociation curves shown in Appendix D (Figure D 1 to Figure D 4). At this pH, the partition coefficients of nicotine range between 4.28 and 8.43 what indicate a preferential partitioning for

the IL-rich phase. As observed before with the neutral molecules of the remaining alkaloids, a maximum with the system composed of $[C_6mim]Cl$ is observed, followed by a decrease. Therefore, for positively charged species, the formation of micelles is not favorable for improved extractions. In addition, the increase of the IL free volume decreases the repulsion forces between the positive "head" cation and the positive charged nicotine molecule. Thus, it is possible to explain the maximum observed at $[C_6mim]Cl$. For longer alkyl chains, the formation of micelles, in which the positive cation "heads" stay outside and the alkyl side chains are turned to inside of the micelles, leads to repulsion forces which further decrease the partition coefficients.

At pH 9 the nicotine molecule is preferentially in a neutral form (58 % of neutral molecule and 42 % of positively charged molecule) and the partition coefficient behavior is completely the inverse to that observed at pH 7 (98 % of positively charged molecule). These different patterns can be explained based on the alkaloids hydrophobicities (*cf.* Table 4). Among all the alkaloids, nicotine is the most hydrophobic compound and thus can display a different behavior. It is probably that in the presence of micelles (with ILs $[C_8mim]Cl$ and $[C_{10}mim]Cl$) nicotine stays inside of the ILs aggregates (within the aliphatic hydrophobic tails) while the other alkaloids tend to remain in the most hydrophilic side of the micelle (outside of micelle). In this way, the formation of micelles is favorable for the extraction of the neutral nicotine and is unfavorable for the extraction of the neutral molecules of caffeine, theophylline and theobromine.

In summary, for the first time, it was confirmed that micelle-mediated extractions with IL-based ATPS are favorable for negatively charged ions which can act as counterions or for the extraction of neutral molecules with a high hydrophobicity.

To prove the presence of micelles and to support all the statements discussed above, Figure 19 presents one microscope image of the IL-rich phase of ATPS composed of $[C_8mim]Cl + C_6H_5K_3O_7 + H_2O$. In Figure 19 it is possible to distinguish the IL aggregates, which support the justifications given for the obtained results. Additional capturing of microscope images confirmed the presence of micelles in systems composed of $[C_7mim]Cl$ and $[C_{10}mim]Cl$, while no aggregates were observed for $[C_4mim]Cl$-based systems. Moreover, it should be remarked that this type of aggregates were only visible in the IL-rich phase. If they exist in the salt-rich phase they are too small to be visualized by optical microscopy.

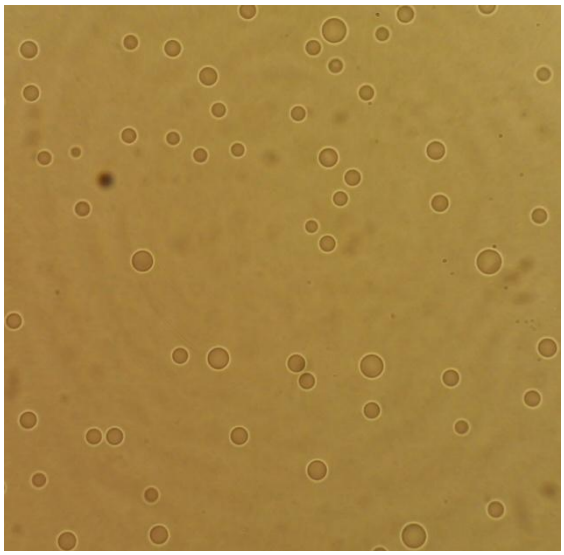

Figure 19. Microscope images of aggregates in the IL-rich phase of the [C_8mim]Cl-based ATPS (50 times magnification).

3.4. Conclusions

The combination of the gathered results with different alkaloids and different pH values allowed to provide novel information on the impact of self-aggregation of ILs towards their extraction efficiencies. It was possible to study and prove that micelles formation has a significant impact in the extraction processes, and for the first time, that self-aggregation of ILs is already verified for [C_7mim]Cl. The interactions between the different species at different stages and the presence of free ILs or their aggregates are in the base of the obtained results. In conclusion, it was observed that negatively charged species are preferentially extracted for IL-rich phases of ILs with long alkyl side chains and ability to self-aggregate.

4. Extraction of BPA with IL-based ATPS

4.1. Bisphenol A (BPA)

Bisphenol A (BPA, 4,4'-(propane-2,2-diyl)diphenol) with the chemical formula $[4\text{-}(OH)C_6H_4]_2C(CH_3)_2$ and the chemical structure presented in Figure 20, is a solid organic compound, with white color and mild phenolic odor. This compound has two phenol functional groups. It is soluble in acetic acid, aqueous alkaline solutions, alcohols and acetone; yet, poorly soluble in water at room temperature[121-123]. The physicochemical properties of BPA are reported in Table 5.

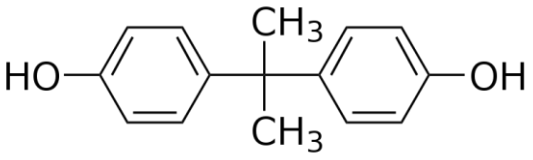

Figure 20. Chemical structure of BPA.

Table 5. Physicochemical properties of BPA[124, 125].

Molecular Weight	228.29	$g \cdot mol^{-1}$
Density at 298 K	1.19	$g \cdot cm^{-3}$
Melting Point	428	K
Boiling Point	671	K
Solubility in Water at 298 K	0.12	$g \cdot dm^{-3}$
$\log K_{OW}$	3.32 – 3.82	
pK_a at 298 K	9.59 – 11.30	

BPA was first synthesized in 1891 by A.P. Dianin[126] and it is obtained by the condensation of acetone with two equivalents of phenol in the presence of a strong acid, such as HCl, or an acidic ion exchange resin as a catalyst[127]. Since 1950 it has been widely used in the plastic industry as an intermediate in the production of epoxy resins and polycarbonate plastics and in the manufacture of thermal paper[128]. These applications account for 95 % of worldwide BPA consumption (over 3.8 million tons *per* year) for the fabrication of regular daily products, *e.g.* baby bottles, food and beverage containers, plastic tableware, toys, eyeglass lenses, sports equipment, medical devices, household electronics, industrial floorings, adhesives, automotive primers and printed circuit boards[129, 130].

BPA is worldwide produced at a rate of about six billion pounds *per* year[131]. Although the volatility of the BPA is lower than that of water, it is released into the atmosphere at a rate of 100 tons *per* year as a consequence of its industrial production[124]. The open burning of plastics in domestic wastes represents also a significant emission source of BPA to atmosphere[132]. In this

way, as shown recently by Pingquin et al.[133], this compound is nowadays a ubiquitous component in the atmosphere.

In the last years, BPA has gained significant public attention due to its potential association with adverse human health effects. The leaching of this compound, particularly from food storing items, became a matter of concern for governmental agencies after its recognition as an endocrine disruptor[134]. In humans, it exerts hormone-like properties leading to altered immune functions, imbalanced hormone ratios[134], decreased semen quality[135], obesity, diabetes, heart disease[136], and behavioral alterations in children[137]. The detection of BPA in 92.6 % of human urine samples, collected among the US population between 2003 and 2004, played a strong role in raising the awareness of its hazards amongst the popular press[138, 139]. Since then, it has been identified in air, water, sediments, soil[140] and house dust[141], food items[142], and other human biological fluids (including serum, plasma, placenta, semen and breast milk)[143]. These findings pointed out the need to establish regulations regarding the production and market placement of BPA. Canada has classified BPA as a toxic substance and has established a provisional tolerable daily intake (TDI) of 25 µg BPA/kg body weight *per* day, whereas in Europe the TDI is 50 µg BPA/kg body weight *per* day[144-146]. This higher TDI value is actually recommended by the US Environmental Protection Agency[144]. Yet, some criticism has been raised regarding the difficulties in detecting and quantifying BPA[138]. The low content of BPA in biological samples is the major obstacle towards its identification and accurate quantification. Usually, liquid-liquid or solid-liquid extractions are used to increase BPA concentrations from food and biological samples[128]; yet, they are time-consuming and require large quantities of volatile organic solvents. In this context, IL-based ATPS may represent a new vehicle for extracting BPA from human fluids. Although one report regarding BPA extraction using ILs has been found in the literature[147], this study made use of expensive, toxic, and non-water-stable fluorinated ILs[88].

In this work, we tested the ability of several hydrophilic ILs combined with K_3PO_4 (a strong salting-out species) as constituents of ATPS for extracting BPA and improving its detection *via* conventional analytical techniques. Both model aqueous systems and more complex matrices, such as human urine-type samples, were investigated. These systems were selected taking into account improved results obtained previously for the extraction of bioactive drugs[59]. Indeed, it was previously verified that IL-based systems formed by the addition of K_3PO_4 provide high extraction efficiencies due to the presence of the strong salting-out salt[59].

4.2. Experimental section

4.2.1. Chemicals

BPA, 4,4'-(propane-2,2-diyl)diphenol, ≥ 99 wt % pure, was supplied by Aldrich. The ILs used in the ATPS composition were: 1-ethyl-3-methylimidazolium chloride, [C_2mim]Cl (> 98 wt %); 1-butyl-3-methylimidazolium chloride, [C_4mim]Cl (99 wt %); 1-hexyl-3-methylimidazolium chloride, [C_6mim]Cl (> 98 wt %); 1-allyl-3-methylimidazolium chloride, [amim]Cl (> 98 wt %); 1-butyl-1-methylpyrrolidinium chloride, [C_4mpyr]Cl (99 wt %); tetrabutylphosphonium chloride, [P_{4444}]Cl (98 wt %); tetrabutylammonium chloride, [N_{4444}]Cl (≥ 97 wt %); and choline chloride, [N_{1112OH}]Cl (≥ 98 wt %). The ILs molecular structures are shown in Figure 21. All ILs used in this work were supplied by Iolitec with the exception of [P_{4444}]Cl that was kindly supplied by Cytec Industries Inc., [N_{4444}]Cl that was from Aldrich and [N_{1112OH}]Cl that was from Sigma. It should be noted that [N_{4444}]Cl and [N_{1112OH}]Cl have melting points above 100 °C, however, along the present work they will be so-called ILs. To reduce the water and volatile compounds content to negligible values, ILs individual samples were dried under constant stirring at vacuum and moderate temperature (≈ 353 K) for a minimum of 24 h. After this step, the purity of each IL was checked by ^{1}H and ^{13}C NMR spectra. Urea, 99 wt % pure, was supplied by Panreac and was used without further purification. K_3PO_4, 98 wt % pure, and NaCl, 99.9 wt % pure, were from Sigma and Normapur, respectively. The water used was ultra-pure water, double distilled, passed by a reverse osmosis system and further treated with a Milli-Q plus 185 water purification apparatus.

Synthetic human urine was prepared by the dissolution of urea and NaCl in pure water, at the concentrations of 1.2 g·dm^{-3} and 4.0 g·dm^{-3}, respectively.

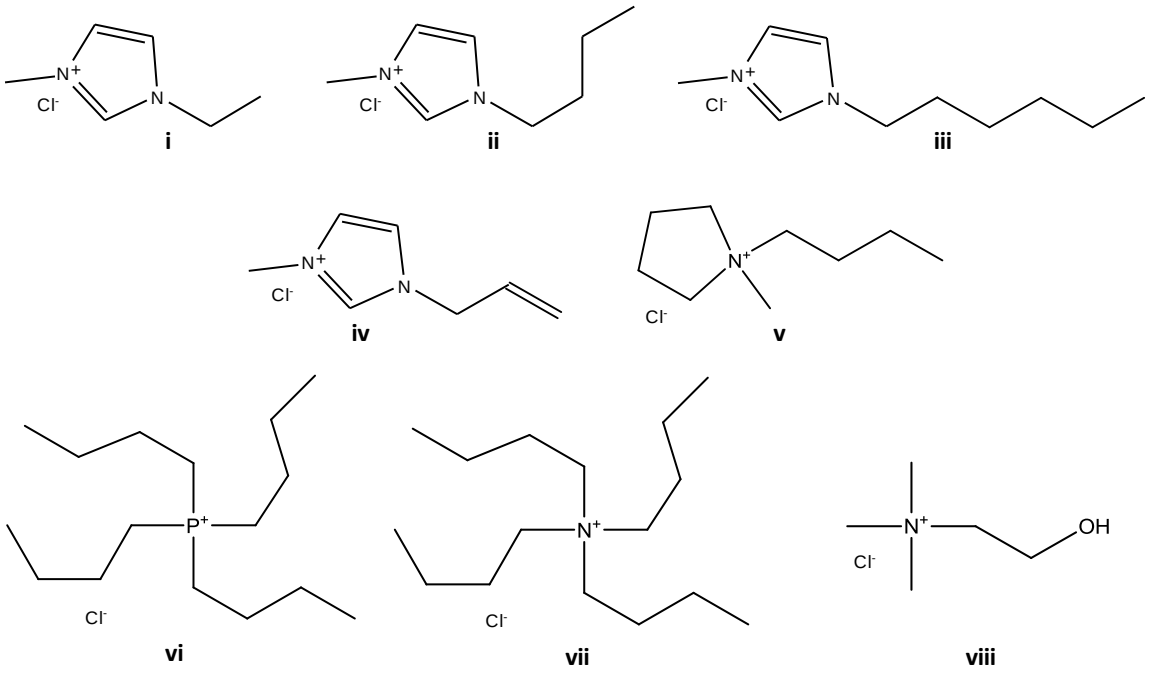

Figure 21. Chemical structure of the ILs studied: (i) [C_2mim]Cl; (ii) [C_4mim]Cl; (iii) [C_6mim]Cl; (iv) [amim]Cl; (v) [C_4mpyr]Cl; (vi) [P_{4444}]Cl; (vii) [N_{4444}]Cl; (viii) [N_{1112OH}]Cl.

4.2.2. Experimental procedures

4.2.2.1. Phase diagrams

New phase diagrams for the IL [C_4mpyr]Cl, [P_{4444}]Cl and [N_{4444}]Cl were determined in this work, while the ternary phase diagrams for [C_2mim]Cl, [C_4mim]Cl, [C_6mim]Cl and [N_{1112OH}]Cl were taken from literature[52, 148]. The experimental procedure adopted was similar to the one described in Section 2.2.2. The ternary phase diagrams were determined through the cloud point titration method[60] at (298 ± 1) K and atmospheric pressure. Aqueous solutions of K_3PO_4 at 50 wt % and aqueous solutions of the different hydrophilic ILs, with concentrations ranging from 60-70 %, were prepared gravimetrically and used for the determination of the binodal curves. Repetitive drop-wise addition of the aqueous inorganic salt solution to each IL aqueous solution was carried out until the detection of a cloudy solution (biphasic region), followed by the drop-wise addition of ultra-pure water until the detection of a clear and limpid solution (monophasic region). Drop-wise additions were carried out under constant stirring. The ternary system compositions were determined by the weight quantification of all components added within an uncertainty of ± 10^{-4} g.

The TLs were determined by the gravimetric method described by Merchuck et al.[92] and presented in Section 2.2.2.

The pH of both IL and organic salt aqueous phases was measured at 298 K using a METTLER TOLEDO SevenMulti pH meter within an uncertainty of ± 0.02.

4.2.2.4. Partitioning and extraction efficiencies of BPA

A ternary mixture within the biphasic region was prepared containing 15 wt % of K_3PO_4, 25 wt % of IL and 60 wt % of a BPA aqueous solution with a concentration of 4.3×10^{-4} mol·dm^{-3}. Only for $[N_{1112OH}]Cl$ a different composition (15 wt % of K_3PO_4, 40 wt % of IL and 45 wt % of the aqueous solution of BPA) was used due to the smaller biphasic region obtained with this IL. As already mentioned in Section 3.2.2, each mixture was vigorously stirred and left to equilibrate for at least 12 h to achieve a complete BPA partitioning between the two phases. It was checked again that for all the ternary mixtures evaluated, and at the compositions used, the IL-rich aqueous phase is the top layer while the K_3PO_4-rich aqueous phase is the bottom layer. After a careful separation of the two phases, the BPA quantification in each phase was carried by UV-spectroscopy, using a SHIMADZU UV-1700, Pharma-Spec Spectrometer, at wavelength of 293 nm and using calibration curves previously established (*cf.* Appendix C - Figure C 6 and Figure C 7). The characteristic alkaline pH that K_3PO_4 confers to the aqueous system, shifts the maximum absorbance of BPA to 293 nm. Therefore, the calibration curve was established at a pH of 13 and blank control samples were always used since interferences of the inorganic salt and ILs with the analytical method were identified. At least three individual samples of each phase were quantified in order to determine the BPA partition coefficients and the respective standard deviations. The stability of BPA in the coexisting phases of all systems was confirmed and it is safe to admit that the molecule is stable at least up to 72 h in the ATPS investigated.

The percentage extraction efficiencies of BPA (EE_{BPA}%) are defined as the percentage ratio between the amount of BPA in the IL-rich aqueous phase and that in the total mixture, according to Equation 8,

$$EE_{\mathrm{BPA}}\% = \frac{m_{BPA}^{IL}}{m_{BPA}^{IL} + m_{BPA}^{Salt}} \tag{8}$$

where m_{BPA}^{IL} and m_{BPA}^{Salt} are the amount of BPA in the IL-rich and in the K_3PO_4-rich aqueous phases, respectively.

4.3. Results and discussion

The new phase diagrams for the ILs [C_4mpyr]Cl, [P_{4444}]Cl and [N_{4444}]Cl are illustrated in Figure 22, against the ternary phase diagrams previously reported for [C_2mim]Cl, [C_4mim]Cl, [C_6mim]Cl and [N_{1112OH}]Cl [52, 148]. Figure 22 indicates that the IL cation ability to form ATPS, at 1.0 mol·kg^{-1} of K_3PO_4, follows the order: $[P_{4444}]^+$ > $[N_{4444}]^+$ >> $[C_6mim]^+$ > $[C_4mpyr]^+$ > $[C_4mim]^+$ > $[amim]^+$ > $[C_2mim]^+$ >> $[N_{1112OH}]^+$.

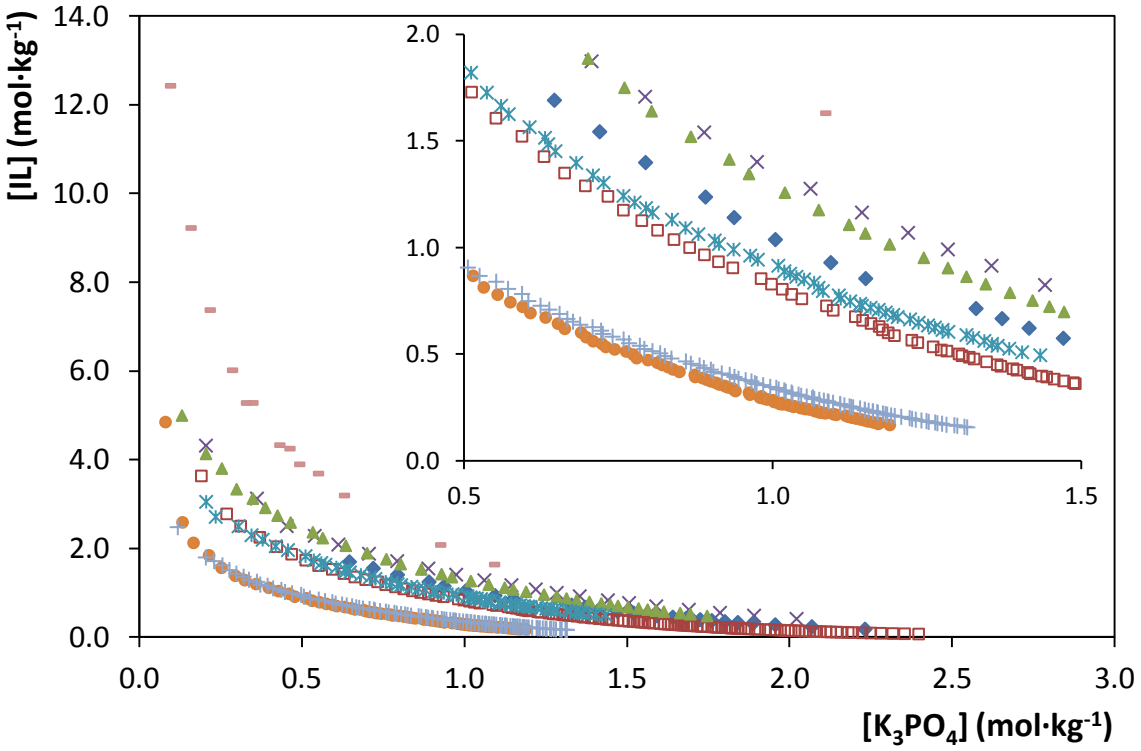

Figure 22. Evaluation of the cation influence in the ternary phase diagrams composed of IL + H_2O + K_3PO_4: [C_2mim]Cl (×); [C_4mim]Cl (◆); [C_6mim]Cl (□); [amim]Cl (▲); [C_4mpyr]Cl (✳); [P_{4444}]Cl (●); [N_{4444}]Cl (+); [N_{1112OH}]Cl (-).

Neves et al.[52] reported that with the increase of the cation alkyl side chain length, the ILs ability for the formation of ATPS also increases. In fact, and has discussed in Section 2, ILs with longer aliphatic chains at the cation are more hydrophobic, and thus, the IL solubility in water decreases. For the IL [amim]Cl, the double bond at the allyl group present at the imidazolium cation decreases the ability for the formation of ATPS[52].

The trend that can be seen with the ILs [C_4mpyr]Cl, [P_{4444}]Cl and [N_{4444}]Cl is associated with the ability of the cation to be solvated by water, which is inherently related with their

hydrophobicity. The four butyl chains present in phosphonium- and ammonium-based cations are responsible for a higher hydrophobicity which induces a higher ability for the formation of ATPS.

Finally, the lower ability of $[N_{1112OH}]Cl$ for the formation of ATPS is related with its smaller size compared to the other cations and with the presence of a terminal hydroxyl group - which increases the IL affinity for water.

The experimental binodal data were fitted by the empirical relationship described by Equation 1. The fitted parameters and respective correlation coefficients are presented in Table 6. The experimental TLs and their respective TLLs are reported in Table 7.

Table 6. Correlation parameters used to describe the experimental binodals data by Equation 1.

IL	$A \pm \sigma$	$B \pm \sigma$	$10^5(C \pm \sigma)$	R^2
$[C_2mim]Cl$[52]	78.2 ± 2.8	-0.339 ± 0.013	2.70 ± 0.25	0.9964
$[C_4mim]Cl$[52]	72.6 ± 0.7	-0.318 ± 0.004	4.07 ± 0.08	0.9994
$[C_6mim]Cl$[52]	84.0 ± 0.5	-0.356 ± 0.002	5.46 ± 0.04	0.9997
[amim]Cl[52]	72.0 ± 0.4	-0.292 ± 0.002	4.09 ± 0.05	0.9998
$[C_4mpyr]Cl$	64.6 ± 1.2	-0.300 ± 0.007	5.26 ± 0.28	0.9984
$[P_{4444}]Cl$	105.2 ± 2.3	-0.506 ± 0.010	9.01 ± 0.51	0.9936
$[N_{4444}]Cl$	74.6 ± 0.4	-0.387 ± 0.002	10.07 ± 0.09	0.9997
$[N_{1112OH}]Cl$	100.6 ± 1.0	-0.281 ± 0.005	1.78 ± 0.27	0.9980

Table 7. Experimental data for TLs and TLLs of IL + K_3PO_4 ATPS.

IL	Weight fraction percentage (wt %)								TLL
	$[IL]_{IL}$	$[Salt]_{IL}$	pH_{IL}	$[IL]_{M}$	$[Salt]_{M}$	$[IL]_{Salt}$	$[Salt]_{Salt}$	pH_{Salt}	
$[C_2mim]Cl$	28.03	8.85	13.18	21.99	15.12	3.69	34.14	13.09	35.10
	34.06	5.94	13.13	24.96	14.96	2.45	37.25	13.18	44.63
	39.52	4.04	13.32	27.97	14.98	1.66	39.90	13.04	52.14
	43.73	2.94	13.28	31.02	15.08	0.69	44.96	13.63	60.15
$[C_4mim]Cl$	37.11	4.40	13.05	25.02	15.02	1.79	35.42	12.97	47.01
$[C_6mim]Cl$	39.51	4.43	12.93	24.94	15.29	1.64	32.66	12.92	47.24
[amim]Cl	35.73	5.62	13.25	25.03	15.02	2.18	35.08	13.24	44.65
$[C_4mpyr]Cl$	39.32	2.71	13.40	25.03	15.03	0.97	35.75	13.07	50.62
$[P_{4444}]Cl$	47.45	2.47	13.04	24.98	14.99	0.90	28.41	12.69	53.30
$[N_{4444}]Cl$	45.36	1.64	13.37	25.08	15.05	0.38	31.38	13.11	53.92
$[N_{1112OH}]Cl$	37.37	11.71	13.11	25.03	22.07	7.55	36.78	12.99	38.96
	39.09	10.78	13.14	26.02	21.89	6.23	38.72	13.00	43.13
	44.57	8.18	13.18	27.95	22.15	4.37	41.97	13.01	52.51
	48.84	6.52	13.25	30.74	22.12	2.47	46.51	12.22	61.23

The extraction efficiencies of BPA in the ATPS formed by chloride-based salts, K_3PO_4 and water are depicted in Figure 23. The composition of the phases for the mixtures used for the extraction of BPA are depicted in Table 7. The extraction efficiencies percentages values and respective standard deviations, are presented in Appendix D (Table D 3 and Table D 4).

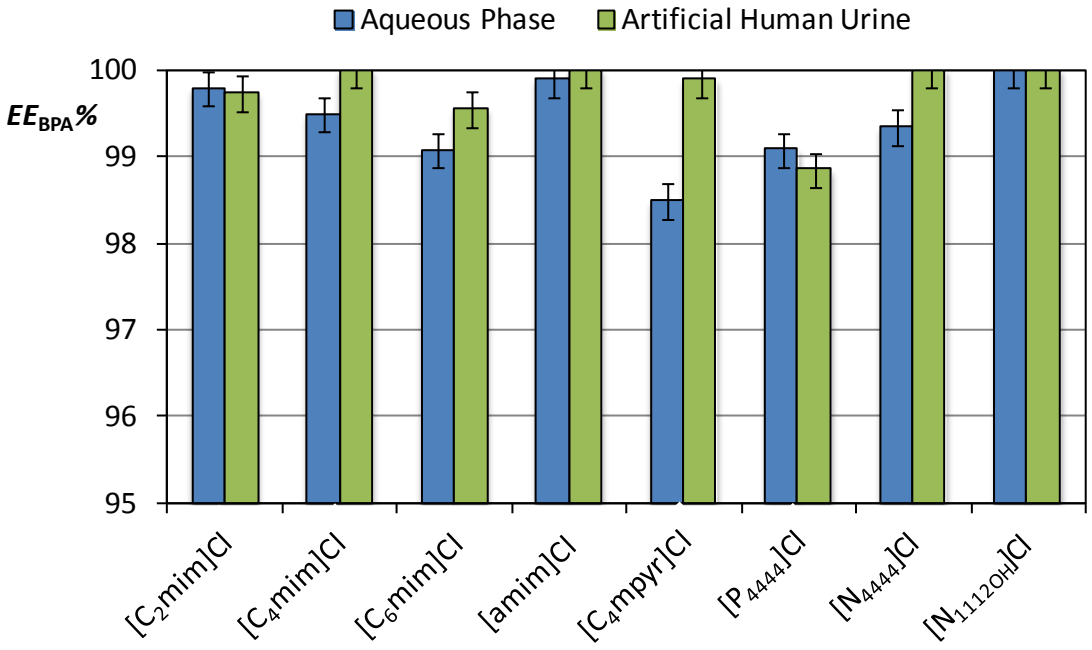

Figure 23. Percentage extraction efficiencies of BPA, EE_{BPA}%, in different ATPS at 298 K. All ATPS are composed of 15 wt % of K_3PO_4 + 25 wt % of chloride-based IL + 60 wt % of aqueous phase/artificial human urine, except for the $[N_{1112OH}]Cl$-based system with a concentration of 15 wt % of K_3PO_4 + 40 wt % of $[N_{1112OH}]Cl$ + 45 wt % of aqueous phase/artificial human urine.

Remarkably, extraction efficiencies of BPA larger than 98.5 % were attained for all the investigated systems. This feature mirrors that of the low affinity of BPA for water and preferential partitioning for organic-rich phases. Indeed, the reported logK_{OW} value (octanol-water partition coefficient) of BPA varies from 3.32 to 3.82[124]. Nevertheless, the high extraction efficiencies obtained are also a direct result of the strong salting-out ability of K_3PO_4 (high-charge density anion with an improved ability to create hydration complexes) and which leads to the "exclusion" of BPA from the inorganic-salt-rich phase to the more "organic" IL-rich phase. Albeit BPA is in a charged form (pK_a = 9.59 - 11.30)[125] due to the alkaline medium used for extraction, it seems that the electrostatic interactions between the salt cation (K^+) and the BPA negative ion are of low importance, with the endocrine disruptor migrating preferentially for the IL-rich phase. On the other hand, the counterions of the chloride-based salts also play a role in the migration of BPA between the coexisting phases and which could indicate the presence of electrostatic interactions between each IL cation and the charged BPA. Taking into account the "neutral" molecular structure of BPA (two large phenyl groups, as well as two electron-rich hydroxyl groups and two methyl groups) and the range of ILs employed, the following interactions can be expected:

(i) hydrogen-bonding interactions; (ii) π···π interactions between the aromatic groups; and (iii) dispersive-type interactions between the aliphatic groups. The results show that an increase in the cation side alkyl chain length of the [$C_n$mim]-based ILs leads to a decrease in the extraction efficiencies of BPA. Moreover, the use of quaternary ammonium- and phosphonium-based ILs also decreases the extraction efficiencies when compared with the imidazolium-based fluids. This effect of the imidazolium alkyl chain length and the four butyl chains at [P_{4444}]Cl and [N_{4444}]Cl seems to indicate that although there is a need to accommodate the non-polar parts of BPA, the dispersive-type interactions are non-favorable for its enhanced extraction. In fact, it seems that π···π interactions and hydrogen-bonding interactions are vital requirements for the complete extraction of BPA. Examples of such factors at work can be noticed with [C_4mim]Cl and [C_4mpyr]Cl (aromatic and non-aromatic five-sided rings) and with [amim]Cl (enhanced hydrogen-bonding capability due to the allyl group). Even with [N_{1112OH}]Cl this tendency is confirmed since the hydroxyl group at the longest aliphatic chain favors the hydrogen-bonding between the choline cation and BPA.

Figure 23 compares ATPS made up of different ILs. Nevertheless, in order to create more economic and environmentally benign processes, the amount of IL added was optimized without losing the high extraction efficiencies of BPA. Therefore, while maintaining the inorganic salt concentration, it was studied the BPA extraction efficiencies in a range of concentrations of [C_2mim]Cl and [N_{1112OH}]Cl – two of the best candidates for the extraction of BPA (*cf.* Appendix D - Figure D 5 and Figure D 6, with the representation of the selected compositions in the ternary phase diagram) . Figure 24 shows the effect of the IL concentration in the extraction of BPA.

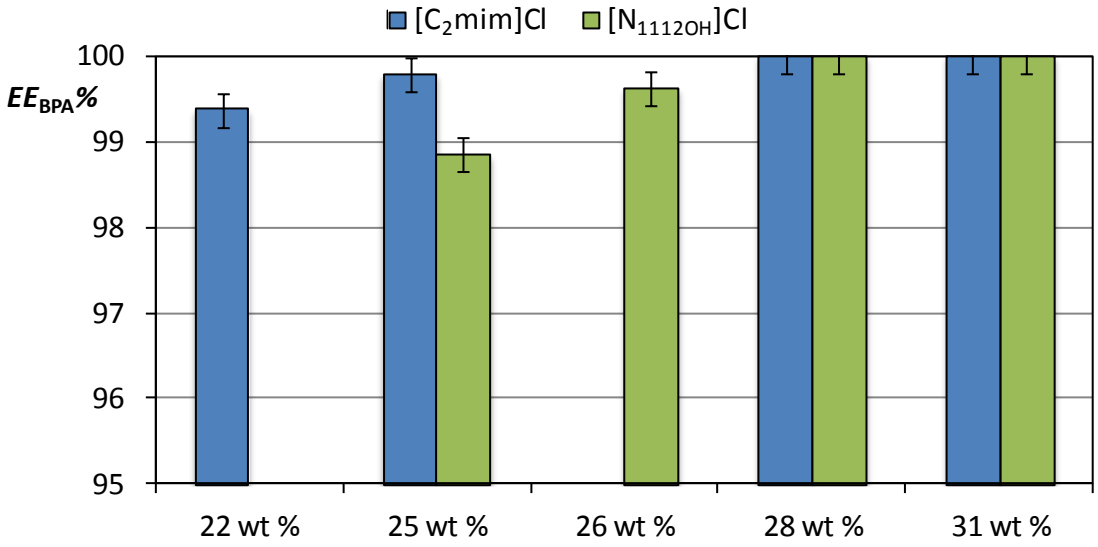

Figure 24. Percentage extraction efficiencies of BPA, EE_{BPA}%, at 298 K, in the ATPS composed of 15 wt % of K_3PO_4 + $[C_2mim]Cl$ at different concentrations and 22 wt % of K_3PO_4 + $[N_{1112OH}]Cl$ at different concentrations.

In general, an increase in the IL concentration, *i.e.,* an increase in the TLL, leads to improved extraction efficiencies. However, to achieve complete extractions of BPA, the minimum concentrations of 15 wt % of K_3PO_4 + 25 wt % of $[C_2mim]Cl$ and 22 wt% of K_3PO_4 + 28 wt % of $[N_{1112OH}]Cl$ are required (or mixture compositions with higher amounts of inorganic salt and less IL and which fit within the same TL).

To guarantee that the concentration of BPA in the aqueous phase neither provides erroneous results nor leads to the saturation of the phases, the extraction efficiencies of BPA at concentrations of 100, 50, 5 and 1 $\mu g \cdot g^{-1}$ were determined in the two systems composed of 15 wt % of K_3PO_4 + 25 wt % $[C_2mim]Cl$ and 15 wt % of K_3PO_4 + 40 wt % of $[N_{1112OH}]Cl$. In all of these studies, complete extraction of BPA for the IL-rich phase was observed and the mass balance was always confirmed. It is well know that BPA is poorly water soluble. If the saturation of the phases is reached, erroneous results could appear in clinical trials providing lower contents than the real ones. From the gathered data it is safe to admit that concentrations up to 100 $\mu g \cdot g^{-1}$ of BPA can be analyzed, and supports the applicability of the proposed systems to real samples since this value is well above to those recently found in human biological fluids[143, 149].

As pointed out before, one of the major concerns related with the BPA analysis is its very low concentration in body fluids. In order to explore the maximum concentration of BPA achievable, several extractions were carried out at different compositions in the same TL (*cf.* Appendix D -

Figure D 5, Figure D 6 and Table D 3). The main goal is to reduce the volume of the IL-rich phase up to a minimum capable of concentrating the BPA that is actually present in a larger volume of an aqueous medium, for instance, in biological fluids. The various initial compositions are along the same TL; yet, different initial concentrations lead a different volume ratio. The results obtained are depicted in Figure 25. Detailed information and the representation of the composition mixtures at the phase diagrams are provided in Appendix D (Figure D 5 and Figure D 6).

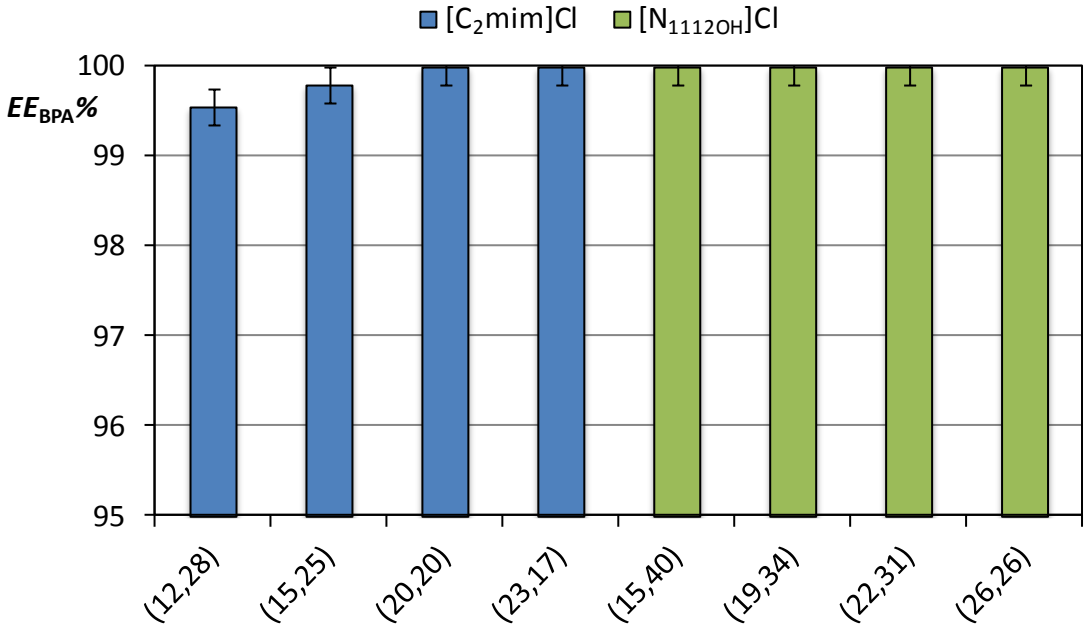

Figure 25. Extraction efficiencies percentages of BPA, $EE_{BPA}\%$, in IL + K_3PO_4 ATPS at 298 K and at different mixture compositions along the same TL (*x*,*y* at the *xx* axis represent the percentage weight fractions of the salt and IL, respectively).

The results shown in Figure 25 indicate that along the same TL it is possible to control the volume ratio of the aqueous phases, aiming at decreasing the volume of the IL-rich phase, while keeping the complete extraction of BPA in a single-step. In Figure 25, the volume ratio (IL-rich/salt-rich phase) ranges between 4 and 0.5 (as determined by the lever-arm rule). Therefore, different mixture compositions along these TLs lead always to the complete extraction of BPA. In this context, the concentration of BPA can be increased at least up to 100-fold by the reduction of the total volume of the extractive phase (making use, for instance, of the following mixture compositions: 2.5 wt % of $[N_{1112OH}]Cl$ + 45 wt % of K_3PO_4 or 2.7 wt% of $[C_2mim]Cl$ + 37 wt % of K_3PO_4).

After fine-tuning the ILs and respective compositions with model systems composed of water, direct extraction of BPA from artificial human urine was further evaluated to ascertain on the applicability of these systems as novel extractive techniques from human biological fluids. The urine sample results appear in Figure 23. In general, the presence of a more complex matrix, now including NaCl and urea, favors the partitioning of BPA for the IL-rich phase. Indeed, for most systems, a 100 % extraction was attained.

The pre-concentration of BPA and related metabolites from biological fluids is traditionally carried out by eminent solid-phase extraction (SPE) techniques and involve, according to well-known adopted protocols, the use of organic solvents (*e.g.* methanol, ethyl acetate, or MTBE)[143, 150]. Besides the requirement on the use of organic and toxic molecular solvents, there is also the need of SPE cartridges which are usually of high cost. Therefore, the alternative process presented in this work is, in comparison to the latter, greener, safer, time saving and (arguably one of the most important characteristics in modern science) more economical. Besides the replacement of the conventional volatile organic solvents, the systems herein proposed, especially those composed of $[C_2mim]Cl$ and $[N_{1112OH}]Cl$, require small amounts of ILs of low toxicity and low cost[151]. Moreover, it should be stressed that the most used analytical method for the determination of BPA is high-performance liquid chromatography (HPLC), either combined with mass spectrometry (MS) using electrospray ionization (ESI) interface or with an electrochemical detector (ED)[152]. There is already evidence that, for instance, the direct quantification of opium alkaloids, testosterone and epitestosterone in IL-rich phases using HPLC is possible, and no interferences with the phase forming components of ATPS were found[53, 54].

4.4. Conclusions

In this work, it was reported for the first time, the remarkable ability of IL-based ATPS to extract BPA from aqueous biological samples in a single-step process. For all the investigated systems, the extraction efficiencies of BPA are higher than 98.5 %. The effect of the IL cation nature was studied and the results obtained indicated that the extraction of BPA is strongly associated with π···π and hydrogen-bonding interactions. It was shown that by obtaining a complete extraction and possible concentration up to 100-fold, human fluid samples can be effortlessly checked for their BPA content. Besides the replacement of the conventional VOCs, the systems proposed, especially those composed of $[C_2mim]Cl$ and $[N_{1112OH}]Cl$, require small amounts of ILs of low toxicity and low cost[151].

In conclusion, small kits containing the optimized ILs and K_3PO_4 in fixed amounts, to which the human biological fluids could be simply added, can be conceptualized as a new and commercial complement to analytical/clinical strategies where the identification/quantification of BPA is required.

5. Final remarks

5.1. Conclusions

In this work it was possible to evaluate novel IL-based ATPS, ranging from their phase diagrams to their application in the extraction of bioactive compounds. The application of organic salts, such as tri-potassium citrate, showed to be a good option for the substitution of the commonly used inorganic salts, and novel ternary phase diagrams were provided. For the first time, it was addressed the effect of micelles formation and their impact on the extraction of (bio)molecules. Finally, proper IL-based ATPS showed to be improved extractive techniques for concentrating an endocrine disruption of human concern, BPA, from biological fluids.

5.2. Future work

In the future it would be interesting to continue the study of finding novel ATPS composed of ILs and other organic salts and to study their potential application in the extraction of different added-value compounds of biotechnological interest.

To support the finding of the micelle-mediated extraction further tests must be conducted. The use of transmission electron microscopy (TEM) could be highly advantageous to detect micelles not observed by optical microscopy and to analyze the form and shape of such aggregates.

Regarding the proposed technique for concentrating BPA it would be of high value to apply it to real body fluid samples, aiming at providing a general overview of the levels of BPA in the Portuguese population and its relation with several cancer types, autoimmune diseases and allergies, infertility, type 2 diabetes and obesity.

6. References

1. Walden, P., *Ueber die Molekulargrösse und elektrische Leitfähigkeit einiger geschmolzener Salze (Molecular weights and electrical conductivity of several fused salts).* Bulletin de l'Académie Impérial des Sciences de St.-Pétersbourg, 1914. **8**: p. 405-422.

2. Charles, G., *Cellulose solution*. 1934, US Patent 1943176.

3. Hurley, F.H., *Electrodeposition of Aluminium*. 1948, US Patent 4446331.

4. T. P. Wier, F.H.H. 1948, US Patente 4446349.

5. Seddon, K.R., *Ionic Liquids for Clean Technology.* Journal of Chemical Technology & Biotechnology, 1997. **68**(4): p. 351-356.

6. Seddon, K.R., *Room-temperature ionic liquids: Neoteric solvents for clean catalysis.* Kinetics and Catalysis, 1996. **37**(5): p. 693-697.

7. Bonhote, P.,Dias, A.P.,Papageorgiou, N.,Kalyanasundaram, K., and Gratzel, M., *Hydrophobic, highly conductive ambient-temperature molten salts.* Inorganic Chemistry, 1996. **35**(5): p. 1168-1178.

8. Elaiwi, A.,Hitchcock, P.B.,Seddon, K.R.,Srinivasan, N.,Tan, Y.M.,Welton, T., and Zora, J.A., *Hydrogen-Bonding in Imidazolium Salts and Its Implications for Ambient-Temperature Halogenoaluminate(III) Ionic Liquids.* Journal of the Chemical Society-Dalton Transactions, 1995(21): p. 3467-3472.

9. Stegemann, H.,Rohde, A.,Reiche, A.,Schnittke, A., and Fullbier, H., *Room-Temperature Molten Polyiodides.* Electrochimica Acta, 1992. **37**(3): p. 379-383.

10. Jungnickel, C.,Łuczak, J.,Ranke, J.,Fernández, J.F.,Müller, A., and Thöming, J., *Micelle formation of imidazolium ionic liquids in aqueous solution.* Colloids and Surfaces A: Physicochemical and Engineering Aspects, 2008. **316**(1-3): p. 278-284.

11. Earle, M.J.,Esperanca, J.M.S.S.,Gilea, M.A.,Canongia Lopes, J.N.,Rebelo, L.P.N.,Magee, J.W.,Seddon, K.R., and Widegren, J.A., *The distillation and volatility of ionic liquids.* Nature, 2006. **439**(7078): p. 831-834.

12. Santos, L.M.N.B.F.,Canongia Lopes, J.N.,Coutinho, J.A.P.,Esperança, J.M.S.S.,Gomes, L.R.,Marrucho, I.M., and Rebelo, L.P.N., *Ionic Liquids: First Direct Determination of their Cohesive Energy.* Journal of the American Chemical Society, 2006. **129**(2): p. 284-285.

13. Rogers, R.D. and Seddon, K.R., *Ionic Liquids--Solvents of the Future?* Science, 2003. **302**(5646): p. 792-793.

14. G. Huddleston, J. and D. Rogers, R., *Room temperature ionic liquids as novel media for 'clean' liquid-liquid extraction.* Chemical Communications, 1998(16): p. 1765-1766.

15. Haddleton, D.M.,Welton, T., and Carmichael, A.J., *Polymer Synthesis in Ionic Liquids*, in *Ionic Liquids in Synthesis*. 2008, Wiley-VCH Verlag GmbH & Co. KGaA. p. 619-640.

16. Visser, A.E.,Swatloski, R.P., and Rogers, R.D., *pH-Dependent partitioning in room temperature ionic liquids provides a link to traditional solvent extraction behavior.* Green Chemistry, 2000. **2**(1): p. 1-4.

17. Swatloski, R.P.,Spear, S.K.,Holbrey, J.D., and Rogers, R.D., *Dissolution of Cellose with Ionic Liquids.* Journal of the American Chemical Society, 2002. **124**(18): p. 4974-4975.

18. Sheldon, R., *Catalytic reactions in ionic liquids.* Chemical Communications, 2001(23): p. 2399-2407.

19. Jain, N.,Kumar, A.,Chauhan, S., and Chauhan, S.M.S., *Chemical and biochemical transformations in ionic liquids.* Tetrahedron, 2005. **61**(5): p. 1015-1060.

20. Zhao, H.,Xia, S., and Ma, P., *Use of ionic liquids as `green' solvents for extractions.* Journal of Chemical Technology & Biotechnology, 2005. **80**(10): p. 1089-1096.

21. Wong, H.-t.,Han, S., and Livingston, A.G., *The effect of ionic liquids on product yield and catalyst stability.* Chemical Engineering Science, 2006. **61**(4): p. 1338-1341.

22. Endres, F. and Zein El Abedin, S., *Air and water stable ionic liquids in physical chemistry.* Physical Chemistry Chemical Physics, 2006. **8**(18): p. 2101-2116.

23. Hussey, C.L., in *Chemistry of Nonaqueous Solutions* 1994, ed. G. Mamantov, A. I. Popov, VCH: Weinheim. p. 227-276.

24. M. Gordon, C.,D. Holbrey, J.,R. Kennedy, A., and R. Seddon, K., *Ionic liquid crystals: hexafluorophosphate salts.* Journal of Materials Chemistry, 1998. **8**(12): p. 2627-2636.

25. Bowlas, C.J.,Bruce, D.W., and Seddon, K.R., *Liquid-crystalline ionic liquids.* Chemical Communications, 1996(14): p. 1625-1626.

26. Park, S. and Kazlauskas, R.J., *Biocatalysis in ionic liquids – advantages beyond green technology.* Current Opinion in Biotechnology, 2003. **14**(4): p. 432-437.

27. van Rantwijk, F. and Sheldon, R.A., *Biocatalysis in ionic liquids.* Chemical Reviews, 2007. **107**(6): p. 2757-2785.

28. Earl, M.J. and Seddon, K.R., *Ionicliquids. Green solvents for the future.* Pure Appl. Chem., 2000. **72**: p. 1391–1398.

29. Ranke, J.,Stolte, S.,Störmann, R.,Arning, J., and Jastorff, B., *Design of Sustainable Chemical ProductsThe Example of Ionic Liquids.* Chemical Reviews, 2007. **107**(6): p. 2183-2206.

30. Wasserscheid, P. and Welton, T., *Ionic liquids in synthesis*. 2008: Wiley-VCH.

31. Welton, T., *Room-Temperature Ionic Liquids. Solvents for Synthesis and Catalysis.* Chemical Reviews, 1999. **99**(8): p. 2071-2083.

32. Couling, D.J.,Bernot, R.J.,Docherty, K.M.,Dixon, J.K., and Maginn, E.J., *Assessing the factors responsible for ionic liquid toxicity to aquatic organisms via quantitative structure-property relationship modeling.* Green Chemistry, 2006. **8**(1): p. 82-90.

33. Docherty, K.M. and Kulpa, J.C.F., *Toxicity and antimicrobial activity of imidazolium and pyridinium ionic liquids.* Green Chemistry, 2005. **7**(4): p. 185-189.

34. Freire, M.G.,Carvalho, P.J.,Gardas, R.L.,Marrucho, I.M.,Santos, L.M.N.B.F., and Coutinho, J.A.P., *Mutual Solubilities of Water and the [Cnmim][Tf2N] Hydrophobic Ionic Liquids.* The Journal of Physical Chemistry B, 2008. **112**(6): p. 1604-1610.

35. Freire, M.G.,Neves, C.M.S.S.,Carvalho, P.J.,Gardas, R.L.,Fernandes, A.M.,Marrucho, I.M.,Santos, L.M.N.B.F., and Coutinho, J.A.P., *Mutual Solubilities of Water and Hydrophobic Ionic Liquids.* The Journal of Physical Chemistry B, 2007. **111**(45): p. 13082-13089.

36. Ranke, J.,Müller, A.,Bottin-Weber, U.,Stock, F.,Stolte, S.,Arning, J.,Störmann, R., and Jastorff, B., *Lipophilicity parameters for ionic liquid cations and their correlation to in vitro cytotoxicity.* Ecotoxicology and Environmental Safety, 2007. **67**(3): p. 430-438.

37. Ventura, S.P.M.,Marques, C.S.,Rosatella, A.A.,Afonso, C.A.M.,Gonçalves, F., and Coutinho, J.A.P., *Toxicity assessment of various ionic liquid families towards Vibrio fischeri marine bacteria.* Ecotoxicology and Environmental Safety, 2012. **76**(0): p. 162-168.

38. Seddon, K.R.,Stark, A., and Torres, M.J., *Influence of chloride, water, and organic solvents on the physical properties of ionic liquids.* Pure and Applied Chemistry, 2000. **72**(12): p. 2275-2287.

39. Martínez-Aragón, M.,Burghoff, S.,Goetheer, E.L.V., and de Haan, A.B., *Guidelines for solvent selection for carrier mediated extraction of proteins.* Separation and Purification Technology, 2009. **65**(1): p. 65-72.

40. Kula, M.-R.,Kroner, K.H., and Hustedt, H., Advanced Biochemical Engineering/ Biotechnology, 1982. **24**: p. 73.

41. Daugulis, A.J.,Axford, D.B.,Ciszek, B., and Malinowski, J.J., *Continuous fermentation of high-strength glucose feeds to ethanol.* Biotechnology Letters, 1994. **16**(6): p. 637-642.

42. Rydberg, J.,Musikas, C., and Choppin, G.R., *Principles and practices of solvent extraction*. 1992: M. Dekker.

43. Albertsson, P.Å., *Partition of proteins in liquid polymer-polymer two-phase systems.* Nature, 1958. **182**(4637): p. 709-711.

44. Albertsson, P.A., *Partitioning of Cell Particles and Macromolecules*. 3 ed. 1986, New York: Wiley-Interscience.

45. Walter, H.,Brooks, D.E., and Fisher, D., *Partitioning in Aqueous Two-Phase Systems*. 1985, New York: Academic Press:.

46. Zaslavsky, B.Y., *Aqueous Two-Phase Partitioning, Physical Chemistry and Bioanalytical Applications*. 1995, New York: Dekker.

47. Willauer, H.D.,Huddleston, J.G., and Rogers, R.D., *Solvent Properties of Aqueous Biphasic Systems Composed of Polyethylene Glycol and Salt Characterized by the Free Energy of Transfer of a Methylene Group between the Phases and by a Linear Solvation Energy Relationship.* Industrial & Engineering Chemistry Research, 2002. **41**(11): p. 2591-2601.

48. D.Rogers, R. and Zhang, J., *New Technologies for Metal Ion Separations Polyethylene Glycol Based-Aqueous Biphasic Systems and Aqueous Biphasic Extraction Chromatography.*, in *Ion Exchange Solvent Extraction*. 1997, Marinsky, J. A., Marcus, Y., Eds., Dekker: New York. p. 141-193.

49. Gutowski, K.E.,Broker, G.A.,Willauer, H.D.,Huddleston, J.G.,Swatloski, R.P.,Holbrey, J.D., and Rogers, R.D., *Controlling the Aqueous Miscibility of Ionic Liquids: Aqueous Biphasic Systems of Water-Miscible Ionic Liquids and Water-Structuring Salts for Recycle, Metathesis, and Separations.* Journal of the American Chemical Society, 2003. **125**(22): p. 6632-6633.

50. Zafarani-Moattar, M.T. and Hamzehzadeh, S., *Liquid-liquid equilibria of aqueous two-phase systems containing 1-butyl-3-methylimidazolium bromide and potassium phosphate or dipotassium hydrogen phosphate at 298.15 K.* Journal of Chemical and Engineering Data, 2007. **52**(5): p. 1686-1692.

51. Ventura, S.P.M.,Neves, C.M.S.S.,Freire, M.G.,Marrucho, I.M.,Oliveira, J., and Coutinho, J.A.P., *Evaluation of anion influence on the formation and extraction capacity of ionic-liquid-based aqueous biphasic systems.* Journal of Physical Chemistry B, 2009. **113**(27): p. 9304-9310.

52. Neves, C.M.S.S.,Ventura, S.P.M.,Freire, M.G.,Marrucho, I.M., and Coutinho, J.A.P., *Evaluation of cation influence on the formation and extraction capability of ionic-liquid-based aqueous biphasic systems.* Journal of Physical Chemistry B, 2009. **113**(15): p. 5194-5199.

53. He, C.,Li, S.,Liu, H.,Li, K., and Liu, F., *Extraction of testosterone and epitestosterone in human urine using aqueous two-phase systems of ionic liquid and salt.* Journal of Chromatography A, 2005. **1082**(2): p. 143-149.

54. Li, S.,He, C.,Liu, H.,Li, K., and Liu, F., *Ionic liquid-based aqueous two-phase system, a sample pretreatment procedure prior to high-performance liquid chromatography of opium alkaloids.* Journal of Chromatography B, 2005. **826**(1-2): p. 58-62.

55. Soto, A.,Arce, A., and Khoshkbarchi, M.K., *Partitioning of antibiotics in a two-liquid phase system formed by water and a room temperature ionic liquid*. Separation and Purification Technology, 2005. **44**(3): p. 242-246.

56. Najdanovic-Visak, V.,Canongia Lopes, J.N.,Visak, Z.P.,Trindade, J., and Rebelo, L.P.N., *Salting-out in aqueous solutions of ionic liquids and K3PO 4: Aqueous biphasic systems and salt precipitation.* International Journal of Molecular Sciences, 2007. **8**(8): p. 736-748.

57. Hofmeister, F., *Arch. Exp. Pathol. Pharmakol.* Vol. XXV. 1888.

58. Domínguez-Pérez, M.,Tomé, L.I.N.,Freire, M.G.,Marrucho, I.M.,Cabeza, O., and Coutinho, J.A.P., *(Extraction of biomolecules using) aqueous biphasic systems formed by ionic liquids and aminoacids.* Separation and Purification Technology, 2010. **72**(1): p. 85-91.

59. Freire, M.G.,Neves, C.M.S.S.,Marrucho, I.M.,Canongia Lopes, J.N.,Rebelo, L.P.N., and Coutinho, J.A.P., *High-performance extraction of alkaloids using aqueous two-phase systems with ionic liquids.* Green Chemistry, 2010. **12**(10): p. 1715-1718.

60. Louros, C.L.S.,Cláudio, A.F.M.,Neves, C.M.S.S.,Freire, M.G.,Marrucho, I.M.,Pauly, J., and Coutinho, J.A.P., *Extraction of Biomolecules Using Phosphonium-Based Ionic Liquids + K3PO4 Aqueous Biphasic Systems.* International Journal of Molecular Sciences, 2010. **11**(4): p. 1777-1791.

61. Freire, M.G.,Louros, C.L.S.,Rebelo, L.P.N., and Coutinho, J.A.P., *Aqueous biphasic systems composed of a water-stable ionic liquid + carbohydrates and their applications.* Green Chemistry, 2011. **13**(6): p. 1536-1545.

62. Dreyer, S.,Salim, P., and Kragl, U., *Driving forces of protein partitioning in an ionic liquid-based aqueous two-phase system.* Biochemical Engineering Journal, 2009. **46**(2): p. 176-185.

63. Ruiz-Angel, M.J.,Pino, V.,Carda-Broch, S., and Berthod, A., *Solvent systems for countercurrent chromatography: An aqueous two phase liquid system based on a room temperature ionic liquid.* Journal of Chromatography A, 2007. **1151**(1–2): p. 65-73.

64. Cláudio, A.F.M.,Freire, M.G.,Freire, C.S.R.,Silvestre, A.J.D., and Coutinho, J.A.P., *Extraction of vanillin using ionic-liquid-based aqueous two-phase systems.* Separation and Purification Technology, 2010. **75**(1): p. 39-47.

65. Cláudio, A.F.M.,Ferreira, A.M.,Freire, C.S.R.,Silvestre, A.J.D.,Freire, M.G., and Coutinho, J.A.P., *Optimization of the gallic acid extraction using ionic-liquid-based aqueous two-phase systems.* Separation and Purification Technology, 2012(0).

66. Zhang, D.,Deng, Y., and Chen, J., *Enrichment of Aromatic Compounds Using Ionic Liquid and Ionic Liquid-Based Aqueous Biphasic Systems.* Separation Science and Technology, 2010. **45**(5): p. 663-669.

67. Akama, Y.,Ito, M., and Tanaka, S., *Selective separation of cadmium from cobalt, copper, iron (III) and zinc by water-based two-phase system of tetrabutylammonium bromide.* Talanta, 2000. **53**(3): p. 645-650.

68. Akama, Y. and Sali, A., *Extraction mechanism of Cr(VI) on the aqueous two-phase system of tetrabutylammonium bromide and (NH4)2SO4 mixture.* Talanta, 2002. **57**(4): p. 681-686.

69. Freire, M.G.,Claudio, A.F.M.,Araujo, J.M.M.,Coutinho, J.A.P.,Marrucho, I.M.,Lopes, J.N.C., and Rebelo, L.P.N., *Aqueous biphasic systems: a boost brought about by using ionic liquids.* Chemical Society Reviews, 2012. **41**(14): p. 4966-4995.

70. Freire, M.G.,Neves, C.M.S.S.,Canongia Lopes, J.N.,Marrucho, I.M.,Coutinho, J.A.P., and Rebelo, L.P.N., *Impact of Self-Aggregation on the Formation of Ionic-Liquid-Based Aqueous Biphasic Systems.* The Journal of Physical Chemistry B, 2012.

71. Mourão, T.,Cláudio, A.F.M.,Boal-Palheiros, I.,Freire, M.G., and Coutinho, J.A.P., *Evaluation of the impact of phosphate salts on the formation of ionic-liquid-based aqueous biphasic systems.* The Journal of Chemical Thermodynamics, (0).

72. Shahriari, S.,Neves, C.M.S.S.,Freire, M.G., and Coutinho, J.A.P., *Role of the Hofmeister Series in the Formation of Ionic-Liquid-Based Aqueous Biphasic Systems.* The Journal of Physical Chemistry B, 2012. **116**(24): p. 7252-7258.

73. Zhang, J.,Zhang, Y.,Chen, Y., and Zhang, S., *Mutual coexistence curve measurement of aqueous biphasic systems composed of [bmim][BF4] and glycine, L-serine, and L-proline, respectively.* Journal of Chemical and Engineering Data, 2007. **52**(6): p. 2488-2490.

74. Wu, B.,Zhang, Y., and Wang, H., *Phase behavior for ternary systems composed of ionic liquid + saccharides + water.* Journal of Physical Chemistry B, 2008. **112**(20): p. 6426-6429.

75. Wu, B.,Zhang, Y.,Wang, H., and Yang, L., *Temperature dependence of phase behavior for ternary systems composed of ionic liquid + sucrose + water.* Journal of Physical Chemistry B, 2008. **112**(41): p. 13163-13165.

76. Chen, Y.,Wang, Y.,Cheng, Q.,Liu, X., and Zhang, S., *Carbohydrates-tailored phase tunable systems composed of ionic liquids and water.* The Journal of Chemical Thermodynamics, 2009. **41**(9): p. 1056-1059.

77. Li, Z.,Pei, Y.,Liu, L., and Wang, J., *(Liquid plus liquid) equilibria for (acetate-based ionic liquids plus inorganic salts) aqueous two-phase systems.* The Journal of Chemical Thermodynamics, 2010. **42**(7): p. 932-937.

78. Han, J.,Yu, C.,Wang, Y.,Xie, X.,Yan, Y.,Yin, G., and Guan, W., *Liquid–liquid equilibria of ionic liquid 1-butyl-3-methylimidazolium tetrafluoroborate and sodium citrate/tartrate/acetate aqueous two-phase systems at 298.15 K: Experiment and correlation.* Fluid Phase Equilibria, 2010. **295**(1): p. 98-103.

79. Zafarani-Moattar, M.T. and Hamzehzadeh, S., *Phase Diagrams for the Aqueous Two-Phase Ternary System Containing the Ionic Liquid 1-Butyl-3-methylimidazolium Bromide and Tri-potassium Citrate at T = (278.15, 298.15, and 318.15) K.* Journal of Chemical & Engineering Data, 2008. **54**(3): p. 833-841.

80. Han, J.,Pan, R.,Xie, X.,Wang, Y.,Yan, Y.,Yin, G., and Guan, W., *Liquid–Liquid Equilibria of Ionic Liquid 1-Butyl-3-Methylimidazolium Tetrafluoroborate + Sodium and Ammonium Citrate Aqueous Two-Phase Systems at (298.15, 308.15, and 323.15) K.* Journal of Chemical & Engineering Data, 2010. **55**(9): p. 3749-3754.

81. Sadeghi, R.,Golabiazar, R., and Shekaari, H., *The salting-out effect and phase separation in aqueous solutions of tri-sodium citrate and 1-butyl-3-methylimidazolium bromide.* The Journal of Chemical Thermodynamics, 2010. **42**(4): p. 441-453.

82. Zafarani-Moattar, M.T. and Hamzehzadeh, S., *Salting-out effect, preferential exclusion, and phase separation in aqueous solutions of chaotropic water-miscible ionic liquids and kosmotropic salts: Effects of temperature, anions, and cations.* Journal of Chemical and Engineering Data, 2010. **55**(4): p. 1598-1610.

83. Zafarani-Moattar, M.T. and Hamzehzadeh, S., *Effect of pH on the phase separation in the ternary aqueous system containing the hydrophilic ionic liquid 1-butyl-3-methylimidazolium bromide and the kosmotropic salt potassium citrate at T = 298.15 K.* Fluid Phase Equilibria, 2011. **304**(1-2): p. 110-120.

84. Han, J.,Wang, Y.,Li, Y.,Yu, C., and Yan, Y., *Equilibrium Phase Behavior of Aqueous Two-Phase Systems Containing 1-Alkyl-3-methylimidazolium Tetrafluoroborate and Ammonium Tartrate at Different Temperatures: Experimental Determination and Correlation.* Journal of Chemical & Engineering Data, 2011. **56**(9): p. 3679-3687.

85. Han, J.,Wang, Y.,Yu, C.-l.,Yan, Y.-s., and Xie, X.-q., *Extraction and determination of chloramphenicol in feed water, milk, and honey samples using an ionic liquid/sodium citrate aqueous two-phase system coupled with high-performance liquid chromatography.* Analytical and Bioanalytical Chemistry, 2011. **399**(3): p. 1295-1304.

86. Lu, Y.,Lu, W.,Wang, W.,Guo, Q., and Yang, Y., *Thermodynamic studies of partitioning behavior of cytochrome c in ionic liquid-based aqueous two-phase system.* Talanta, 2011. **85**(3): p. 1621-1626.

87. Zafarani-Moattar, M.T. and Hamzehzadeh, S., *Partitioning of amino acids in the aqueous biphasic system containing the water-miscible ionic liquid 1-butyl-3-methylimidazolium bromide and the water-structuring salt potassium citrate.* Biotechnology Progress, 2011. **27**(4): p. 986-997.

88. Freire, M.G.,Neves, C.M.S.S.,Marrucho, I.M.,Coutinho, J.o.A.P., and Fernandes, A.M., *Hydrolysis of Tetrafluoroborate and Hexafluorophosphate Counter Ions in Imidazolium-Based Ionic Liquids†.* The Journal of Physical Chemistry A, 2009. **114**(11): p. 3744-3749.

89. Bridges, N.J.,Gutowski, K.E., and Rogers, R.D., *Investigation of aqueous biphasic systems formed from solutions of chaotropic salts with kosmotropic salts (salt-salt ABS).* Green Chemistry, 2007. **9**(2): p. 177-183.

90. Pei, Y.,Wang, J.,Liu, L.,Wu, K., and Zhao, Y., *Liquid−Liquid Equilibria of Aqueous Biphasic Systems Containing Selected Imidazolium Ionic Liquids and Salts.* Journal of Chemical & Engineering Data, 2007. **52**(5): p. 2026-2031.

91. Cláudio, A.F.M.,Ferreira, A.M.,Shahriari, S.,Freire, M.G., and Coutinho, J.o.A.P., *Critical Assessment of the Formation of Ionic-Liquid-Based Aqueous Two-Phase Systems in Acidic Media.* The Journal of Physical Chemistry B, 2011. **115**(38): p. 11145-11153.

92. Merchuk, J.C.,Andrews, B.A., and Asenjo, J.A., *Aqueous two-phase systems for protein separation Studies on phase inversion.* Journal of Chromatography B, 1998. **711**(1-2): p. 285-293.

93. Wilkes, J.S.,Levisky, J.A.,Wilson, R.A., and Hussey, C.L., *Dialkylimidazolium chloroaluminate melts: a new class of room-temperature ionic liquids for electrochemistry, spectroscopy and synthesis.* Inorganic Chemistry, 1982. **21**(3): p. 1263-1264.

94. Ning, W.,Xingxiang, Z.,Haihui, L., and Benqiao, H., *1-Allyl-3-methylimidazolium chloride plasticized-corn starch as solid biopolymer electrolytes.* Carbohydrate Polymers, 2009. **76**(3): p. 482-484.

95. *Online Database of Chemicals from Around the World*. 2011 [cited 2011 December]; Available from: www.chemblink.com.

96. Ventura, S.P.M.,Sousa, S.G.,Serafim, L.S.,Lima, Á.S.,Freire, M.G., and Coutinho, J.A.P., *Ionic Liquid Based Aqueous Biphasic Systems with Controlled pH: The Ionic Liquid Cation Effect.* Journal of Chemical & Engineering Data, 2011. **56**(11): p. 4253-4260.

97. Freire, M.G.,Neves, C.M.S.S.,Ventura, S.P.M.,Pratas, M.J.,Marrucho, I.M.,Oliveira, J.,Coutinho, J.A.P., and Fernandes, A.M., *Solubility of non-aromatic ionic liquids in water and correlation using a QSPR approach.* Fluid Phase Equilibria, 2010. **294**(1–2): p. 234-240.

98. Lungwitz, R. and Spange, S., *A hydrogen bond accepting (HBA) scale for anions, including room temperature ionic liquids.* New Journal of Chemistry, 2008. **32**(3): p. 392-394.

99. Blesic, M.,Marques, M.H.,Plechkova, N.V.,Seddon, K.R.,Rebelo, L.P.N., and Lopes, A., *Self-aggregation of ionic liquids: micelle formation in aqueous solution.* Green Chemistry, 2007. **9**(5): p. 481-490.

100. Bowers, J.,Butts, C.P.,Martin, P.J.,Vergara-Gutierrez, M.C., and Heenan, R.K., *Aggregation Behavior of Aqueous Solutions of Ionic Liquids.* Langmuir, 2004. **20**(6): p. 2191-2198.

101. Dorbritz, S.,Ruth, W., and Kragl, U., *Investigation on Aggregate Formation of Ionic Liquids.* Advanced Synthesis & Catalysis, 2005. **347**(9): p. 1273-1279.

102. Miskolczy, Z.,Sebök-Nagy, K.,Biczók, L., and Göktürk, S., *Aggregation and micelle formation of ionic liquids in aqueous solution.* Chemical Physics Letters, 2004. **400**(4-6): p. 296-300.

103. El Seoud, O.A.,Pires, P.A.R.,Abdel-Moghny, T., and Bastos, E.L., *Synthesis and micellar properties of surface-active ionic liquids: 1-Alkyl-3-methylimidazolium chlorides.* Journal of Colloid and Interface Science, 2007. **313**(1): p. 296-304.

104. Dong, B.,Li, N.,Zheng, L.,Yu, L., and Inoue, T., *Surface Adsorption and Micelle Formation of Surface Active Ionic Liquids in Aqueous Solution.* Langmuir, 2007. **23**(8): p. 4178-4182.

105. Baltazar, Q.Q.,Chandawalla, J.,Sawyer, K., and Anderson, J.L., *Interfacial and micellar properties of imidazolium-based monocationic and dicationic ionic liquids.* Colloids and Surfaces A: Physicochemical and Engineering Aspects, 2007. **302**(1-3): p. 150-156.

106. Modaressi, A.,Sifaoui, H.,Mielcarz, M.,Domańska, U., and Rogalski, M., *Influence of the molecular structure on the aggregation of imidazolium ionic liquids in aqueous solutions.* Colloids and Surfaces A: Physicochemical and Engineering Aspects, 2007. **302**(1-3): p. 181-185.

107. Moniruzzaman, M.,Kamiya , N.,Nakashima, K., and Goto , M., *Formation of Reverse Micelles in a Room-Temperature Ionic Liquid.* ChemPhysChem, 2008. **9**(5): p. 689-692.

108. Marták, J. and Schlosser, Š., *Phosphonium ionic liquids as new, reactive extractants of lactic acid.* Chemical Papers, 2006. **60**(5): p. 395-398.

109. García-Río, L. and Méndez, M., *First Kinetic Determination of Partition Coefficients for Organic Compounds between the Three Microenvironments of AOT-Based Microemulsions.* ChemPhysChem, 2007. **8**(14): p. 2112-2118.

110. Rösler, A.,Vandermeulen, G.W.M., and Klok, H.-A., *Advanced drug delivery devices via self-assembly of amphiphilic block copolymers.* Advanced Drug Delivery Reviews, 2001. **53**(1): p. 95-108.

111. Sakono, M.,Kawashima, Y.-m.,Ichinose, H.,Maruyama, T.,Kamiya, N., and Goto, M., *Direct Refolding of Inclusion Bodies Using Reversed Micelles.* Biotechnology Progress, 2004. **20**(6): p. 1783-1787.

112. Vestal, C.R. and Zhang, Z.J., *Synthesis of CoCrFeO4 Nanoparticles Using Microemulsion Methods and Size-Dependent Studies of Their Magnetic Properties.* Chemistry of Materials, 2002. **14**(9): p. 3817-3822.

113. Visser, A.E.,Swatloski, R.P.,Reichert, W.M.,Mayton, R.,Sheff, S.,Wierzbicki, A.,Davis, J.J.H., and Rogers, R.D., *Task-specific ionic liquids for the extraction of metal ions from aqueous solutions.* Chemical Communications, 2001(1): p. 135-136.

114. Visser, A.E.,Swatloski, R.P.,Reichert, W.M.,Mayton, R.,Sheff, S.,Wierzbicki, A.,Davis, J.H., and Rogers, R.D., *Task-Specific Ionic Liquids Incorporating Novel Cations for the Coordination and Extraction of Hg2+ and Cd2+: Synthesis, Characterization, and Extraction Studies.* Environmental Science & Technology, 2002. **36**(11): p. 2523-2529.

115. Machatha, S.G. and Yalkowsky, S.H., *Comparison of the octanol/water partition coefficients calculated by ClogP®, ACDlogP and KowWin® to experimentally determined values.* International Journal of Pharmaceutics, 2005. **294**(1–2): p. 185-192.

116. Sangster, J., *Octanol-Water Partition Coefficients: Fundamentals and Physical Chemistry*. 1997: Wiley.

117. *ChemSpider - The free chemical database*. 2012 [cited 2012 April]; Available from: www.chemspider.com.

118. Pérez-Marŕinez, I.,Sagrado, S., and Medina-Hernández, M.J., *A rapid procedure for the determination of caffeine, theophylline and theobromine in urine by micellar liquid chromatography and direct sample injection.* Analytica Chimica Acta, 1995. **304**(2): p. 195-201.

119. Aswal, V.K. and Goyal, P.S., *Dependence of the size of micelles on the salt effect in ionic micellar solutions.* Chemical Physics Letters, 2002. **364**(1–2): p. 44-50.

120. Corrin, M.L. and Harkins, W.D., *The Effect of Salts on the Critical Concentration for the Formation of Micelles in Colloidal Electrolytes.* Journal of the American Chemical Society, 1947. **69**(3): p. 683-688.

121. O'Neil, M.J. and et al., *The Merck Index - An Encyclopedia of Chemicals, Drugs, and Biologicals (14th Edition - Version 14.8)*. 2006, Merck Sharp & Dohme Corp., a subsidiary of Merck & Co., Inc. p. 211.

122. Lewis, R.J., Sr., *Hawley's Condensed Chemical Dictionary (14th Edition)*. 2002, John Wiley & Sons. p. 147.

123. Lide, D. and Milne, G.W.A., *Handbook of Data on Organic Compounds*. 3 ed. Vol. I. 1994: CRC Press, Inc. Boca Raton.

124. Staples, C.A.,Dome, P.B.,Klecka, G.M.,Oblock, S.T., and Harris, L.R., *A review of the environmental fate, effects, and exposures of bisphenol A.* Chemosphere, 1998. **36**(10): p. 2149-2173.

125. Cousins, I.T.,Staples, C.A.,Klečka, G.M., and Mackay, D., *A Multimedia Assessment of the Environmental Fate of Bisphenol A.* Human and Ecological Risk Assessment: An International Journal, 2002. **8**(5): p. 1107-1135.

126. Dianin, A.P., Zhurnal russkogo fiziko-khimicheskogo obshchestva, 1891. **23**: p. 492.

127. Uglea, C.V. and Negulescu, I.I., *Synthesis and characterization of oligomers*. 1991: CRC Press. 103.

128. Meeting, J.F.W.E., *Toxicological and Health Aspects of Bisphenol A: Summary Report*. 2010: Ottawa.

129. EU, *European Union Risk Assessment Report - Environment Addendum of April 2008 - 4,4'-Isopropylidenediphenol(Bisphenol-A) - Part 1 Environment*. 2010.

130. Mendum, T.,Stoler, E.,VanBenschoten, H., and Warner, J.C., *Concentration of bisphenol A in thermal paper.* Green Chemistry Letters and Reviews, 2010. **99999**(1): p. 1-6.

131. Mendum, T.,Stoler, E.,VanBenschoten, H., and Warner, J.C., *Concentration of bisphenol A in thermal paper.* Green Chemistry Letters and Reviews, 2010. **4**(1): p. 81-86.

132. Sidhu, S.,Gullett, B.,Striebich, R.,Klosterman, J.,Contreras, J., and DeVito, M., *Endocrine disrupting chemical emissions from combustion sources: diesel particulate emissions and domestic waste open burn emissions.* Atmospheric Environment, 2005. **39**(5): p. 801-811.

133. Fu, P. and Kawamura, K., *Ubiquity of bisphenol A in the atmosphere.* Environmental Pollution, 2010. **158**(10): p. 3138-3143.

134. Clayton, E.M.R.,Todd, M.,Dowd, J.B., and Aiello, A.E., *The Impact of Bisphenol A and Triclosan on Immune Parameters in the U.S. Population, NHANES 2003–2006.* Environ Health Perspect, 2010. **119**(3).

135. Meeker, J.D.,Ehrlich, S.,Toth, T.L.,Wright, D.L.,Calafat, A.M.,Trisini, A.T.,Ye, X., and Hauser, R., *Semen quality and sperm DNA damage in relation to urinary bisphenol A among men from an infertility clinic.* Reproductive Toxicology, 2010. **30**(4): p. 532-539.

136. Lang, I.A.,Galloway, T.S.,Scarlett, A.,Henley, W.E.,Depledge, M.,Wallace, R.B., and Melzer, D., *Association of Urinary Bisphenol A Concentration With Medical Disorders and Laboratory Abnormalities in Adults.* JAMA: The Journal of the American Medical Association, 2008. **300**(11): p. 1303-1310.

137. Braun, J.M.,Kalkbrenner, A.E.,Calafat, A.M.,Yolton, K.,Ye, X.,Dietrich, K.N., and Lanphear, B.P., *Impact of Early-Life Bisphenol A Exposure on Behavior and Executive Function in Children.* Pediatrics, 2011. **128**: p. 873.

138. Borrell, B., *Toxicology: The big test for bisphenol A* Nature Biotechnology, 2010. **464**: p. 1122-1124.

139. Calafat, A.M.,Ye, X.,Wong, L.-Y.,Reidy, J.A., and Needham, L.L., *Exposure of the U.S. Population to Bisphenol A and 4-tertiary-Octylphenol: 2003–2004.* Environ Health Perspect, 2007. **116**(1): p. 39-44.

140. Kang, J.-H.,Kondo, F., and Katayama, Y., *Human exposure to bisphenol A.* Toxicology, 2006. **226**(2–3): p. 79-89.

141. Loganathan, S. and Kannan, K., *Occurrence of Bisphenol A in Indoor Dust from Two Locations in the Eastern United States and Implications for Human Exposures.* Archives of Environmental Contamination and Toxicology, 2011. **61**(1): p. 68-73.

142. Schecter, A.,Malik, N.,Haffner, D.,Smith, S.,Harris, T.R.,Paepke, O., and Birnbaum, L., *Bisphenol A (BPA) in U.S. Food.* Environmental Science & Technology, 2010. **44**(24): p. 9425-9430.

143. Zhang, Z.,Alomirah, H.,Cho, H.-S.,Li, Y.-F.,Liao, C.,Minh, T.B.,Mohd, M.A.,Nakata, H.,Ren, N., and Kannan, K., *Urinary Bisphenol A Concentrations and Their Implications for Human Exposure in Several Asian Countries.* Environmental Science & Technology, 2011. **45**(16): p. 7044-7050.

144. USEPA, *Integrated Risk Information System (IRIS) (1993)*. 1993, www.epa.gov/ncea/iris/subst/0356.htm.

145. CEPA, *Order Adding a Toxic Substance to Schedule 1 to the Canadian Environmental Protection Act, 1999*, in *Canada Gazette*. 2010.

146. EFSA, *Scientific Opinion on Bisphenol A: evaluation of a study investigating its neurodevelopmental toxicity, review of recent scientific literature on its toxicity and advice on the Danish risk assessment of Bisphenol A.* EFSA Journal, 2010. **8 (9)**: p. 1829.

147. Fan, J.,Fan, Y.,Pei, Y.,Wu, K.,Wang, J., and Fan, M., *Solvent extraction of selected endocrine-disrupting phenols using ionic liquids.* Separation and Purification Technology, 2008. **61**(3): p. 324-331.

148. Louros, C.L.S., Master thesis, *Extraction of Biomolecules with Aqueous Two Phases Systems*, in Chemistry Department. 2009, University of Aveiro: Aveiro

149. Carwile, J.L. and Michels, K.B., *Urinary bisphenol A and obesity: NHANES 2003-2006.* Environmental Research, 2011. **111**(6): p. 825-830.

150. Markham, D.A.,Waechter, J.M.,Wimber, M.,Rao, N.,Connolly, P.,Chuang, J.C.,Hentges, S.,Shiotsuka, R.N.,Dimond, S., and Chappelle, A.H., *Development of a Method for the Determination of Bisphenol A at Trace Concentrations in Human Blood and Urine and Elucidation of Factors Influencing Method Accuracy and Sensitivity.* Journal of Analytical Toxicology, 2010. **34**(6): p. 293-303.

151. *The UFT / Merck Ionic Liquids Biological Effects Database*. 2011 [cited 2012 February]; Available from: www.il-eco.uft.uni-bremen.de.

152. Sajiki, J.,Takahashi, K., and Yonekubo, J., *Sensitive method for the determination of bisphenol-A in serum using two systems of high-performance liquid chromatography.* Journal of Chromatography B: Biomedical Sciences and Applications, 1999. **736**(1–2): p. 255-261.

7. List of publications

Co-author in:

- Helena Passos, Ana R. Ferreira, Ana Filipa M. Cláudio, João A. P. Coutinho and Mara G. Freire, *Characterization of Aqueous Biphasic Systems Composed of Ionic Liquids and a Citrate-Based Biodegradable Salt*, Biochemical Engineering Journal, 2012, 67, 68-76.
- Helena Passos, Ana C. A. Sousa, M. Ramiro Pastorinho, António J. A. Nogueira, Luís Paulo N. Rebelo, João A. P. Coutinho and Mara G. Freire, *Ionic-Liquid-Based Aqueous Biphasic Systems for Improved Detection of Bisphenol A in Human Fluids*, Analytical Methods, 2012. DOI: 10.1039/C2AY25536G.
- Hugo F. D. Almeida, Helena Passos, José A. Lopes-da-Silva, Ana M. Fernandes, Mara G. Freire and João A. P. Coutinho, *Thermophysical Properties of Acetate-Based Ionic Liquids*, Journal of Chemical and Engineering Data, 2012, accepted for publication.
- Helena Passos, João A. P. Coutinho and Mara G. Freire, *Extraction of Alkaloids: The Impact of Self-Aggregation in Ionic-Liquid-Based Aqueous Biphasic Systems*, Journal of Colloid and Interface Science, 2012, in preparation.

Appendix A

Experimental binodal curves

A.1. Experimental binodal data for systems composed of IL + $C_6H_5K_3O_7$ + H_2O

The phase diagrams of the ternary systems composed of IL + $C_6H_5K_3O_7$ + H_2O obtained in this work with the ones presented in literature are shown in Figure A 1.

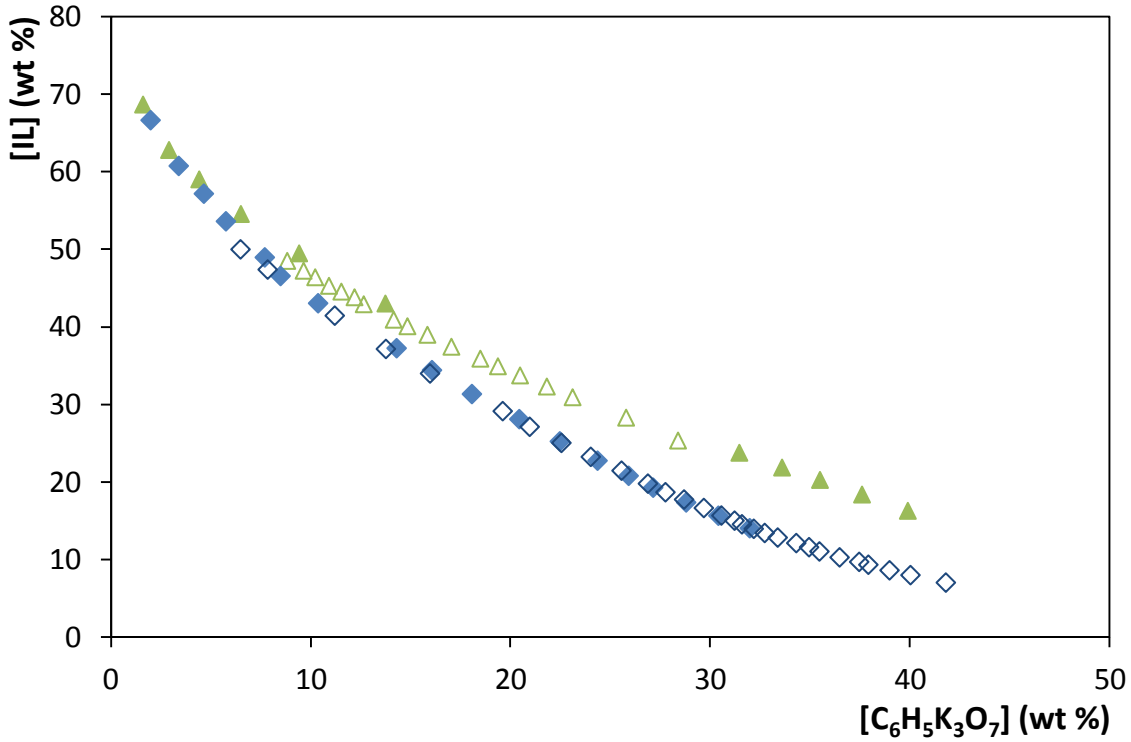

Figure A 1. Phase diagram for the ternary systems composed of IL + $C_6H_5K_3O_7$ + H_2O at 298 K: [C_4mim]Br - this work (◆); literature data (◇)[79]; [C_4mim]Cl – this work (▲); literature data (△)[82].

The experimental weight fraction data for the phase diagrams of the systems composed of IL + $C_6H_5K_3O_7$ + H_2O are presented in Table A 1 to Table A 11.

Table A 1. Experimental weight fraction data for the systems composed of IL (1) + $C_6H_5K_3O_7$ (2) + H_2O (3) at 298 K and atmospheric pressure.

[C_4mim]Cl		[C_4mim]Br		[C_4mim][SCN]	
Mw = 174.67		*Mw* = 219.12		*Mw* = 197.19	
100 w_1	100 w_2	100 w_1	100 w_2	100 w_1	100 w_2
68.640	1.600	66.625	1.978	68.822	1.592
62.787	2.900	60.731	3.387	52.817	2.690
59.000	4.413	57.156	4.645	46.887	3.764
54.537	6.500	53.597	5.749	42.895	4.814
49.469	9.417	48.945	7.697	36.831	6.376
43.003	13.735	46.546	8.486	34.198	6.976
23.776	31.460	43.039	10.365	30.769	8.039
21.874	33.600	37.247	14.297	28.980	8.359
20.279	35.497	34.419	16.068	26.125	9.166
18.395	37.603	31.342	18.068	23.497	10.079
16.299	39.897	28.108	20.440	22.085	10.452
		25.239	22.470	20.634	11.180
		22.755	24.360	20.101	11.467
		20.806	25.918	19.465	11.763
		19.278	27.144	18.609	12.082
		17.375	28.796	18.205	12.316
		15.665	30.410	17.797	12.398
		14.056	31.978	14.635	13.826
				14.309	14.104

Table A 2. Experimental weight fraction data for the systems composed of IL (1) + $C_6H_5K_3O_7$ (2) + H_2O (3) at 298 K and atmospheric pressure.

$[C_4mim][CF_3CO_2]$		$[C_4mim][CF_3SO_3]$			
Mw = 252.23		*Mw* = 288.29			
100 w_1	100 w_2	100 w_1	100 w_2	100 w_1	100 w_2
67.014	1.745	68.129	1.839	12.205	11.709
62.327	3.932	48.631	3.192	11.912	12.364
57.309	6.131	42.434	3.789	11.683	12.405
43.435	10.783	37.824	4.369	11.333	12.893
41.599	11.329	33.839	4.732	11.186	13.006
38.836	12.922	31.666	5.115	10.919	13.256
35.143	14.900	29.577	5.405	10.655	13.462
34.052	15.291	27.890	5.727	10.505	13.527
32.219	16.362	26.419	6.195	10.380	13.635
30.428	17.522	24.369	6.360	10.140	13.838
29.436	17.898	23.618	6.750	9.991	14.106
27.975	18.931	22.614	7.007		
26.334	19.855	21.656	7.266		
25.033	20.610	20.722	7.393		
23.931	21.325	20.168	7.611		
22.782	21.981	19.765	7.853		
21.714	22.665	19.120	8.151		
20.266	23.563	18.475	8.361		
19.320	24.146	17.832	8.561		
18.553	24.725	17.280	8.799		
17.797	25.202	16.905	9.093		
17.141	25.615	16.356	9.260		
16.326	26.200	16.031	9.583		
15.650	26.685	15.537	9.766		
15.190	26.945	15.117	9.929		
14.794	27.096	14.873	10.101		
14.017	27.858	14.510	10.279		
13.723	28.011	14.196	10.412		
13.187	28.627	13.875	10.552		
12.730	28.968	13.464	10.991		
12.345	29.303	13.111	11.314		
12.083	29.423	12.864	11.411		
11.565	30.039	12.614	11.525		
10.928	30.516	12.450	11.661		

Table A 3. Experimental weight fraction data for the systems composed of IL (1) + $C_6H_5K_3O_7$ (2) + H_2O (3) at 298 K and atmospheric pressure.

$[C_4mim][N(CN)_2]$					
Mw = 205.14					
100 w_1	100 w_2	100 w_1	100 w_2	100 w_1	100 w_2
67.802	1.905	16.725	15.356	10.444	19.241
54.433	2.898	16.429	15.538	10.332	19.406
48.910	4.026	16.071	15.706	10.229	19.557
44.529	4.917	15.865	15.812	10.035	19.728
41.224	5.736	15.555	15.919	9.839	19.932
38.737	6.495	15.245	16.039	9.653	20.021
36.848	7.164	15.010	16.251	9.547	20.122
34.973	7.800	14.691	16.356	9.415	20.348
33.335	8.221	14.474	16.554	9.320	20.442
31.963	8.691	14.182	16.595	9.236	20.515
30.685	9.137	13.978	16.788	9.142	20.621
29.487	9.582	13.802	16.932	9.017	20.828
28.609	10.142	13.628	17.084	8.943	20.930
27.520	10.506	13.363	17.155	8.856	20.990
26.555	10.953	13.174	17.314	8.765	21.080
25.572	11.309	13.011	17.471	8.691	21.147
24.755	11.708	12.859	17.590	8.575	21.387
23.881	12.038	12.685	17.768	8.431	21.533
23.058	12.334	12.482	17.850	8.338	21.579
22.532	12.736	12.380	17.689	8.231	21.810
21.774	13.013	12.160	17.698	8.123	22.037
21.074	13.210	12.023	17.846	7.993	22.160
20.644	13.542	11.893	17.980	7.895	22.309
20.069	13.734	11.651	18.256	7.744	22.522
19.607	13.898	11.488	18.261	7.567	22.810
19.182	14.249	11.271	18.557	7.423	23.035
18.656	14.414	11.031	18.797	7.312	23.137
18.161	14.568	10.874	18.845	7.137	23.457
17.826	14.816	10.758	18.939	7.010	23.654
17.354	14.892	10.655	19.034	6.867	23.930
17.066	15.186	10.559	19.120	6.714	24.195

Table A 4. Experimental weight fraction data for the systems composed of IL (1) + $C_6H_5K_3O_7$ (2) + H_2O (3) at 298 K and atmospheric pressure.

$[C_4mim][PO_4(CH_3)_2]$		$[C_4mim][CH_3SO_3]$		$[C_4mim][CH_3CO_2]$	
Mw = 264.14		*Mw* = 234.20		*Mw* = 198.15	
100 w_1	100 w_2	100 w_1	100 w_2	100 w_1	100 w_2
59.812	11.891	52.647	13.214	57.496	9.381
58.622	12.673	51.116	14.824	55.050	11.664
56.744	13.949	48.295	17.427	52.977	13.539
55.598	14.823	43.981	21.106	49.263	16.366
54.202	15.778	42.403	22.498	47.595	17.725
50.972	17.787	40.801	23.963	44.390	20.420
49.948	18.601	39.247	25.430	41.940	22.596
47.972	20.192			40.074	24.385
46.027	21.712				
42.157	25.014				
40.216	26.722				
37.679	28.836				

Table A 5. Experimental weight fraction data for the systems composed of IL (1) + $C_6H_5K_3O_7$ (2) + H_2O (3) at 298 K and atmospheric pressure.

$[C_6mim]Cl$				$[C_7mim]Cl$	
Mw = 202.72				*Mw* = 216.75	
100 w_1	100 w_2	100 w_1	100 w_2	100 w_1	100 w_2
69.004	1.408	69.846	1.754	26.908	26.546
63.451	3.048	63.264	3.595	25.513	27.957
60.865	4.153	56.471	5.946	23.435	29.815
58.119	5.411	51.755	8.401	22.224	31.061
55.576	6.465	48.032	10.314	21.171	32.504
53.213	7.495	39.414	16.296	20.907	33.261
49.909	9.395	38.439	17.065	18.189	35.979
46.825	11.107	34.924	19.623	16.627	38.094
42.778	13.693	34.193	20.242	15.616	40.157
38.176	17.016	33.114	21.060		
30.372	23.272	31.779	22.136		
24.096	28.319	28.346	25.303		

Table A 6. Experimental weight fraction data for the systems composed of IL (1) + $C_6H_5K_3O_7$ (2) + H_2O (3) at 298 K and atmospheric pressure.

[C_8mim]Cl *Mw* = 230.78				[C_{10}mim]Cl *Mw* = 258.83	
100 w_1	100 w_2	100 w_1	100 w_2	100 w_1	100 w_2
50.047	10.383	30.412	24.564	39.466	18.518
45.875	12.817	28.407	26.431	38.139	19.307
43.466	14.349	27.245	27.700	34.597	22.148
40.812	16.152	26.180	28.774	30.918	25.223
37.953	18.198	23.691	31.174	28.553	27.081
35.652	19.944	21.986	32.866	22.956	32.338
33.751	21.496	20.502	34.653	19.112	36.536
32.300	22.709	18.848	36.604	17.579	38.897

Table A 7. Experimental weight fraction data for the systems composed of IL (1) + $C_6H_5K_3O_7$ (2) + H_2O (3) at 298 K and atmospheric pressure.

[C_4mpyr]Cl *Mw* = 177.72					
100 w_1	100 w_2	100 w_1	100 w_2	100 w_1	100 w_2
65.681	2.063	41.083	12.124	30.793	21.097
50.882	6.008	40.639	12.496	29.661	22.131
46.435	8.525	40.059	12.933	28.914	23.012
46.113	8.735	39.663	13.213	27.755	24.131
45.644	8.976	39.243	13.478	26.752	25.344
45.624	9.118	38.693	13.964	25.061	26.853
45.362	9.195	38.125	14.448	23.918	28.144
45.012	9.429	37.519	14.960	22.801	29.608
44.627	9.682	36.902	15.487	20.619	31.882
44.133	9.947	36.163	16.111	19.108	33.819
43.755	10.214	35.810	16.548	16.286	36.595
43.132	10.582	35.109	17.179	15.362	38.125
42.747	10.850	34.197	17.888	13.203	40.753
42.482	11.096	33.620	18.511	12.070	42.632
42.028	11.462	32.581	19.391		
41.572	11.776	31.397	20.316		

Table A 8. Experimental weight fraction data for the systems composed of IL (1) + $C_6H_5K_3O_7$ (2) + H_2O (3) at 298 K and atmospheric pressure.

[C_4mpy]Cl					
Mw = 185.79					
100 w_1	100 w_2	100 w_1	100 w_2	100 w_1	100 w_2
66.913	2.320	34.202	17.582	24.068	27.126
50.603	6.941	33.820	17.897	23.734	27.680
47.681	8.207	33.458	18.293	22.777	28.596
39.828	13.070	32.705	18.858	21.387	30.025
39.601	13.248	32.331	19.264	20.322	31.068
39.298	13.512	31.894	19.709	19.919	31.826
38.883	13.794	31.042	20.328	19.307	32.418
38.681	13.994	30.742	20.625	18.075	33.471
38.223	14.292	30.206	21.167	17.515	34.338
37.567	14.825	29.621	21.685	16.286	35.736
37.294	15.092	29.155	22.256	14.785	37.204
36.744	15.428	28.557	22.814	14.127	38.257
36.485	15.715	27.950	23.448	13.428	39.142
35.959	16.086	27.283	24.081	12.699	40.250
35.672	16.385	26.512	24.800	11.291	42.535
35.077	16.813	25.733	25.496	10.505	43.823
34.758	17.147	24.932	26.314		

Table A 9. Experimental weight fraction data for the systems composed of IL (1) + $C_6H_5K_3O_7$ (2) + H_2O (3) at 298 K and atmospheric pressure.

[C_4mpip]Cl					
Mw = 191.74					
100 w_1	100 w_2	100 w_1	100 w_2	100 w_1	100 w_2
67.511	1.560	36.908	15.535	27.919	23.904
60.511	3.048	36.529	15.898	26.983	24.819
55.603	4.194	36.050	16.301	26.033	25.760
51.288	6.576	35.544	16.689	25.090	26.738
48.392	7.634	35.045	17.137	24.154	27.693
44.293	10.138	34.778	17.370	23.175	28.768
41.028	12.437	34.127	17.948	21.964	29.940
40.470	12.828	33.462	18.561	21.253	30.862
40.074	13.140	32.825	19.136	19.969	32.201
39.886	13.236	32.783	19.038	19.095	33.251
39.553	13.462	32.039	19.799	17.452	34.864
39.135	13.781	31.513	20.353	16.381	36.255
38.888	13.973	30.866	20.970	15.259	37.672
38.375	14.382	30.213	21.636	13.892	39.389
37.994	14.701	29.457	22.358	13.236	40.261
37.475	15.100	28.428	23.272	11.830	42.027

Table A 10. Experimental weight fraction data for the systems composed of IL (1) + $C_6H_5K_3O_7$ (2) + H_2O (3) at 298 K and atmospheric pressure.

$[P_{4444}]Cl$					
Mw = 294.88					
100 w_1	100 w_2	100 w_1	100 w_2	100 w_1	100 w_2
58.615	5.560	16.018	21.566	9.040	28.109
48.752	6.944	15.632	21.918	8.898	28.217
44.978	7.422	15.301	22.229	8.713	28.453
41.690	8.008	15.083	22.318	8.567	28.587
39.230	8.576	14.701	22.663	8.426	28.738
37.264	9.152	14.377	23.025	8.278	28.912
35.572	9.565	14.133	23.141	8.134	29.082
34.403	10.185	13.756	23.523	7.987	29.293
32.774	10.653	13.550	23.612	7.890	29.370
30.815	11.472	13.266	23.904	7.739	29.576
29.945	11.865	13.097	23.985	7.596	29.753
29.106	12.239	12.960	24.121	7.456	29.932
28.391	12.628	12.663	24.457	7.285	30.149
27.604	13.153	12.491	24.567	7.162	30.303
26.488	14.022	12.249	24.805	7.025	30.471
25.787	14.359	12.092	24.899	6.946	30.530
24.266	15.595	11.802	25.295	6.797	30.736
23.756	15.842	11.647	25.370	6.663	30.921
23.301	16.071	11.505	25.479	6.540	31.089
22.823	16.325	11.235	25.812	6.432	31.234
22.317	16.602	11.015	26.031	6.318	31.384
21.646	17.189	10.880	26.113	6.202	31.544
21.036	17.666	10.676	26.345	6.089	31.692
20.328	18.224	10.458	26.604	5.976	31.870
19.959	18.434	10.339	26.662	5.862	32.033
19.044	19.115	10.072	27.038	5.774	32.132
18.453	19.702	9.919	27.175	5.693	32.228
17.747	20.163	9.750	27.313	5.592	32.387
17.163	20.506	9.529	27.564	5.497	32.531
16.763	20.881	9.339	27.805	5.394	32.675
16.383	21.245	9.222	27.872		

Table A 11. Experimental weight fraction data for the systems composed of IL (1) + $C_6H_5K_3O_7$ (2) + H_2O (3) at 298 K and atmospheric pressure.

$[N_{4444}]Cl$					
Mw = 277.92					
100 w_1	100 w_2	100 w_1	100 w_2	100 w_1	100 w_2
65.990	1.832	25.606	16.428	13.484	26.668
51.102	4.182	24.666	17.106	12.975	27.226
47.501	5.309	23.475	18.135	12.599	27.663
44.345	6.288	22.703	18.635	12.105	28.202
41.938	6.891	21.704	19.547	11.663	28.693
40.414	7.574	20.785	20.377	11.210	29.189
38.715	8.274	19.913	21.053	10.723	29.777
37.262	8.962	19.090	21.823	10.324	30.241
36.035	9.521	18.396	22.481	9.950	30.660
34.211	10.776	17.825	22.918	9.474	31.259
32.973	11.369	16.509	24.126	9.095	31.749
31.370	12.510	15.784	24.843	8.774	32.143
30.391	12.948	15.064	25.599	8.461	32.540
29.070	13.829	14.514	26.080	8.171	32.912
27.632	14.947	14.245	26.156	7.936	33.185
26.587	15.748	13.859	26.408		

A.2. Experimental binodal data for systems composed of IL + $C_6H_5K_3O_7/C_6H_8O_7$ + H_2O

Figure A 2 depicts the ternary phase diagrams for the systems composed of $[C_4mim]Br$ + $C_6H_5K_3O_7/C_6H_8O_7$ + H_2O obtained in this work and reported in literature.

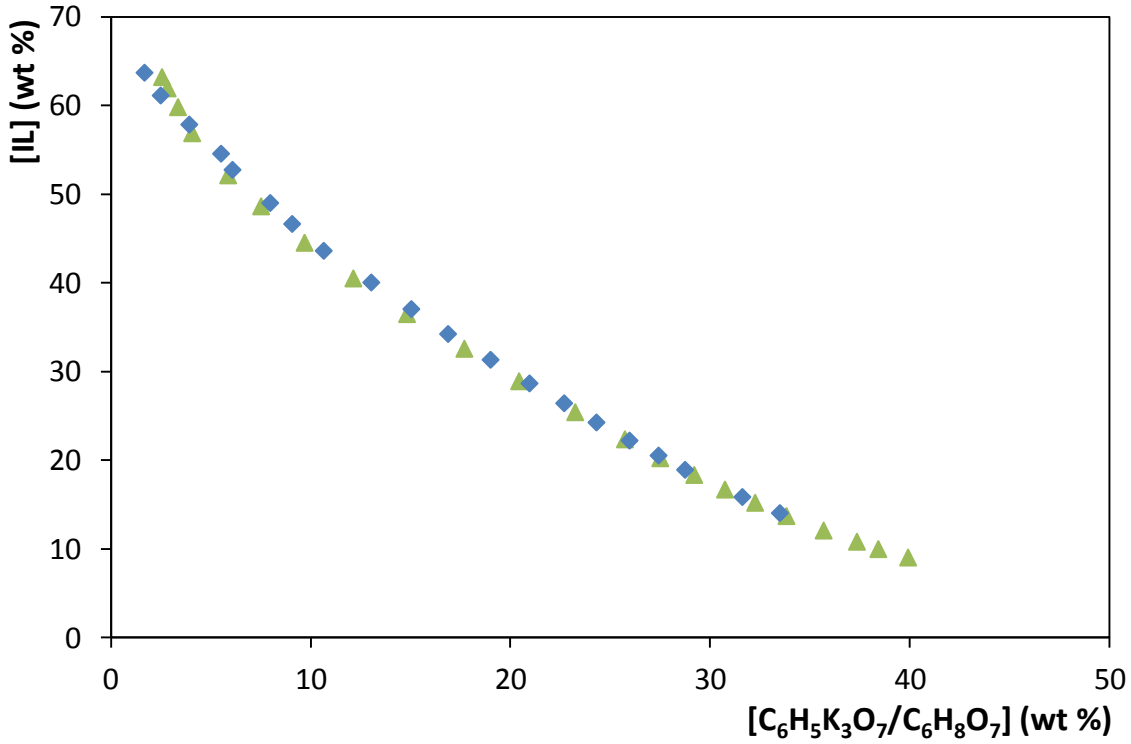

Figure A 2. Phase diagram for the ternary systems composed of $[C_4mim]Br$ + $C_6H_5K_3O_7/C_6H_8O_7$ + H_2O at 298 K: this work (◆); literature data (▲)[83].

The experimental weight fraction data for the systems composed of IL + $C_6H_5K_3O_7/C_6H_8O_7$ + H_2O are presented in Tables A 12 to A 14.

Table A 12. Experimental weight fraction data for the systems composed of IL (1) + $C_6H_5K_3O_7$/$C_6H_8O_7$ (2) + H_2O (3) at 298 K and atmospheric pressure.

[C_4mim]Cl					
Mw = 174.67					
100 w_1	100 w_2	100 w_1	100 w_2	100 w_1	100 w_2
67.890	1.914	42.053	14.439	33.744	21.781
55.757	5.920	41.491	14.776	33.441	22.251
51.509	7.956	41.481	14.928	33.031	22.231
50.129	8.487	41.103	15.122	32.552	22.817
49.906	8.701	40.615	15.543	32.100	23.389
47.945	9.602	40.217	15.835	31.480	23.798
47.529	9.900	39.407	16.624	31.342	24.373
47.241	10.308	39.216	16.609	30.250	24.861
47.109	10.511	38.646	17.256	29.875	25.657
46.566	10.900	38.421	17.339	29.013	26.223
46.181	11.258	37.782	17.929	28.900	26.845
45.424	11.753	37.548	18.082	27.034	28.482
44.806	12.177	37.543	18.390	25.730	30.015
44.083	12.687	36.857	18.697	25.087	30.909
43.964	13.013	36.678	19.158	22.710	33.263
43.497	13.127	36.206	19.275	20.880	35.275
42.822	13.919	35.869	19.908	19.021	37.240
42.746	13.711	35.045	20.302	16.950	39.553
42.581	13.860	34.801	20.824		
42.069	14.317	34.070	21.241		

Table A 13. Experimental weight fraction data for the systems composed of IL (1) + $C_6H_5K_3O_7$/$C_6H_8O_7$ (2) + H_2O (3) at 298 K and atmospheric pressure.

[C_6mim]Cl				[C_7mim]Cl	
Mw = 202.72				*Mw* = 216.75	
100 w_1	100 w_2	100 w_1	100 w_2	100 w_1	100 w_2
64.978	3.843	36.575	18.073	49.703	9.614
57.815	5.325	35.737	19.025	46.378	12.033
52.263	8.138	34.540	19.915	43.489	13.569
45.801	11.674	33.258	21.048	40.357	15.975
44.730	12.344	32.027	22.179	35.702	19.763
43.832	12.957	30.547	23.569	31.217	23.643
43.571	13.547	29.305	24.826	27.359	27.738
42.820	13.583	27.300	26.635	24.028	30.980
41.961	14.172	25.947	28.031	20.246	35.088
41.048	14.753	24.162	29.940	16.528	39.753
40.066	15.472	21.197	33.079		
39.465	15.956	19.323	35.344		
38.682	16.945	17.034	38.251		
37.875	17.133	15.249	40.511		

Table A 14. Experimental weight fraction data for the systems composed of IL (1) + $C_6H_5K_3O_7$/$C_6H_8O_7$ (2) + H_2O (3) at 298 K and atmospheric pressure.

[C_8mim]Cl		[C_{10}mim]Cl	
Mw = 230.78		*Mw* = 258.83	
100 w_1	100 w_2	100 w_1	100 w_2
49.672	10.918	37.892	18.181
45.410	13.664	36.333	19.797
42.690	15.503	34.532	21.813
39.906	17.530	30.351	26.615
36.548	20.151	26.127	30.554
34.740	21.649	22.138	34.874
31.749	24.215	20.506	36.833
29.305	26.480	18.253	41.062
27.590	28.221		
24.626	31.159		
21.615	34.437		

The pH effect in the ternary phase diagrams composed of IL + citrate salt + H_2O is depicted in Figure A 3.

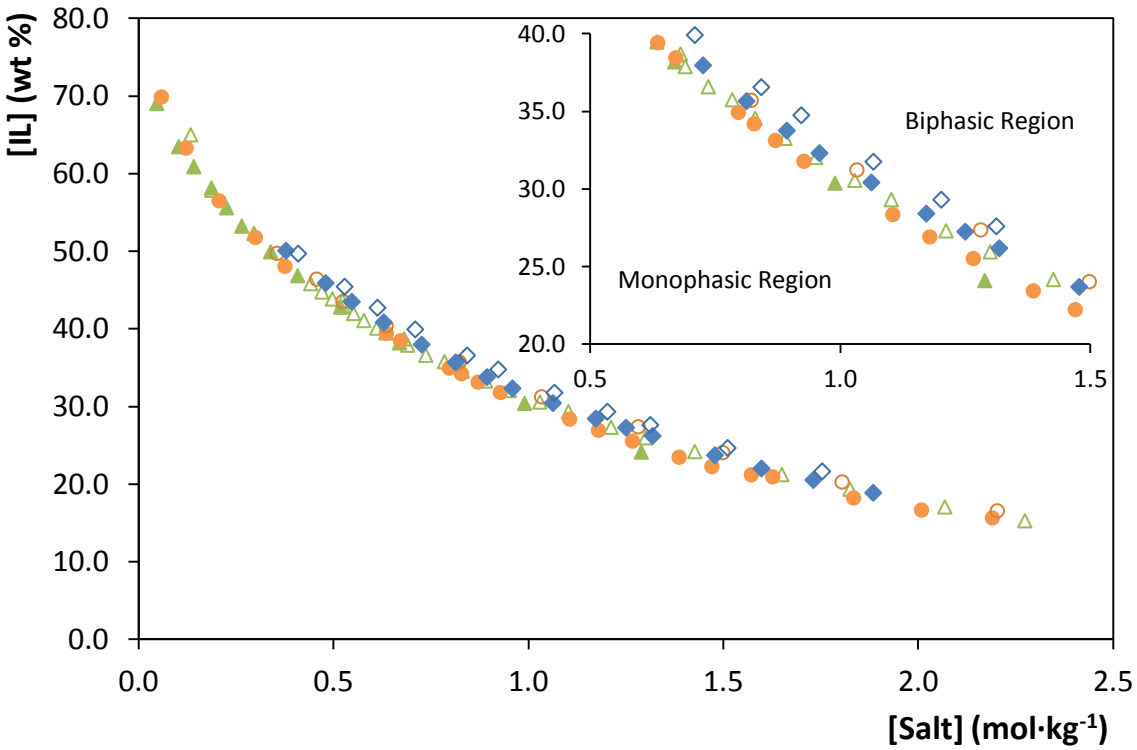

Figure A 3. Evaluation of the pH effect in the ternary phase diagrams composed of $[C_6mim]Cl + H_2O + C_6H_5K_3O_7$ (▲); $[C_6mim]Cl + H_2O + C_6H_5K_3O_7/C_6H_8O_7$ (△); $[C_7mim]Cl + H_2O + C_6H_5K_3O_7$ (●); $[C_7mim]Cl + H_2O + C_6H_5K_3O_7/C_6H_8O_7$ (○); $[C_8mim]Cl + H_2O + C_6H_5K_3O_7$ (◆); $[C_8mim]Cl + H_2O + C_6H_5K_3O_7/C_6H_8O_7$ (◇).

A.3. Experimental binodal data for systems composed of IL + K_3PO_4 + H_2O

In Tables A 15 to Table A 17 are presented the weight fraction data for the systems composed of IL + K_3PO_4 + H_2O.

Table A 15. Experimental weight fraction data for the systems composed of IL (1) + K_3PO_4 (2) + H_2O (3) at 298 K and atmospheric pressure.

[C_4mpyr]Cl					
Mw = 177.72					
100 w_1	100 w_2	100 w_1	100 w_2	100 w_1	100 w_2
35.098	4.192	17.134	14.609	11.627	19.555
32.457	4.757	16.731	15.092	11.497	19.748
30.695	6.096	16.247	15.426	11.362	19.926
28.931	6.834	15.881	15.742	11.180	20.083
28.008	7.462	15.506	16.139	11.026	20.248
26.638	8.185	15.298	16.240	10.875	20.344
25.791	8.857	14.964	16.593	10.724	20.614
24.439	9.798	14.598	16.989	10.490	20.798
23.476	10.237	14.351	17.169	10.309	21.002
22.832	10.629	13.978	17.649	10.160	21.149
22.410	10.839	13.633	17.791	10.003	21.312
21.750	11.407	13.483	17.924	9.866	21.435
21.209	11.822	13.293	18.070	9.646	21.819
20.876	11.908	13.126	18.247	9.443	21.960
20.507	12.100	12.922	18.477	9.235	22.192
19.885	12.649	12.811	18.577	9.027	22.352
19.211	13.085	12.600	18.677	8.892	22.468
18.809	13.361	12.316	19.038	8.689	22.708
18.081	13.871	12.096	19.081	8.439	22.972
17.709	14.155	11.926	19.294	8.221	23.340
17.391	14.443	11.762	19.518		

Table A 16. Experimental weight fraction data for the systems composed of IL (1) + K_3PO_4 (2) + H_2O (3) at 298 K and atmospheric pressure.

$[P_{4444}]Cl$					
Mw = 294.88					
100 w_1	100 w_2	100 w_1	100 w_2	100 w_1	100 w_2
58.808	1.690	11.935	14.729	7.172	17.862
43.217	2.755	11.691	14.850	7.078	17.917
38.450	3.428	11.463	14.996	7.009	18.014
35.139	4.363	11.212	15.118	6.935	18.002
31.460	5.101	10.941	15.277	6.860	18.155
28.856	5.912	10.607	15.654	6.775	18.173
27.349	6.456	10.376	15.663	6.715	18.252
25.966	7.095	10.253	15.844	6.664	18.290
24.585	7.805	10.064	15.950	6.610	18.378
23.314	8.341	9.890	16.049	6.506	18.516
22.236	8.918	9.716	16.173	6.412	18.494
21.055	9.229	9.533	16.252	6.349	18.571
20.363	9.855	9.368	16.378	6.296	18.603
19.332	10.152	9.214	16.450	6.257	18.601
18.675	10.536	9.067	16.568	6.209	18.670
17.976	10.885	8.934	16.603	6.153	18.738
17.545	11.219	8.788	16.639	6.051	18.912
16.960	11.429	8.595	16.959	5.963	18.979
16.529	11.837	8.367	16.982	5.848	19.196
15.935	12.167	8.179	17.255	5.727	19.256
15.426	12.348	8.019	17.219	5.612	19.337
15.056	12.776	7.944	17.287	5.507	19.427
14.590	12.909	7.863	17.359	5.402	19.525
14.177	13.091	7.806	17.392	5.297	19.606
13.917	13.318	7.722	17.523	5.155	19.694
13.591	13.418	7.607	17.566	5.025	19.811
13.341	13.646	7.514	17.553	4.954	19.946
13.125	13.941	7.455	17.625	4.841	19.915
12.802	14.117	7.390	17.742	4.707	20.172
12.424	14.208	7.290	17.679		
12.215	14.494	7.231	17.743		

Table A 17. Experimental weight fraction data for the systems composed of IL (1) + K_3PO_4 (2) + H_2O (3) at 298 K and atmospheric pressure.

$[N_{4444}]Cl$					
Mw= 277.92					
100 w_1	100 w_2	100 w_1	100 w_2	100 w_1	100 w_2
40.732	2.459	12.493	14.605	7.018	18.908
33.216	4.173	12.276	14.798	6.875	19.069
32.175	4.666	12.006	14.914	6.787	19.071
30.945	5.157	11.752	15.077	6.725	19.164
29.500	5.563	11.458	15.437	6.614	19.280
28.344	5.969	11.211	15.557	6.543	19.319
27.359	6.388	11.033	15.772	6.491	19.361
26.348	6.691	10.786	15.875	6.379	19.514
25.642	7.146	10.608	16.046	6.241	19.619
24.663	7.328	10.370	16.104	6.163	19.623
24.227	7.739	10.211	16.310	6.112	19.706
23.308	8.043	10.057	16.500	6.060	19.796
22.715	8.498	9.838	16.613	5.997	19.804
21.937	8.693	9.644	16.711	5.946	19.894
21.406	9.078	9.500	16.882	5.878	19.908
20.803	9.565	9.365	17.019	5.795	20.021
20.110	9.709	9.173	17.100	5.726	20.078
19.410	10.035	9.082	17.141	5.659	20.115
18.915	10.496	8.970	17.295	5.575	20.201
18.295	10.820	8.768	17.461	5.498	20.281
17.852	11.202	8.667	17.603	5.415	20.422
17.222	11.372	8.501	17.659	5.266	20.605
16.802	11.701	8.394	17.789	5.164	20.658
16.449	11.935	8.253	17.825	5.073	20.738
16.057	12.208	8.160	17.957	4.979	20.859
15.599	12.415	8.019	17.979	4.908	20.968
15.338	12.563	7.922	18.120	4.810	21.015
15.053	12.752	7.796	18.181	4.737	21.155
14.825	13.076	7.707	18.307	4.657	21.202
14.490	13.296	7.623	18.449	4.595	21.302
14.178	13.342	7.502	18.429	4.471	21.396
13.918	13.592	7.434	18.482	4.415	21.564
13.644	13.875	7.349	18.595	4.346	21.625
13.277	14.013	7.254	18.700	4.238	21.776
13.028	14.287	7.179	18.788	4.168	21.834
12.709	14.400	7.088	18.809		

Appendix B

NMR spectra

B.1. NMR spectra

The ^{1}H NMR spectra of pure potassium citrate and the pure IL $[C_2mim][N(CN)_2]$ are shown in Figures B 1 and B 2, respectively.

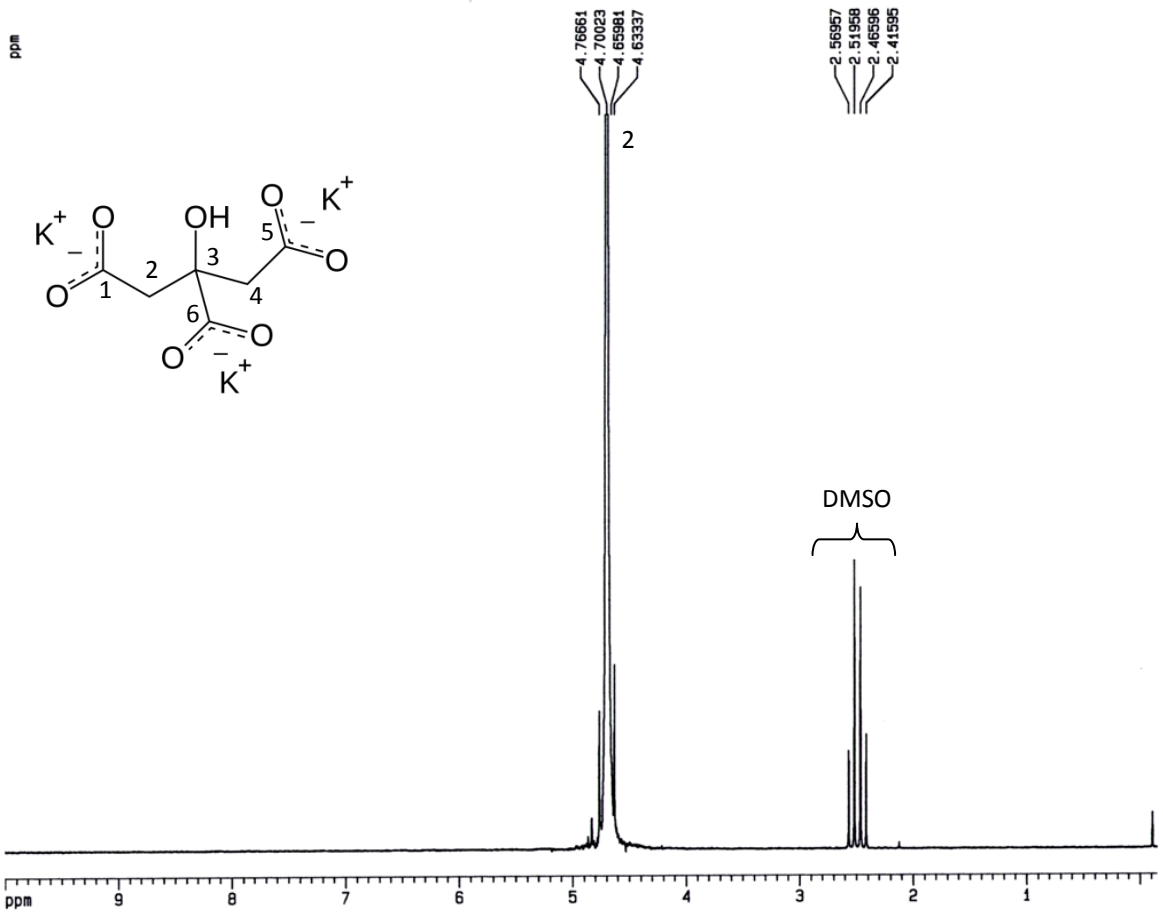

Figure B 1. ^{1}H NMR spectrum of the potassium citrate ($C_6H_5K_3O_7$) in DMSO.

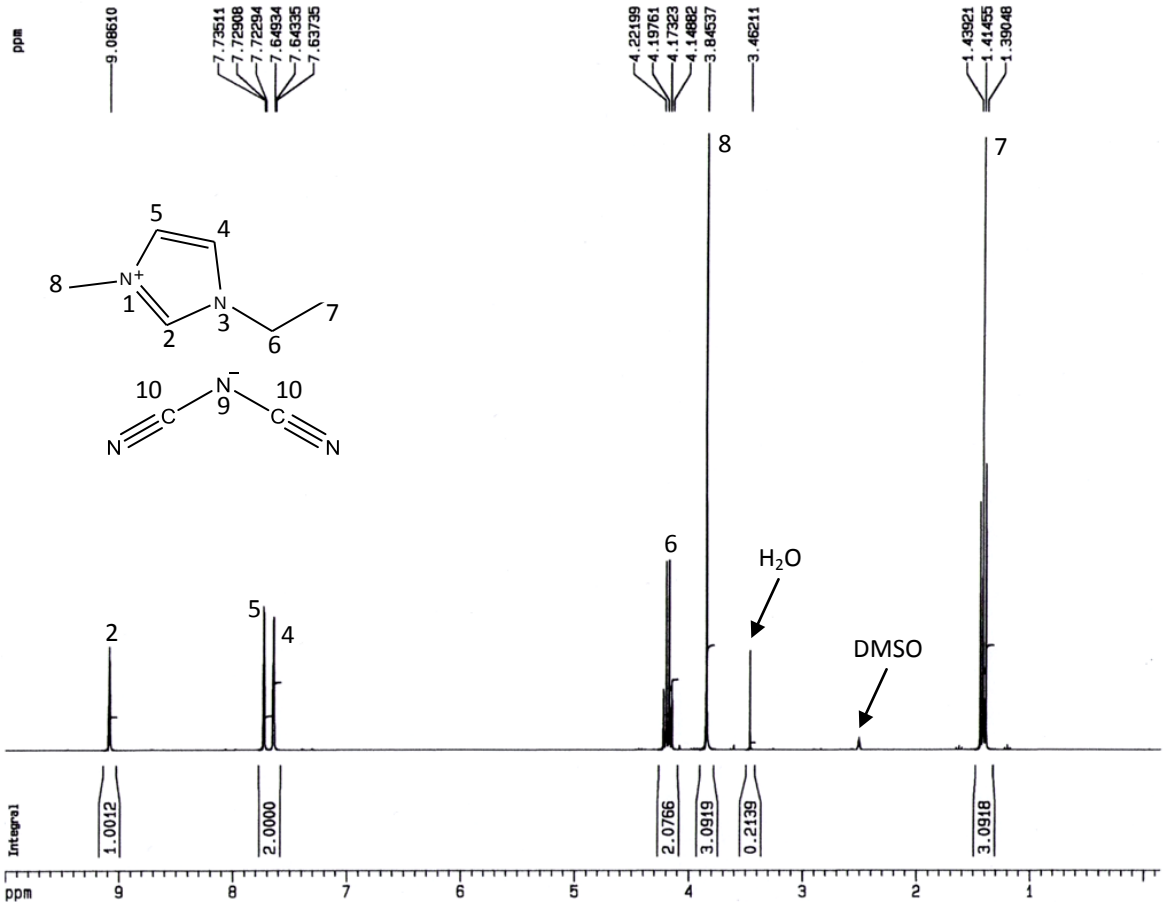

Figure B 2. ^{1}H NMR spectrum of $[C_2mim][N(CN)_2]$ in DMSO.

Figure B 3 presents the ^{1}H RMN spectrum of the solid phase obtained in the determination of ATPS composed of $[C_2mim]Cl + C_6H_5K_3O_7 + H_2O$. Through the comparison of this spectrum with both ^{1}H RMN spectra of pure salt and pure IL it is possible to determine its main composition.

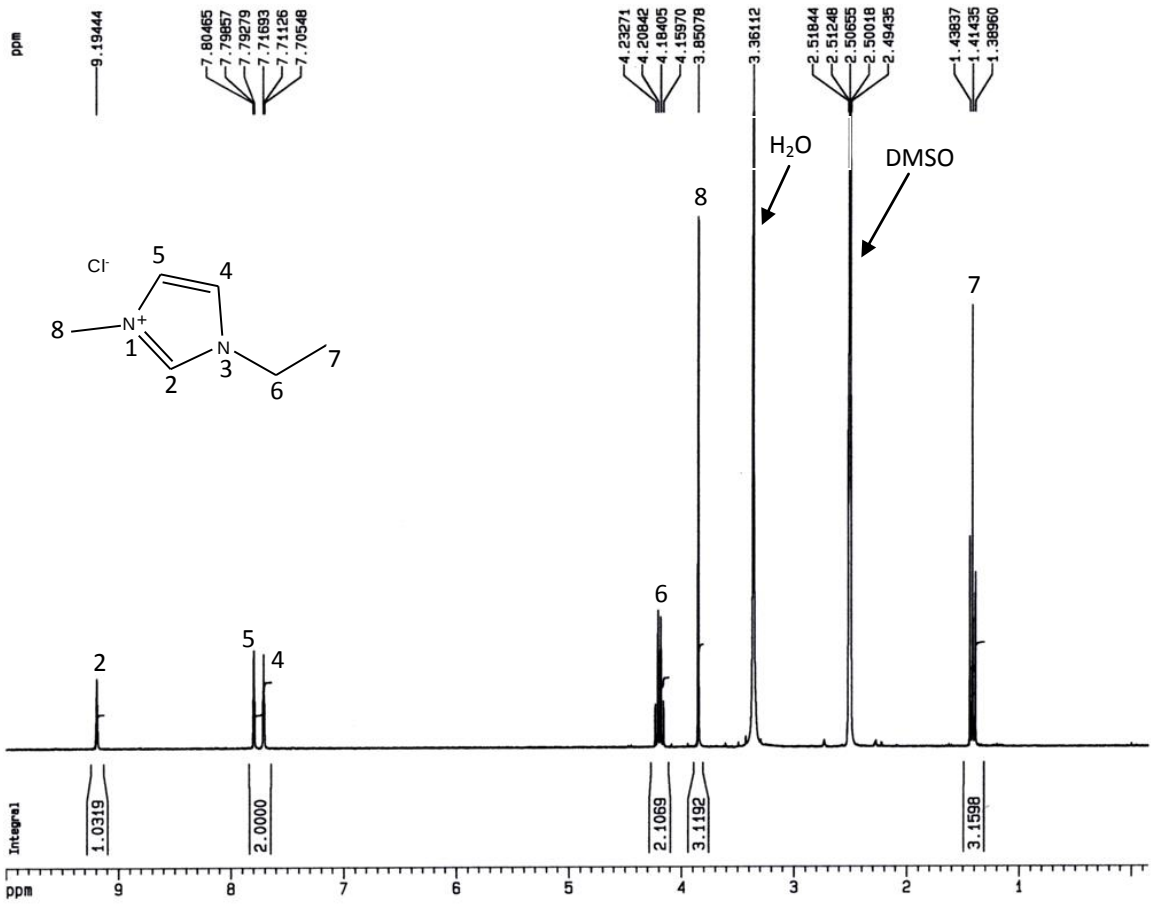

Figure B 3. ^{1}H NMR spectrum of the precipitate observed with the system composed of $[C_2mim]Cl$ + $C_6H_5K_3O_7$ + H_2O.

Appendix C

Calibration curves

C.1. Calibration curves for alkaloids

Figures C 1 to C 4 depict the calibration curves (absorbance *vs.* concentration) of nicotine, caffeine, theophylline and theobromine.

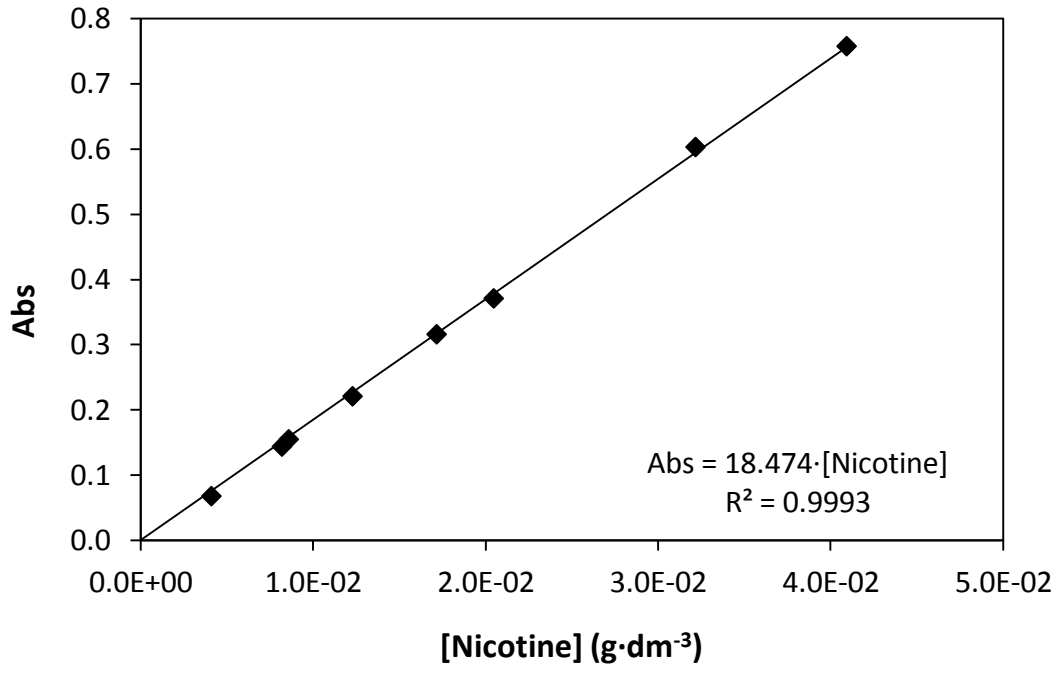

Figure C 1. Calibration curve for nicotine at λ = 260 nm.

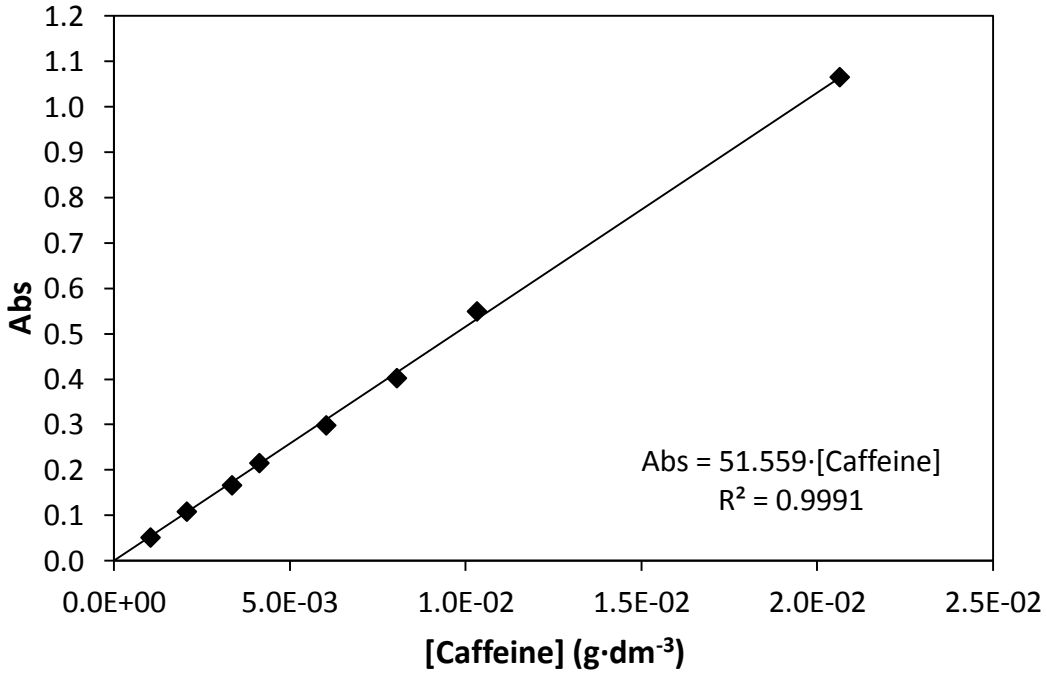

Figure C 2. Calibration curve for caffeine at λ = 273 nm.

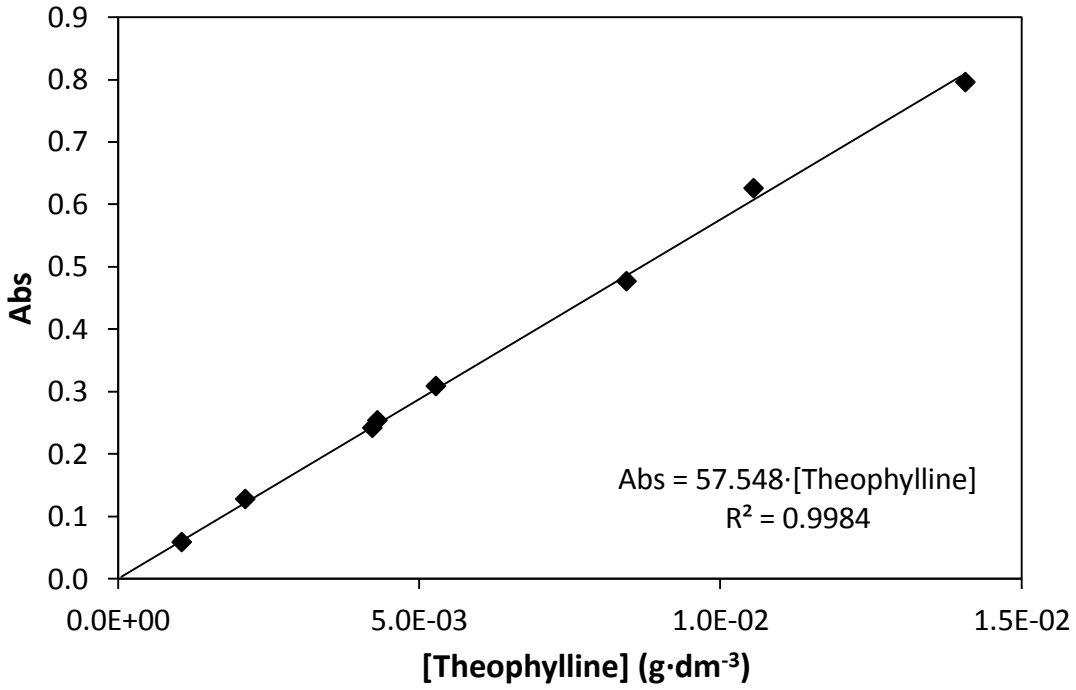

Figure C 3. Calibration curve for theophylline at λ = 272 nm.

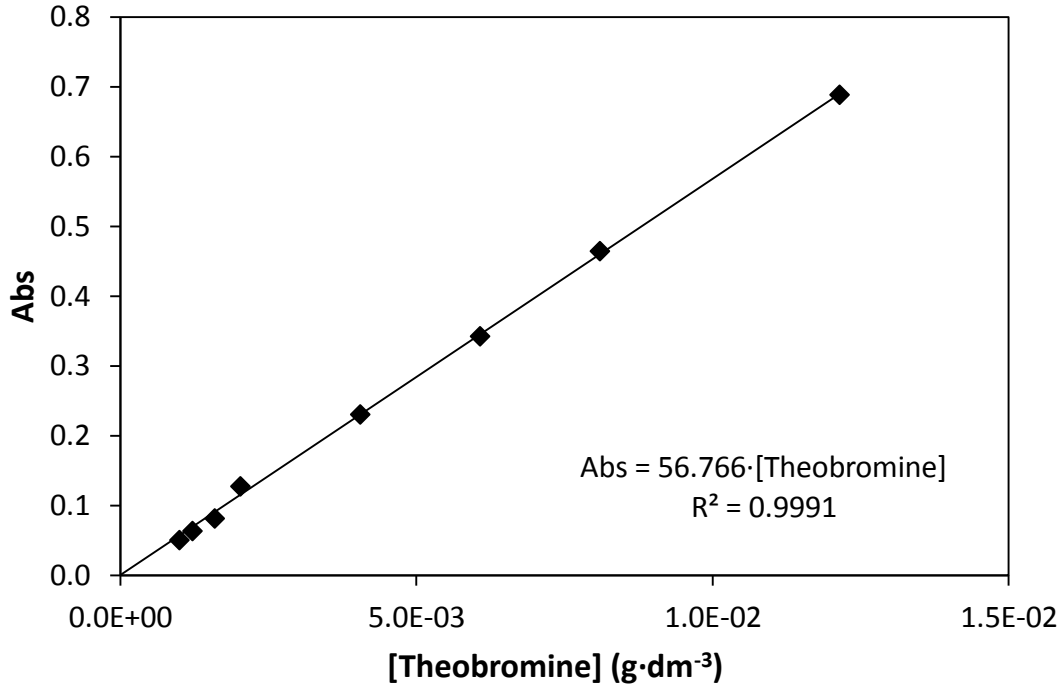

Figure C 4. Calibration curve for theobromine at λ = 273 nm.

C.2. Calibration curve for BPA

In Figure C 5 it is possible to compare the BPA absorbance *vs.* the wavelength behavior at different pH values. Thus, in Figures C 6 and C 7 are presented the calibration curves (absorbance *vs.* concentration) of BPA at the pH values of 7 and 13, respectively.

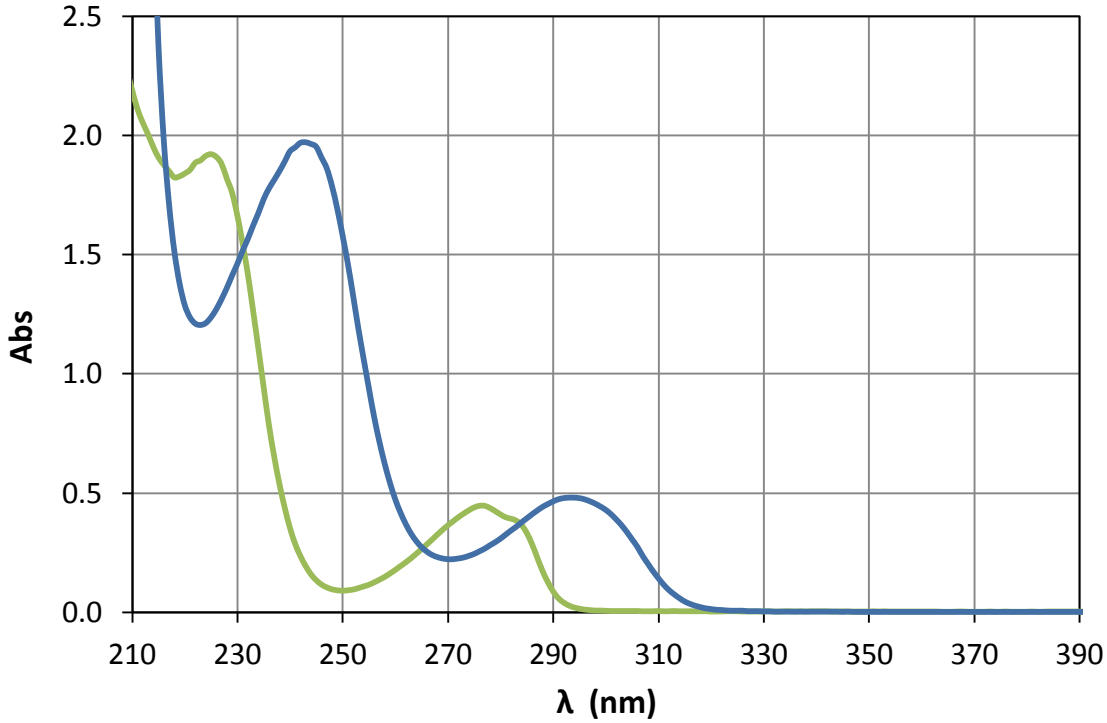

Figure C 5. Absorbance of BPA aqueous solution in function of wavelength: pH ≈ 7 (—); pH ≈ 13 (—).

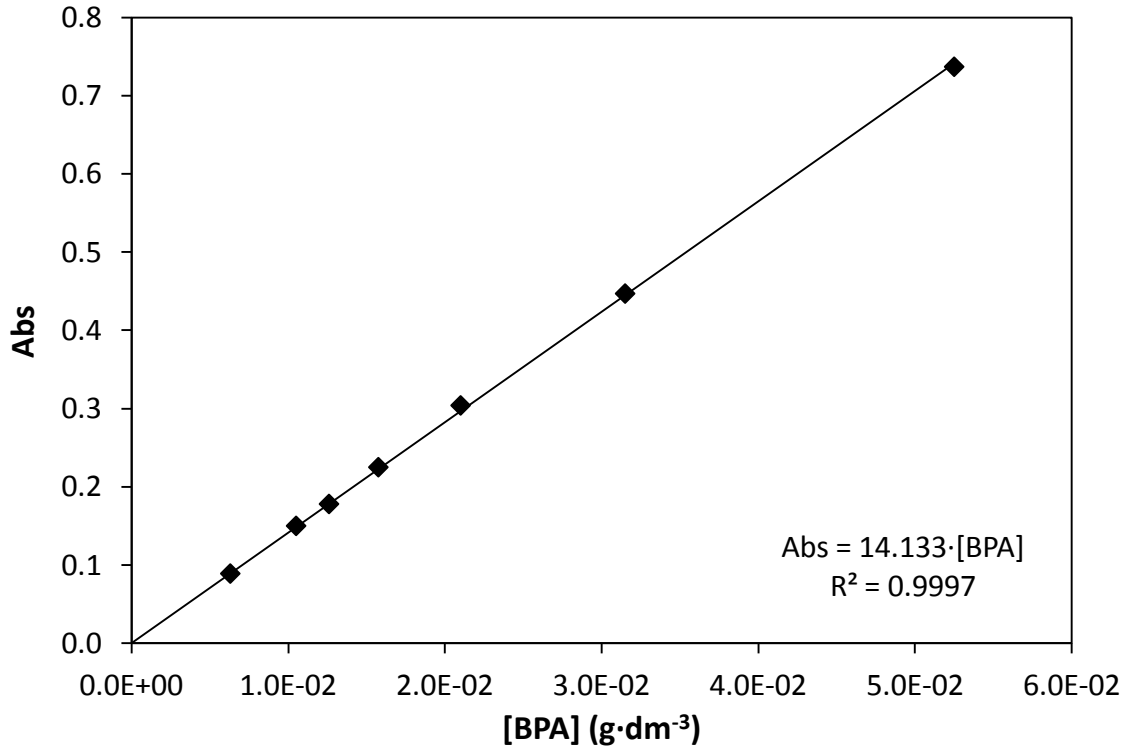

Figure C 6. Calibration curve for BPA at λ= 277 nm and pH ≈ 7.

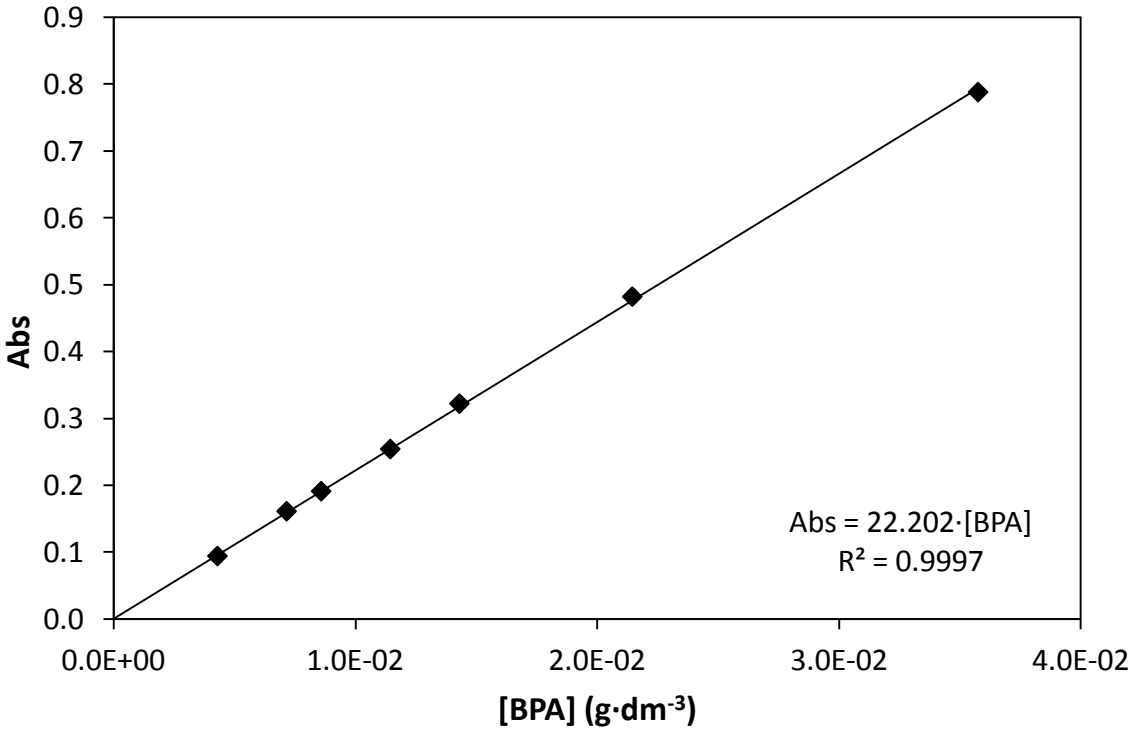

Figure C 7. Calibration curve for BPA at λ = 293 nm and pH ≈ 13.

Appendix D

Experimental data for partitioning of molecules

D.1. Experimental data for partitioning of alkaloids

In Figures D 1 at D 4 are presented the effect of the pH in the concentration of the different molecular species that can exist in aqueous solutions of caffeine, nicotine, theophylline and theobromine, respectively.

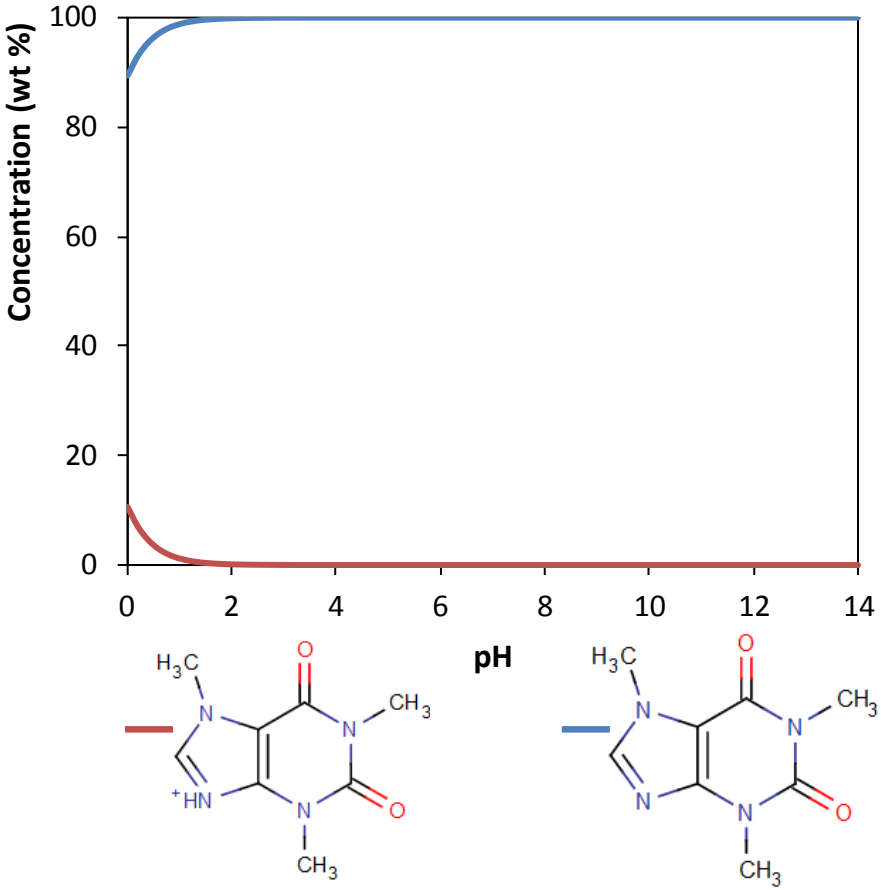

Figure D 1. Speciation diagram of caffeine[117].

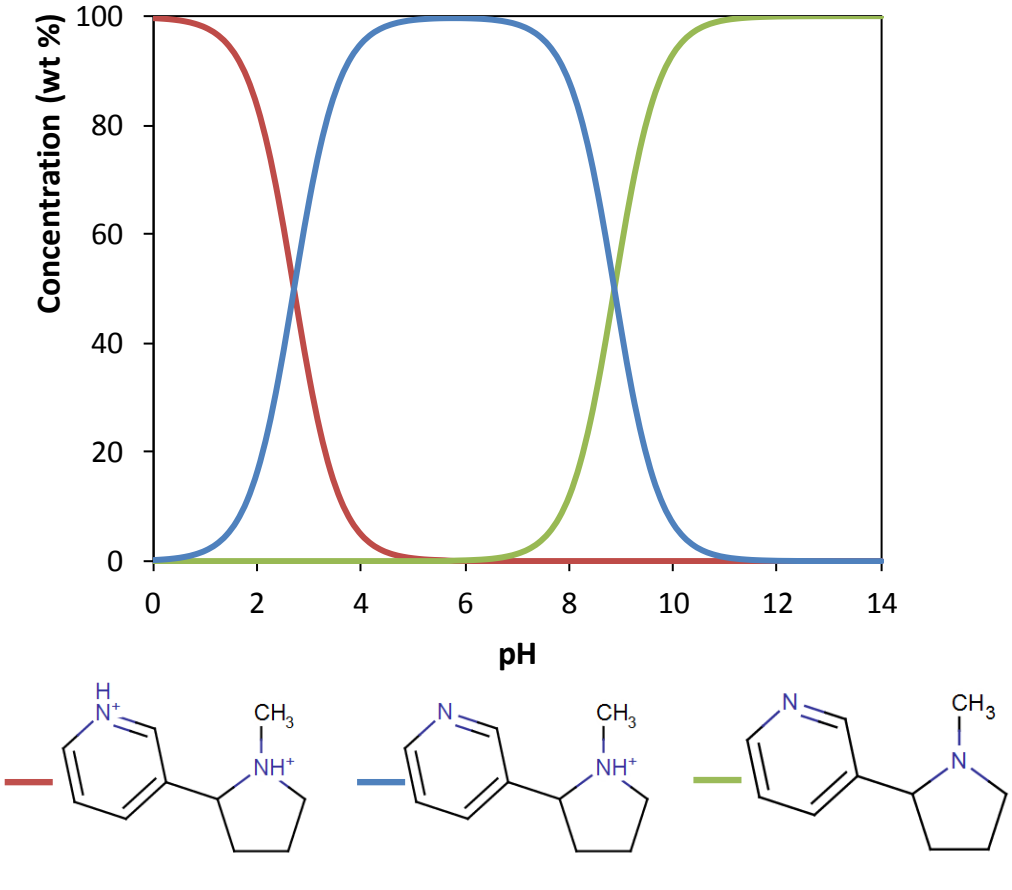

Figure D 2. Speciation diagram of nicotine[117].

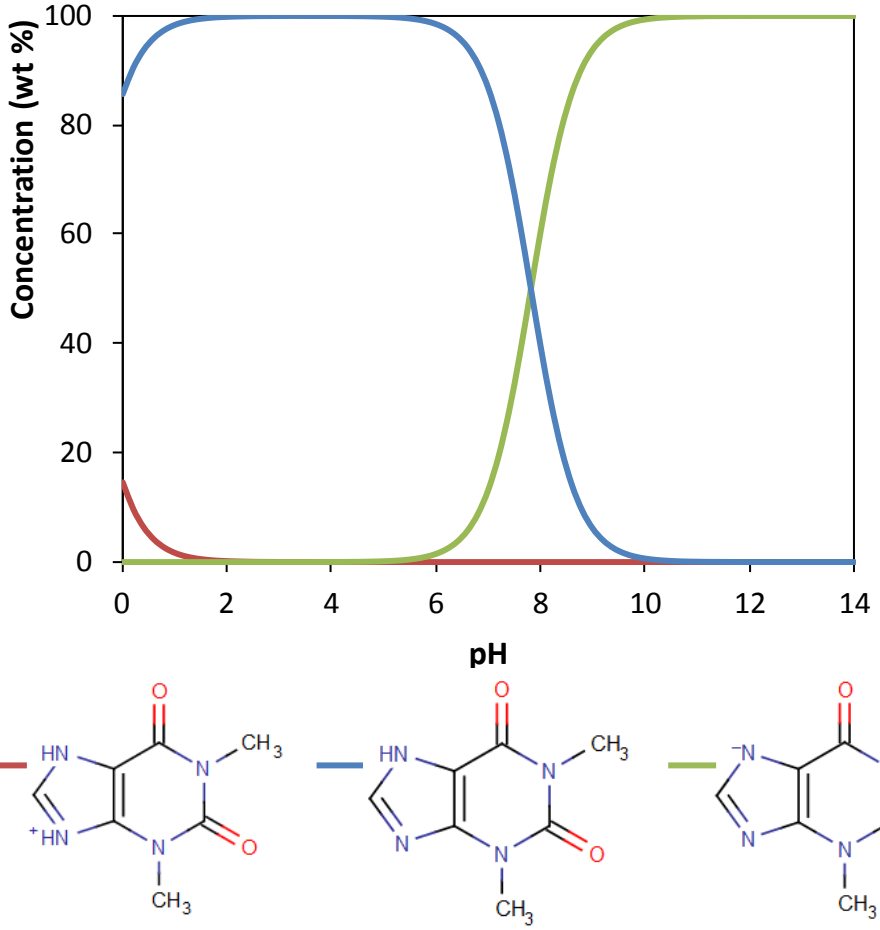

Figure D 3. Speciation diagram of theophylline[117].

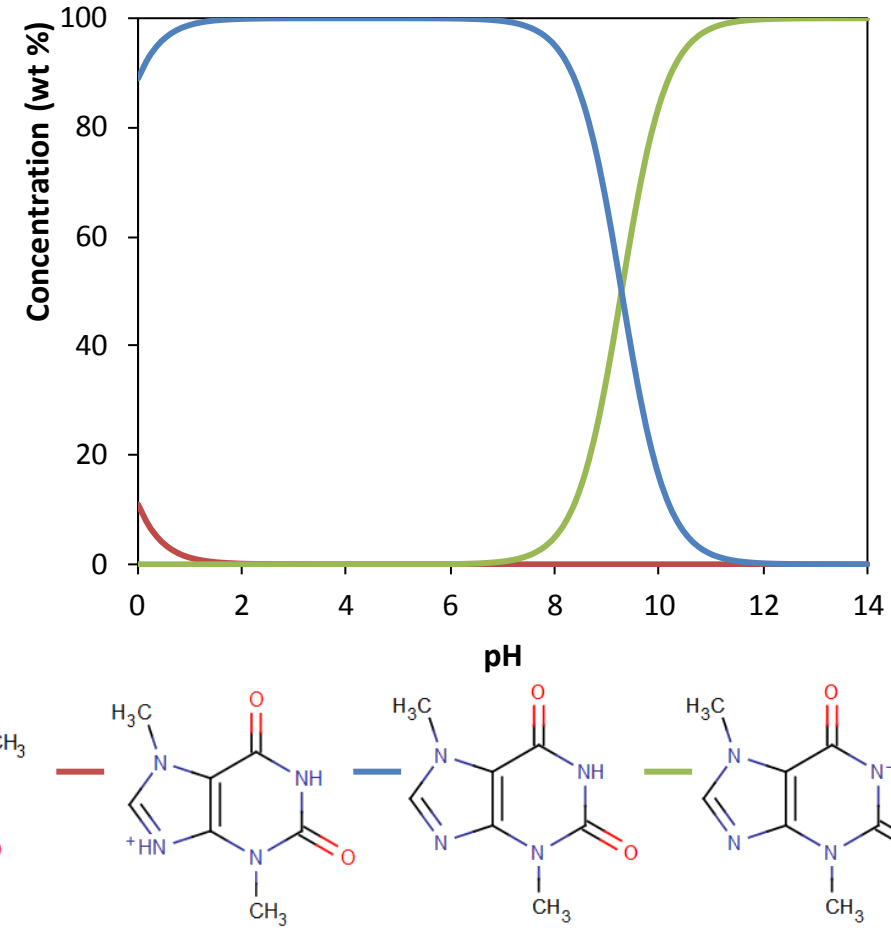

Figure D 4. Speciation diagram of theobromine[117].

Tables D 1 and D 2 present the weight fraction percentage of the extraction points, namely the initial mixture compositions, and respective bottom and top phases compositions and TLLs, and the partition coefficients of the different alkaloids extracted with the systems composed of citrate buffer and tripotassium citrate salt, respectively.

Table D 1. Partition coefficients of nicotine (K_{Nic}), caffeine (K_{Caf}), theophylline (K_{Tph}) and theobromine (K_{Tbr}) in IL + $C_6H_5K_3O_7$/$C_6H_8O_7$ ATPS, mixture compositions and respective TLs and TLLs, and pH values of the coexisting phases.

IL	Weight fraction percentage (wt %)								TLL	K_{Nic}	K_{Caf}	K_{Tph}	K_{Tbr}
	$[IL]_{IL}$	$[Salt]_{IL}$	pH_{IL}	$[IL]_{M}$	$[Salt]_{M}$	$[IL]_{Salt}$	$[Salt]_{Salt}$	pH_{Salt}					
$[C_4mim]Cl$	41.44	14.80	7.13	27.04	29.97	13.11	44.65	7.11	41.16	6.67 ± 0.02	6.34 ± 0.32	5.16 ± 0.10	4.22 ± 0.65
$[C_6mim]Cl$	39.17	16.21	6.91	26.19	30.07	10.70	46.61	7.01	41.65	8.43 ± 0.66	13.00 ± 0.52	12.33 ± 0.19	8.62 ± 0.01
$[C_7mim]Cl$	40.34	15.96	6.85	27.03	29.97	11.40	46.41	6.93	42.01	7.00 ± 0.65	12.87 ± 0.67	10.76 ± 0.08	6.50 ± 0.14
$[C_8mim]Cl$	39.36	17.89	6.94	27.58	29.96	11.98	45.92	6.89	39.19	4.92 ± 0.52	11.53 ± 0.48	9.34 ± 0.68	4.61 ± 0.25
$[C_{10}mim]Cl$	41.24	17.70	7.16	28.19	29.99	13.22	44.10	7.17	38.50	4.28 ± 0.33	7.92 ± 2.17	8.75 ± 1.83	3.12 ± 1.57

Table D 2. Partition coefficients of nicotine (K_{Nic}) and theophylline (K_{Tph}) in IL + $C_6H_5K_3O_7$ ATPS, mixture compositions and respective TLs and TLLs, and pH values of the coexisting phases.

IL	Weight fraction percentage (wt %)								TLL	K_{Nic}	K_{Tph}
	$[IL]_{IL}$	$[Salt]_{IL}$	pH_{IL}	$[IL]_{M}$	$[Salt]_{M}$	$[IL]_{Salt}$	$[Salt]_{Salt}$	pH_{Salt}			
$[C_4mim]Cl$	41.26	15.32	9.18	26.68	29.92	13.04	43.59	9.06	39.94	11.40 ± 0.73	11.48 ± 0.36
$[C_6mim]Cl$	46.52	11.53	8.48	23.49	29.89	8.89	41.53	8.48	48.12	5.29 ± 0.17	2.02 ± 0.20
$[C_8mim]Cl$	39.49	17.02	9.15	27.03	29.87	11.97	45.40	9.20	39.53	13.48 ± 0.19	14.27 ± 1.80
$[C_{10}mim]Cl$	38.70	19.03	8.28	27.75	29.89	13.09	44.42	8.39	36.06	21.0 ± 0.80	16.52 ± 1.20

D.2. Experimental data for the partitioning of BPA

Figure D 5 and Figure D 6 show the diverse mixture compositions evaluated for the extraction of BPA from aqueous phases with $[C_2mim]Cl$- and $[N_{1112OH}]Cl$-based systems.

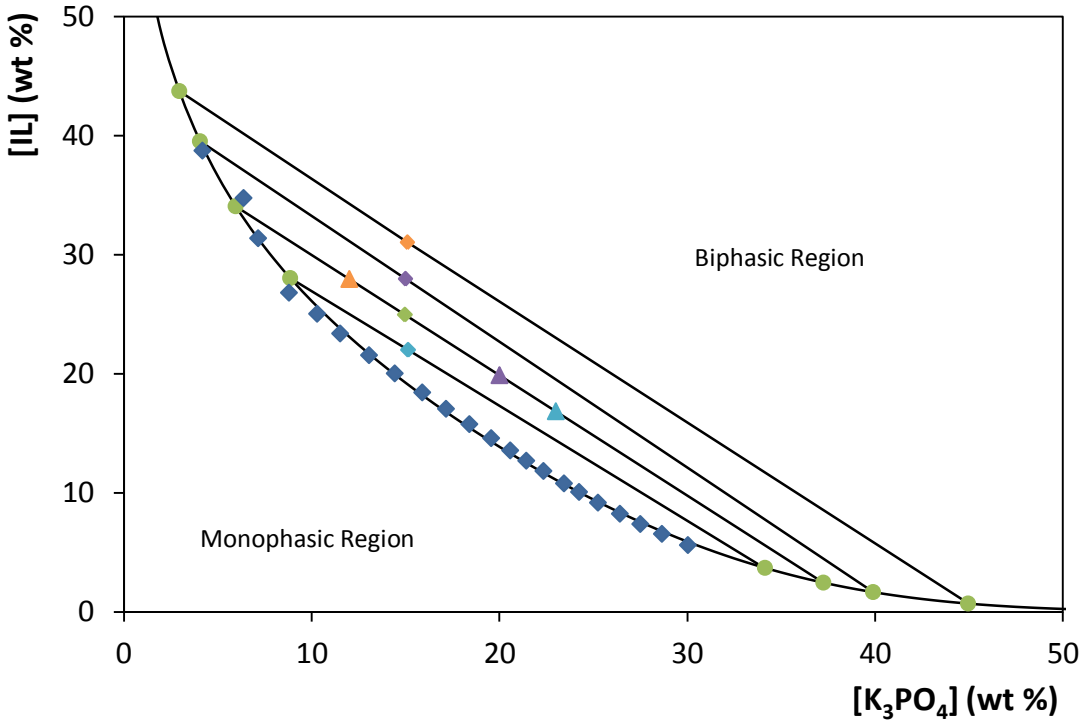

Figure D 5. Phase diagrams for the $[C_2mim]Cl$ + K_3PO_4 ATPS: binodal curve data (◆); fitted curve by Eq.1 (–); TL data (●); extraction points: 12.00 wt % of K_3PO_4 + 27.94 wt % of IL (▲); 20.00 wt % of K_3PO_4 + 19.87 wt % of IL (▲); 23.00 wt % of K_3PO_4 + 16.84 wt % of IL (▲); 15.00 wt % of K_3PO_4 + 22.00 wt % of IL (◆); 15.00 wt % of K_3PO_4 + 25.00 wt % of IL (◆); 15.00 wt % of K_3PO_4 + 28.00 wt % of IL (◆); and 15.00 wt % of K_3PO_4 + 31.00 wt % of IL (◆).

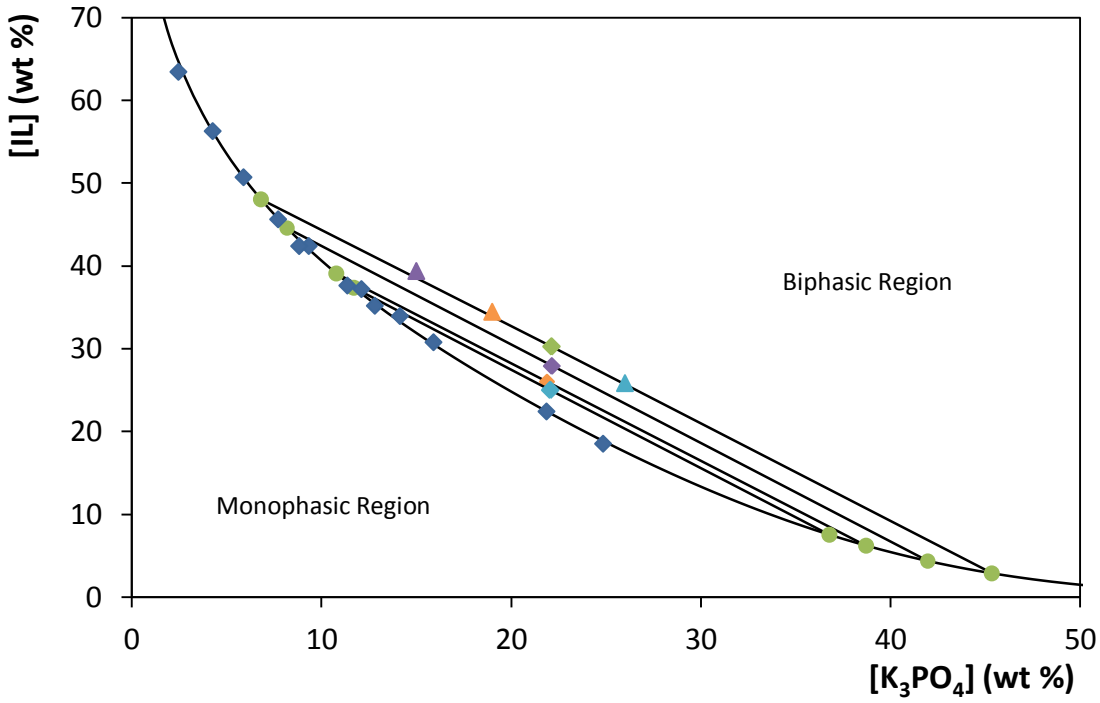

Figure D 6. Phase diagrams for the $[N_{1112OH}]Cl$ + K_3PO_4 ATPS: binodal curve data (◆); fitted curve by Eq.1 (–); TL data (●); extraction points: 15.00 wt % of K_3PO_4 + 40.00 wt % of IL (▲); 19.00 wt % of K_3PO_4 + 34.47 wt % of IL (▲); 26.00 wt % of K_3PO_4 + 25.85 wt % of IL (▲); 22.00 wt % of K_3PO_4 + 25.00 wt % of IL (◆); 22.00 wt % of K_3PO_4 + 26.00 wt % of IL (◆); 22.00 wt % of K_3PO_4 + 28.00 wt % of IL (◆); and 22.00 wt % of K_3PO_4 + 30.77 wt % of IL (◆).

Table D 3 and Table D 4 present the detailed extraction efficiencies of BPA obtained with the several systems investigated and the respective mixture compositions.

Table D 3. Extraction efficiencies of BPA (EE_{BPA}%) in IL-based ATPS and respective mixture compositions.

IL	Weight fraction percentage (wt %)		EE_{BPA}% ± 0.2
	$[IL]_M$	$[Salt]_M$	
$[C_2mim]Cl$	21.99	15.12	99.4
	24.96	14.96	99.8
	27.97	14.98	100.0
	31.02	15.08	100.0
$[C_4mim]Cl$	25.02	15.02	99.5
$[C_6mim]Cl$	24.94	15.29	99.1
[amim]Cl	25.03	15.02	99.9
$[C_4mpyr]Cl$	25.03	15.03	98.5
$[P_{4444}]Cl$	24.98	14.99	99.1
$[N_{4444}]Cl$	25.08	15.05	99.3
$[N_{1112OH}]Cl$	25.03	22.07	98.8
	26.02	21.89	99.6
	27.95	22.15	100.0
	30.74	22.12	100.0

Table D 4. Extraction efficiencies of BPA (EE_{BPA}%) in urine-type IL-based ATPS and respective mixture compositions.

IL	Weight fraction percentage (wt %)		EE_{BPA}% ± 0.2
	$[IL]_M$	$[Salt]_M$	
$[C_2mim]Cl$	24.98	14.99	99.7
$[C_4mim]Cl$	25.05	15.20	100.0
$[C_6mim]Cl$	25.05	15.01	99.6
[amim]Cl	25.06	15.10	100.0
$[C_4mpyr]Cl$	25.01	15.02	99.9
$[P_{4444}]Cl$	25.04	14.99	98.8
$[N_{4444}]Cl$	24.99	14.90	100.0
$[N_{1112OH}]Cl$	40.03	14.85	100.0